To the Graduate Council:

I am submitting herewith a thesis written by Christopher Charles Hood entitled "Characterization of Activated Carbon Adsorption Applied to a Thin Bed System". I have examined the final copy of this thesis for form and content and recommend that it be accepted in partial fulfillment of the requirements for the degree of Masters of Science, with a major in Civil Engineering.

Wayne T. Davis

Wayne T. Davis, Major Professor

We have read this thesis
and recommend its acceptance:

James L. Smoot

Terry L. Miller

Maureen Devor

Accepted for the Council:

Lee Minkel

Associate Vice Chancellor
and Dean of The Graduate School

STATEMENT OF PERMISSION TO USE

In presenting this thesis in partial fulfillment of the requirements for a Master's degree at The University of Tennessee, Knoxville, I agree that the Library shall make it available to borrowers under rules of the Library. Brief quotations form this thesis are allowable without special permission, provided that accurate acknowledgment of the source is made.

Permission for extensive quotation from or reproduction of this thesis may be granted by my major professor, or in his absence, by the Head of Interlibrary Services when, in the opinion of either, the proposed use of the material is for scholarly purposes. Any copying or use of the material in this thesis for financial gain shall not be allowed without my written permission.

Signature Christopher C. Hood

Date 20 August 1993

CHARACTERIZATION OF ACTIVATED CARBON ADSORPTION APPLIED TO A THIN BED SYSTEM

A Thesis

Presented for the

Master of Science Degree

The University of Tennessee, Knoxville

Christopher Charles Hood

December 1993

DEDICATION

This thesis is dedicated to my wife, daughter, parents and grandparents:

Laura Crozier Hood

Rebecca Ashley Hood

Thomas Charles Hood

Virginia Johnson Hood

Harold Johnson

Priscella Johnson

Helena Hood

Max Kay Hood

I thank them for their inspiration and support.

ACKNOWLEDGMENTS

I would like to thank my major professor, Dr. Wayne T. Davis, for his patience, commitment and time. He has been a continual example of the type of professional which I am striving to become. I appreciate all of his work and effort in the completion of my graduate studies. I would also like to thank the other members of my committee, Dr. Terry Miller, Dr. James Smoot, and Dr. Maureen Dever, for their comments and advice.

This research was funded in part by the U.S. ARMY Natick Research, Development and Engineering Center, Natick, MA and was conducted within the laboratories of TANDEC (the Textiles and Nonwovens Development Center) and the Environmental Engineering Program of the Civil Engineering Department at the University of Tennessee.

ABSTRACT

Research has been conducted by Textiles and Nonwoven Development Center (TANDEC) and the University of Tennessee Civil and Environmental Engineering Department to investigate the possible use of non-woven materials impregnated with activated carbon as a potential liner for chemical warfare suits. The objectives of this thesis were to evaluate the breakthrough time and capacity of these materials in a bench scale adsorption system, and then conduct preliminary modeling of the system using existing adsorption theory. The theory is based on the adsorbent and adsorbate following a Freundlich type isotherm of the form:

$$C_e = \alpha(X_{sat})^{\beta}$$

where C_e is the concentration of the adsorbate in the gas phase, α is an adjustable constant with units of concentration, β is an adjustable constant that is a pure number and X_{sat} is the solid phase adsorption capacity (gram of adsorbate/gram of adsorbent). This representation allows one to develop a set of equations that describe the velocity of the mass transfer zone, the width of the zone, and the time required for the zone to pass through the bed.

In order to make the appropriate comparisons to existing theory, the activated carbon was evaluated to determine pore volume, surface area and density. This allowed for a complete physical characterization of the adsorbent.

This study of carbon loaded laminates provided insight to how the bed weight, bed depth and carbon distribution affect the breakthrough time and adsorption wave. In order to fully understand how the weight and depth affect the adsorption system, the adsorption mass transfer zone was evaluated. The shape of the adsorption zone changed as these characteristics

were varied which in turn affected the point at which breakthrough occurred and the time required to reach total capacity.

The experimental information in conjunction with existing adsorption theoretical models were used to develop a computer program to attempt to simulate a thin bed adsorption systems. The theoretical model was based on conventional thick bed adsorption theory. Although the theoretical results were not directly comparable to the experimental, useful information was gathered for understanding the development of the adsorption zone.

TABLE OF CONTENTS

CHAPTER		PAGE
1.	INTRODUCTION	1
2.	LITERATURE REVIEW	3
	Introduction	3
	Adsorption Background	3
	Adsorbent	4
	Adsorbate	9
	Development of the Testing Method and Procedures.	11
	Adsorption Theory Characteristics	12
	Modeling the Adsorption Mass Transfer Process	28
3.	THEORETICAL DEVELOPMENT	35
4.	EXPERIMENTAL METHOD	40
	Test Materials	40
	Test Carbons	43
	Test Gas	45
	Test Apparatus	45
	Detector	47
	Testing Procedure	48
	Data Analysis Process	49
5.	RESULTS	51
	Experimental Results	51
	Theoretical Model	66
	Conclusions	79
6.	FUTURE WORK	81
	LIST OF REFERENCES	83
	APPENDIX	88
	APPENDIX A. Chemical properties and toxicity of TCE	90
	APPENDIX B. Basic computer code based on Wark and Warner's theoretical model	91
	APPENDIX C. Carbon Surface Area Analysis	95
	APPENDIX D. Detailed Miran 1A information	125
	APPENDIX E. Detailed Spreadsheet Mass Balance Analysis	127
	VITA	130

LIST OF TABLES

TABLE		PAGE
4-1	Laminate characteristics.....	41
4-2	Miran 1A Detector settings.....	47
5-1	Characteristic breakthrough curve time and adsorption capacity.....	52
5-2	Adsorption model sensitivity analysis.....	68
5-3	Film Coefficient and molecular weight relationship.....	73
5-4	Effect of bed depth and density variation.....	79

LIST OF FIGURES

FIGURE		PAGE
2-1	Pore structure of Activated Carbon as presented by Noll et. al.....	6
2-2	Relationship between breakthrough time, T_b and adsorption bed depth, L: Noll et. al.....	13
2-3	Adsorption zone and breakthrough curve in a thick bed adsorption system: Treybal.....	15
2-4	The development of the adsorption wave, Stern, Air Pollution 3rd version.....	18
2-5	Transmission of a gas through an adsorbent: Klotz.....	19
2-6	Steady-state adsorption wave development.....	20
2-7	Unsteady-state adsorption wave development.....	20
2-8	Types of Isotherms for Gaseous Adsorption: Noll.	23
2-9	The effect of bed depth and superficial air flow velocity on breakthrough time.....	32
3-1	Variables for a mass balance between inlet and outlet of a thick bed adsorber.....	36
4-1	Photograph of calendered laminate.....	44
4-2	Photograph of non-calendered laminate.....	44
4-3	Experimental set-up illustration.....	46
4-4	Comparison of gravimetric and spreadsheet values.....	50
5-1	Overall breakthrough curves for BDO and NG7-72..	53
5-2	Behavior at breakthrough for BDO and NG7-72.....	53
5-3	Breakthrough time versus the areal density for HSA and STD carbons.....	55
5-4	Photograph of NG13F-40: poor distribution of STD carbon.....	57
5-5	HSA and STD carbon calendered laminates.....	58

LIST OF FIGURES

FIGURE		PAGE
5-6	Noncalendered and calendered HSA carbon laminates	59
5-7	Breakthrough adsorption capacity for all laminates	61
5-8	Isotherm plot of the gas concentration	62
5-9	Log/log plot of concentration versus adsorption capacity	63
5-10	Photograph of laminate shrinkage	65
5-11	Graphical illustration of bleedthrough	66
5-12	Effect of bed depth on breakthrough	68
5-13	Effect of velocity on breakthrough	69
5-14	Effect of beta on breakthrough	71
5-15	Effect of alpha on breakthrough	72
5-16	Effect of inlet concentration on breakthrough	73
5-17	Effect of film coefficient on breakthrough	74
5-18	Effect of density on breakthrough	75
5-19	Theoretically modelled isotherm	76
5-20	Constant adsorbent quantity, density and bed depth variation	77
5-21	Three sections of an adsorption unit	78

LIST OF ABBREVIATIONS

American Society for Testing and Materials.....ASTM
Absorption Unit.....AU
Battle Dress Overgarment.....BDO
Breakthrough time.....t_b
Brunauer, Emmett and Teller.....BET
Centimeter.....cm
Centimeter per second.....cm/s
Cubic foot per minute per foot squared.....cfm/ft^2
Differential change in concentration.....dC
Differential change in distance.....dx
Dimethyl methylphosphonate.....DMMP
Gram.....g
Gram of adsorbate per gram of adsorbent.....g/g
Gram per meter squared.....g/m^2
High Surface Area.....HSA
High-Resolution Transmission Electron Microscopy....HRTEM
International Union of Pure and Applied Chemistry...IUPAC
Isopropyl Methylphosphonofluoridate.....IMPF
Kilogram per meter squared.....kg/m^2
Liter per minute.....lpm
Melt Blown.....MB
Meter.....m
Meter per second.....m/s
Millimeter.....mm
Millimeter per second.....mm/s
Minute.....min
Nanometers.....nm
Nylon.....N
Oak Ridge National Laboratory.....ORNL
Occupational Safety and Health Association.....OSHA
Parts per million.....ppm

Permissible Exposure Limit.....PEL
Polyester.....PET
Polyethylene.....PE
Polypropylene.....PP
Scanning Electron Microscope.....SEM
Spunbond.....SB
Standard.....STD
Textiles and Nonwoven Development Center.....TANDEC
Total Volume Filling Method.....TVFM
Trichloroethylene.....TCE

CHAPTER 1

INTRODUCTION

Carbon has been used as an adsorbent for over a hundred years in applications ranging from remediation of contaminated ground water to separation of chemicals. It is an especially good control technology for gases which are noncombustible, valuable, or in very dilute concentrations. Two terms which are important in understanding the adsorption process are adsorbent and adsorbate. The adsorbent is the media which is adsorbing the adsorbate. The adsorption process may be physical or chemical. Physical adsorption utilizes the surface tension forces, which may be described as weak electrostatic or H-bonding, to form either single or multiple layers of the adsorbate. Chemisorption requires that a chemical reaction takes place resulting in a bond between the adsorbent and the adsorbate. In this later case, the adsorbent may only be covered with a single layer of the adsorbate due to the reaction that must take place. Because a chemical reaction occurs, this process is difficult to reverse. Since chemisorption system are limited to single layer and are difficult to reverse, a physical adsorption system is the most applicable system for adsorbing chemical warfare agents.

U.S. Army personnel are currently (1993) issued an air-permeable overgarment for protection against chemical warfare agents. This garment, the Battle Dress Overgarment (BDO), has two layers. The inner layer consists of a poly(urethane) foam non-woven fabric impregnated with a slurry of latex binder and powdered activated carbon. The finished layer must meet requirements specified in the American Standard Test Method (ASTM) MIL-C-43858B(GL) standard, including a fabric weight of 0.2543-0.3391 kg/m^2 (7.5-10 oz/yd^2), a thickness of 0.07-0.12

inches, a minimum air permeability of 40 cfm/ft^2 at 0.5 inches of water pressure drop, a minimum bursting strength of 75 pounds and a minimum carbon tetrachloride adsorption of 1.8 mg/cm^2. In addition, the BDO must meet specific flexibility, flame resistance, and water resistance requirements. The existing BDO has been found to act as insulators resulting in heat stress to personnel when worn in a dessert climate. A lighter-weight, thinner, more air-permeable, yet highly adsorptive inner layer is desired. The purpose of this study was to develop and test a activated carbon loaded polymer laminate as an alternative to the existing inner layer of the BDO.

Textiles and Nonwoven Development Center (TANDEC) and the Civil Engineering Department have investigated the possible use of nonwoven materials impregnated with activated carbon as a potential liner for the BDO. This thesis evaluates the breakthrough capacity of these materials in a bench scale adsorption system. Results from the testing were then compared to conventional adsorption theory based on thicker beds of carbon through the use of a computer model.

The polymer laminates developed in this study consisted of meltblown (MB) non-woven materials which were used in non-calendered laminates, and sandwiched between two layers of spunbonded (SB) material in the calendered laminates. The MB non-woven web, consisting of small fiber diameters, provided a high surface area for retention of the powdered activated carbon. These webs also exhibited high air permeability. For the calendered laminates the SB material was chosen as the material to sandwich the carbon-loaded MB core because it was lightweight, strong, and had a high air permeability. Each of the laminates was tested before and after calendering to determine the effect of the reduced permeability. Laminates were prepared with loaded activated carbon loadings of nominally 0.04, 0.08, and 0.12 kg/m^2 (40, 80, and 120 g/m^2) using two different activated carbons.

CHAPTER 2

LITERATURE REVIEW

2.1 Introduction

This section provides a general background for understanding the adsorption process and how it can be related to a thin bed adsorption system. The review starts with the basics of adsorption. Then examines procedures related to experimental methods. This is followed by a discussion of the theory of adsorption and experimental results.

2.2 Adsorption Background

Adsorption may be used in applications ranging from remediation of contaminated ground water to separation of chemicals through its use as a molecular sieve. It is an especially good control technology for systems that have gases which are noncombustible, valuable, or in dilute concentrations.[1] Commonly, there is confusion between the differences in adsorption, absorption, and sorption. The process of absorption requires the contaminant to penetrate the surface and become part of the media which is performing the absorption. Adsorption, on the other hand, is only a surface phenomena resulting from an imbalance in the molecular forces. The term sorption refers to situations where adsorption and/or absorption may be taking place.

Two important terms used to describe adsorption are adsorbent and adsorbate. The adsorbent is the media which is adsorbing the adsorbate.[2] For example, if one is trying to recover perchloroethylene from a dry cleaning process, an activated carbon canister may be placed on the exhaust. The activated carbon is the adsorbent and the perchloroethylene is

the adsorbate.

There are two distinct types of adsorption: physical and chemical. In physical adsorption, also referred to as Van der Waals adsorption, the adsorbate is held by the surface tension forces produce by the pores of the adsorbent. These surface tension forces may be described as weak electrostatic or H-bonding.[2] This type of adsorption may be mono-layered or multi-layered and is typically reversible. In chemisorption, also known as activated adsorption, a chemical reaction actually takes place resulting in a bond between the adsorbent and the adsorbate. In this type of system the adsorbent may only be covered with a monolayer of the adsorbate due to sites for the reaction to take place and becomes much more difficult to reverse.

2.3 Adsorbent

The adsorbent is fundamentally the most important part of the adsorption process since it is the media which retains the adsorbate. One must attempt to accurately evaluate it's properties and quantify it's characteristics. This may be done by describing the important properties. Then evaluating the limitations associated with the characterization of adsorbents.

2.3.1 General Characteristics

The characteristics of the adsorbent vary with the type of adsorbent selected. Since activated carbon was the selected adsorbent, this discussion will be limited to its characterization. The parameters of primary importance are carbon type and form, surface area, pore volume and pore diameter.

Activated carbon is predominantly an amorphous solid which may be formed from many different materials. The type

and form of the activated carbon are interdependent characteristics. They both depend on the virgin material and type of processing. Specific applications require different forms of carbon ranging from granular, powdered and shaped.[3] According to American Society for Testing and Materials (ASTM), granular activated carbon has particle sizes predominately greater that 80 mesh and powdered are predominately smaller than 80 mesh. The shaped activated carbon is not defined by these size standards because it can be comprised of either granular, powdered or both.[4] Shaped activated carbon is limited to specific applications and its shape is determined by the application. The type and form of activated carbon effect the surface area, pore volume and pore diameter.

The surface area describes the amount of area per specific unit of volume or fixed amount of mass. Its importance to adsorption is that it describes the number of sites available for adsorption to occur. The Brunauer-Emmett-Teller (BET) model is commonly used to determine the surface area of activated carbons. ASTM D 2652-76 defines surface area (BET) as the total surface area of a solid calculated by the BET equation, from nitrogen adsorption or desorption data obtained under specified conditions. The normal values for surface area of an activated carbon are in the range of 500-2,000 m^2/g; however, there are some activated carbons which have reported surfaces areas of 3,500-5,000 m^2/g.[3]

The pores of an activated carbon are also important to the adsorption process. They are divided into three classes by the International Union of Pure and Applied Chemistry (IUPAC): micropores, width < 2 nanometers (nm); mesopores, width 2-50 nm; and macropores, width > 50 nm.[5] One should recognize that the width of the pore and the diameter of the pore may be used synonymously. Figure 2-1 illustrates the pore structure of an activated carbon. From this illustration it is clear that the volume which is represented by the micropores maybe far

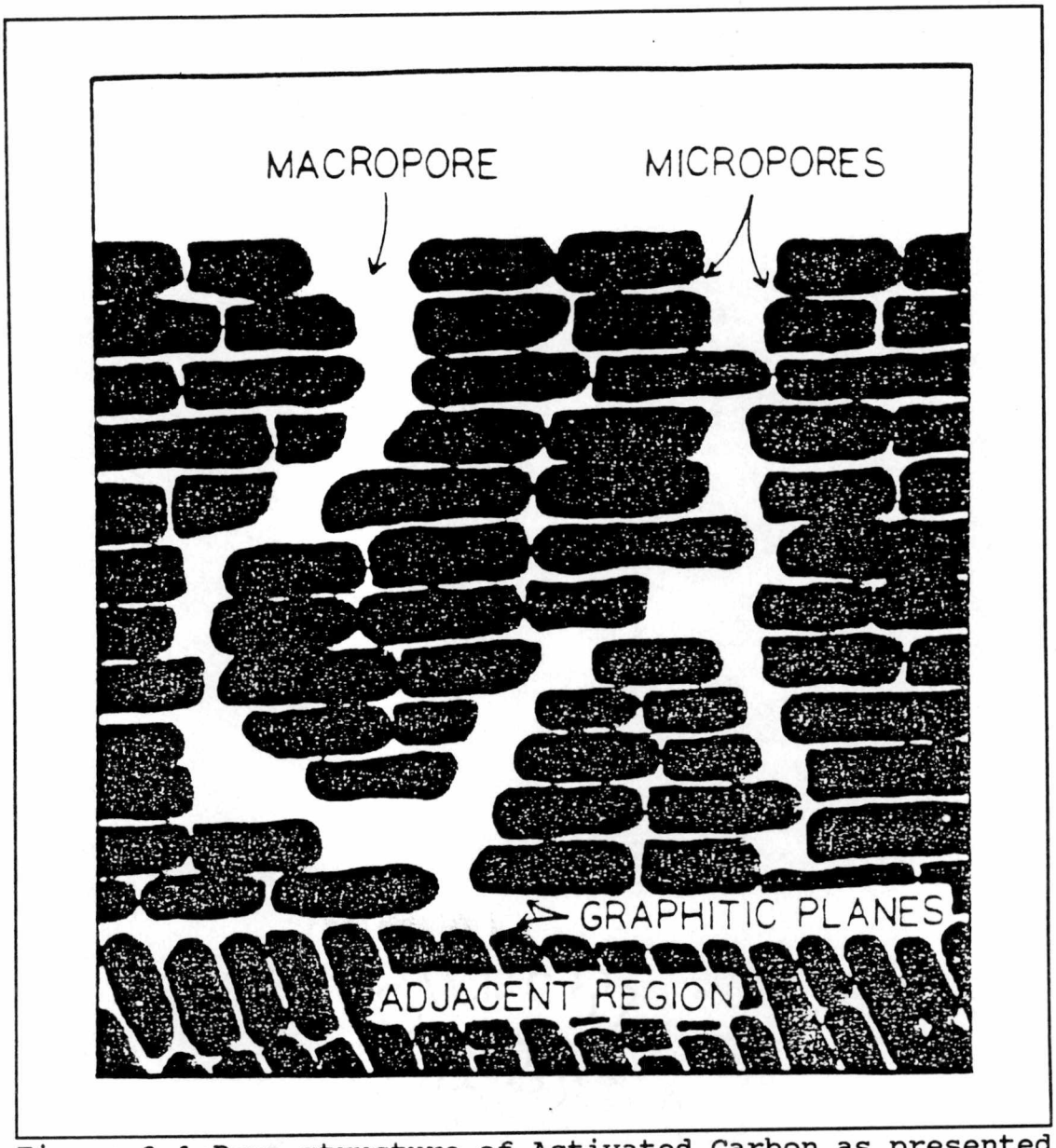


Figure 2-1 Pore structure of Activated Carbon as presented by Noll et. al.

greater than that of the other two classifications.

2.3.2 Description of the micropore structure

The micropore structure accounts for the majority of the adsorption capacity. For a typical activated carbon, these pores constitute the largest part of the internal surface and

may account for 90 percent of the apparent surface area.[6] There has been a great deal of work to characterize the micropore structure over the last decade. The BET surface area analysis method, which has been widely accepted as a method for determining the surface area of activated carbons, has been challenged as to its accuracy when characterizing pores under 2 nm in diameter. Although at this time there is no universal method for characterization of the micropore structure, there are some new "state of the art" techniques for evaluating these small pore diameters.[7]

The mechanism responsible for the micropore's adsorption potential is the superposition of the adsorption forces generated by the opposite walls. As the pore size increases to the mesopore and macropore, the forces of the opposite walls are reduced. This results in a comparatively small amount of adsorption taking place in these larger pores. The new assessment methods used to characterize microporous activated carbon involve "(1) assessing the microporosity, and (2) evaluating the parameters that describe the microporous structure. The most popular methods used for the assessment of the microporosity (e.g., the t-method [7,8] and the $alpha_s$-method[9-12]) are based on a comparison of the shape of a given isotherm with that of a standard isotherm on a nonporous reference solid."[7]

One of the most popular and well documented theories for describing micropores is that of Total Volume Filling Method (TVFM). Innes et. al. describe micropores as pores which have molecular dimensions in which volume filling of pores occurs. Dubinin introduced this in a journal article written for Progress in Surface and Membrane Science.[8] This theory provides an alternative method for determining the total capacity of adsorbents. For the case of activated carbon, the homogeneity of pore structure is an important factor which effects the micropore adsorption. Dubinin discusses the effects of this homogeneity on the TVFM and the resultant

changes in the isotherms. Isotherms are important since they describe the mass transfer for varying concentration of the adsorbate on the adsorbent. This provides the appropriate information to characterize the way in which a system reaches breakthrough. The TVFM only evaluates the way pores are filled and the author presents a detailed empirical method for analysis of micropore performance.[9] This theory is limited in its applicability for design because it is founded in how the system is performing at capacity.

Two other methods which have been developed to evaluate micropore capacity are High-Resolution Transmission Electron Microscopy (HRTEM) and a thermodynamic method based on an expansion of the BET model. These two methods show the diversity of the theories. HRTEM is used as a means for evaluating the pore volume accessible pore width, distribution of the accessible width, measure of the heterogeneity of the material and surface area of the walls are all physical properties of micropore which effect adsorption. The critical chemical property is related to the variety of oxygen groups which are found on the surface edges.[10] This article suggests that both physical and chemical properties of micropores effect the quantity adsorbed and require investigation. This method is also based purely on experimentation. The second method follows the thermodynamic approach which is used in the conventional BET model. Seaton et. al. uses the standard nitrogen adsorption isotherm to determine the relationship between pressure and capillary condensation. Then they determine the pore size associated with each pressure at which capillary condensation will occur. Their theoretical data are compared to conventional values measured using the Micromeritics Digisorb 2500 Sorption Analyzer.[11]

Other characteristics of activated carbon which need to be considered include pore volume, particle size distribution, apparent or bulk density, particle density, abrasion resistance, hardness, and ash content. These properties are

important to both the adsorption capacity and the long term durability of the carbon.[2]

2.3.3 Characteristic Test Methods

There are two standard test methods which ASTM uses to characterize activated carbon for adsorption: 1) ASTM D 3467-88: Standard Test Method for Carbon Tetrachloride Activity of Activated Carbon, and 2) ASTM D 5158-91: Standard Test Method for Determination of the Particle Size of Powdered Activated Carbon. The carbon tetrachloride test identifies activated carbons by determining the "activation level". The activation level is defined as the ratio of carbon tetrachloride adsorbed (weight) to the weight of activated carbon under the listed conditions in the test method. In the test, carbon tetrachloride is adsorbed from a carrier gas. The significance of determining the activity characteristic is that it becomes a basic measure of the pore volume. However, the activity number does not necessarily provide an absolute or relative measure of the effectiveness of the tested carbon on other adsorbates, or at other conditions of operation.[12]

The second test method is used to determine powdered activated carbon particle sizes. The significance and use of this method is for evaluating cake filtration rate and filter penetration. The particle size is also important when selecting and handling powdered activated carbon due to potential operational limitations.[12]

2.4 Adsorbate

The type of adsorbate is as important as the type of adsorbent to understanding the adsorption process. Its chemical properties are essential to understanding how the system will react and in the selection of the adsorbent. Another important consideration is the level of toxicity. If

one is adsorbing an adsorbate which is toxic additional information is required to insure human safety and well being. The final consideration is the detection of the adsorbate. This is important when considering concentration ranges and types of detectors.

2.4.1 Adsorbate Characterization

In the text Mass Transfer Operations by Treybal, he makes the statement that "as a general rule, vapors and gases are more readily adsorbed as their molecular weight increases and the lower the critical temperature, although chemical differences, such as the extent of unsaturation in the molecule also influence the extent of adsorption."[13] This information is supported in the literature and should be considered when approaching any type of adsorption system. In A summary of some of the chemical properties of TCE is included in Appendix A-1. These properties should be considered when evaluating the results of the different adsorbates and may be used as a design parameter for the development of testing. Additional information on other adsorbates can be found in the journal article by G.O. Nelson and C.A Harder. In this article breakthrough curves for 131 different solvents vapors at 1,000 ppm where generated.[14]

2.4.2 Toxicity

Trichloroethylene (TCE) is a halogenated organic compound that has been adsorbed from emissions in many commercial operations. It is halogenated with chlorine and act as solvents. The National Toxicology Program has determined that trichloroethylene is a suspected carcinogen. As a result, Occupational Safety and Health Association (OSHA) has established strict exposure limits for both of these chemicals. For TCE the eight hour permissible exposure limit

(PEL) is 100 ppm.[15] Appendix A-1 gives a detailed summary of other exposure limits which have been established for this chemical.

2.4.3 Adsorbate Detection

The detection of adsorbate penetrating the bed of adsorbent is critical to evaluating an adsorption systems. Gas chromatography, flame ionization, photoionization and infrared absorption are all methods to determine different gas concentrations. The detection may be static or dynamic. Time interval sampling may make one detector more applicable than another. In the literature the majority of tests were performed under continuous monitoring conditions and several utilized infrared absorption technology to monitor the exit gas concentration.

An experiment performed by Wood and Moyer, on the performance of respirator cartridges, utilized the Miran 1A as the detection device. This device uses infared absorption to determine concentration. In the test, the device handled a gas stream velocity of 32 to 115 lpm and measured up to 20% of the inlet concentration of acetone.[16] This device was also used in a similar experiment performed by Mark Ackley.[17] In this experiment, the test conditions were detection of carbon tetrachloride at a concentration of 5,000 ppm. The temperature was between 20 and 25 °C and the superficial velocity was between 12.05 and 30.74 cm/s. Here again the Miran was used to continuously monitor the outlet concentration.

2.5 Development of the Testing Method and Procedures

ASTM D 5160-91, Standard Guide for Gas-Phase Adsorption Testing of Activated Carbon, covers the evaluation of activated carbons for gas-phase adsorption. "It presents a procedure for determining the dynamic adsorption capacity, N_o,

and critical bed depth, d_c, for an activated carbon used to remove a specific adsorbate from a gas stream under conditions chosen by the user."

The guide is written for experiments which utilize a known amount of activated carbon. The user specifies the flow rate, adsorbate concentration, temperature, pressure and relative humidity. These conditions are held constant during each experiment. The breakthrough time for these test conditions is measured repeatedly varying the known amount of carbon. The guide suggests that the relationship between the breakthrough time is linear with the amount of carbon (Figure 2-2). Further, the slope and x-intercept of the line can be used to calculate the dynamic capacity, N_o (expressed as grams adsorbate/grams carbon or grams adsorbate/cm^3 carbon) and critical bed depth, d_c, characteristic of the activated carbon under the conditions used in the test.(ASTM D 5160-91, Standard Guide for Gas-Phase Adsorption Testing of Activated Carbon)

In section 6.1.2 of the guide for gas-phase adsorption testing of activated carbon, the apparatus for the testing is described. The activated carbon is contained in a sample tube and its length should be several times greater that the critical bed depth under the given test conditions. Section 10.2 discusses the determination of breakthrough. "Many techniques can be used to detect adsorbate as it begins to penetrate the bed. A method that gives the instantaneous concentration of adsorbate in the effluent is preferred. Methods such as chemical indicating solutions that respond to cumulative penetration can cause curvature in the breakthrough time versus bed depth plots in cases where the breakthrough curve is shallow."[18]

2.6 Adsorption Theory Characteristics

Understanding the theoretical characteristics that

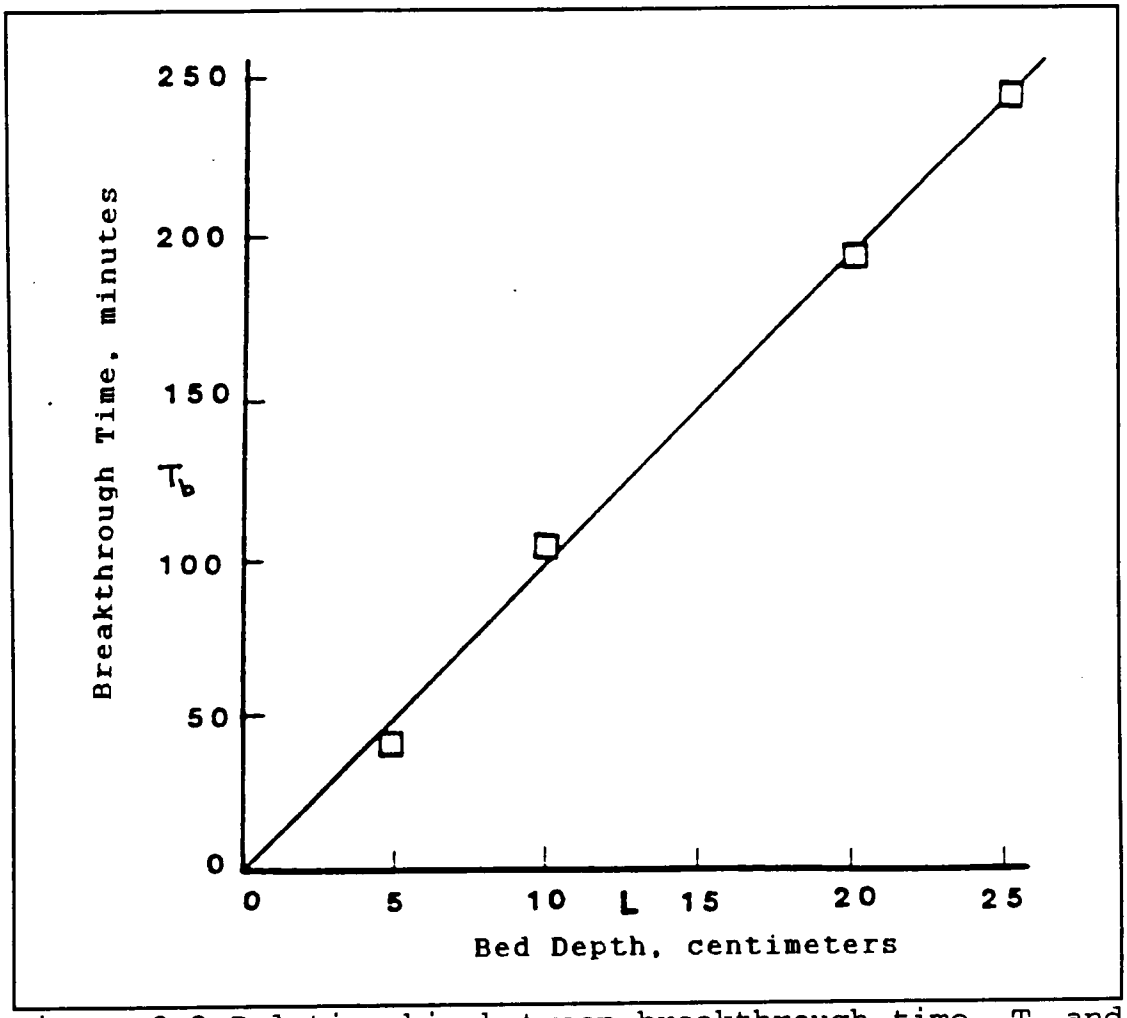


Figure 2-2 Relationship between breakthrough time, T_b and adsorption bed depth, L : Noll et. al.

influence the adsorption process is as important as the understanding the effects of the adsorbate and adsorbent in the actual process. There are three main concepts which must be evaluated to establish a theoretical framework: breakthrough time, adsorption wave, and adsorption isotherm. Each of these is discussed in detail in the following sections.

2.6.1 Breakthrough Time

Breakthrough time can be described as the point at which the outlet concentration reaches a level which is unacceptable

or some appreciable point. In ASTM D 2652-76, Standard Definitions of Terms Related to Activated Carbon, the breakpoint is defined as "the first appearance in the effluent of an adsorbate of interest under specified conditions." Perry's Chemical Engineering Handbook gives a little more latitude to the definition by describing the breakthrough point as "the time of the first nonzero or first nonacceptable value for X" where X is the adsorbate concentration.[19] Another description which some texts use for the breakpoint as the point when the breakthrough curve changes slope or mathematically as a point of inflection. From these definitions, one can see how the quantification of the breakthrough point varies with the application, detection device and experimenter. Referring to Figure 2-3 the point at which the curve changes shape is the breakthrough point designated as C_c; however, this is not the point where the effluent gas does not contain any of the contaminate(i.e. C_b). This figure is representative of a thick bed system.

2.6.1.1 Experimental definitions

Other experimenters have defined breakthrough time in a more quantifiable manner. Typically, they choose a percent of the inlet concentration to define breakthrough. In one such experiment, the author stated that the breakthrough time was 1 percent of inlet concentration. This value was used for predicting the performance and evaluation of respirator sorbent cartridges.[16] This criteria of 1 percent is confirmed in the paper by Jonas et. al. where they state that pseudo first order adsorption kinetics characterize the carbon bed up to first traces of gas penetration (approximately 1 percent inlet concentration).[20]

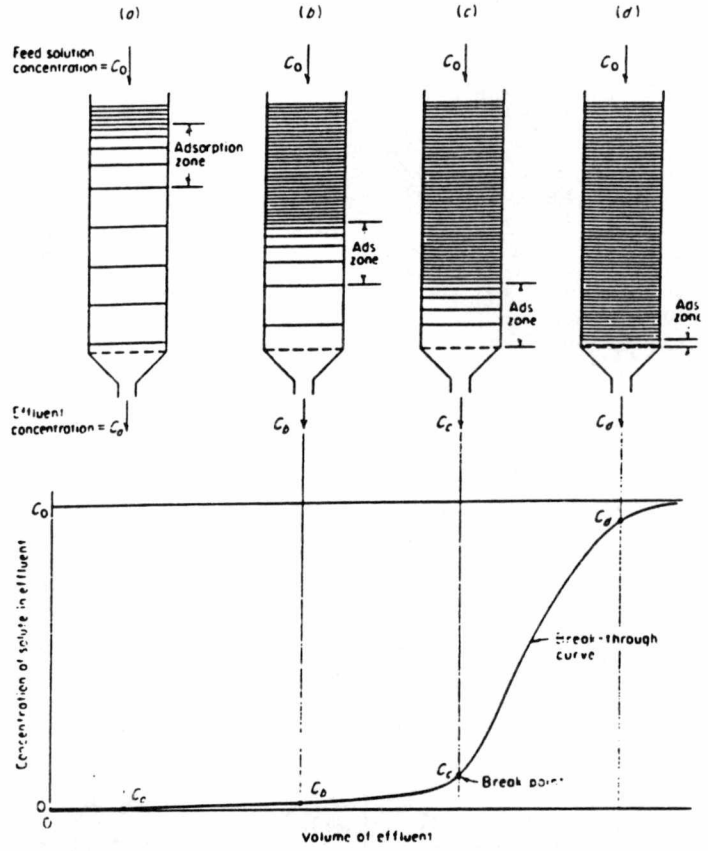


Figure 2-3 Adsorption zone and breakthrough curve in a thick bed adsorption system: Treybal.

2.6.1.2 Factors of influence

Factors which influence the breakthrough time are: the nature of the adsorbent; the nature of the gas to be removed; the geometrical state of the adsorbent; the temperature; the local concentration of the toxic gas, as well as of other gases in the air; the relative amount of the toxic and other gases already adsorbed by the granules; the velocity of the gas-air stream; and the available surface.[21,1] These factors need special consideration if modeling attempts are to be used

to predict the performance of the adsorption unit as related to the adsorption wave and time to breakthrough. One needs to recognize that these factors are competing during the adsorption process and this is one reason why the characterization of the adsorbent and adsorbate is so important. Naturally, the depth of the bed effects the breakthrough time (refer to figure 2-2); however, one cannot discount the other parameters involved in the testing of the material.

2.6.2 Adsorption Wave

2.6.2.1 Definition, description and purpose

The adsorption wave is also known as the adsorption zone or the mass transfer zone. In ASTM D 2652-76 defines the mass transfer zone as "the region in which the concentration of the adsorbate of interest in the fluid decreases from influent concentration to the lowest detectable concentration." The adsorption zone is shown in Figure 2-3.

The adsorption wave is a means for describing the way in which the adsorbate is adsorbed. It is termed as a wave because it is not static in the bed but dynamic and dependent on the systems adsorption characteristics. AP-40 describes the time of appearance and shape of the breakthrough curve as a function of bed operation. Further, "the curves usually have an S shape, but they may be steep or relatively flat and, in some cases, considerably distorted. The actual rate and mechanism of the adsorption process, the nature of the adsorption equilibrium, the fluid velocity, the pollutant concentration in the entering gas, and the adsorber bed length all contribute to the shape of the curve produced for any system."[1]

2.6.2.2 Adsorption Wave verse Breakthrough Curve

A distinction exists between the adsorption wave and the breakthrough curve. The adsorption wave relates to the actual position at which the adsorption mass transfer process is taking place. It is for a specific point in time and position in the bed. The breakthrough curve, on the other hand, describes the way in which the bed performs the adsorption process after breakthrough occurs. If the system reaches steady-state, the adsorption zone is established and is equivalent to the breakthrough curve. As a matter of terminology, as the adsorption zone exits the bed it becomes the breakthrough curve. If the system characteristics are such that the system never reaches steady-state then the adsorption zone and breakthrough curves are different. For these unsteady-state systems the adsorption zone is always dynamic and increasing in width. When it exits the bed it becomes the breakthrough curve; however, the width of the breakthrough curve will continue to increase as the bed reaches capacity.

2.6.2.3 Development of the Adsorption Zone

Irving Klotz in his article "THE ADSORPTION WAVE" presents the concept of the adsorption wave shape being a function of the adsorbent particle size. "If the reaction on the adsorbent were instantaneous, and if the adsorbent were infinitely fine-grained, none of the adsorbable gas would penetrate until some time, t, at which time the adsorbent would be saturated, and then the gas would penetrate at full influent concentration." This is an interesting concept because it challenges the idea that if the bed operates in this fashion, then the gas would travel through the bed as an adsorption line as illustrated by curve A in Figure 2-4. Another perspective presented in this article is the reaction involving a catalyst which is on the activated carbon. The

catalytic reaction with the adsorbate causes the effluent-concentration curve to rise very slowly; this in turn may cause the transmission of gas to never reach the full influent value as illustrated by curve C.

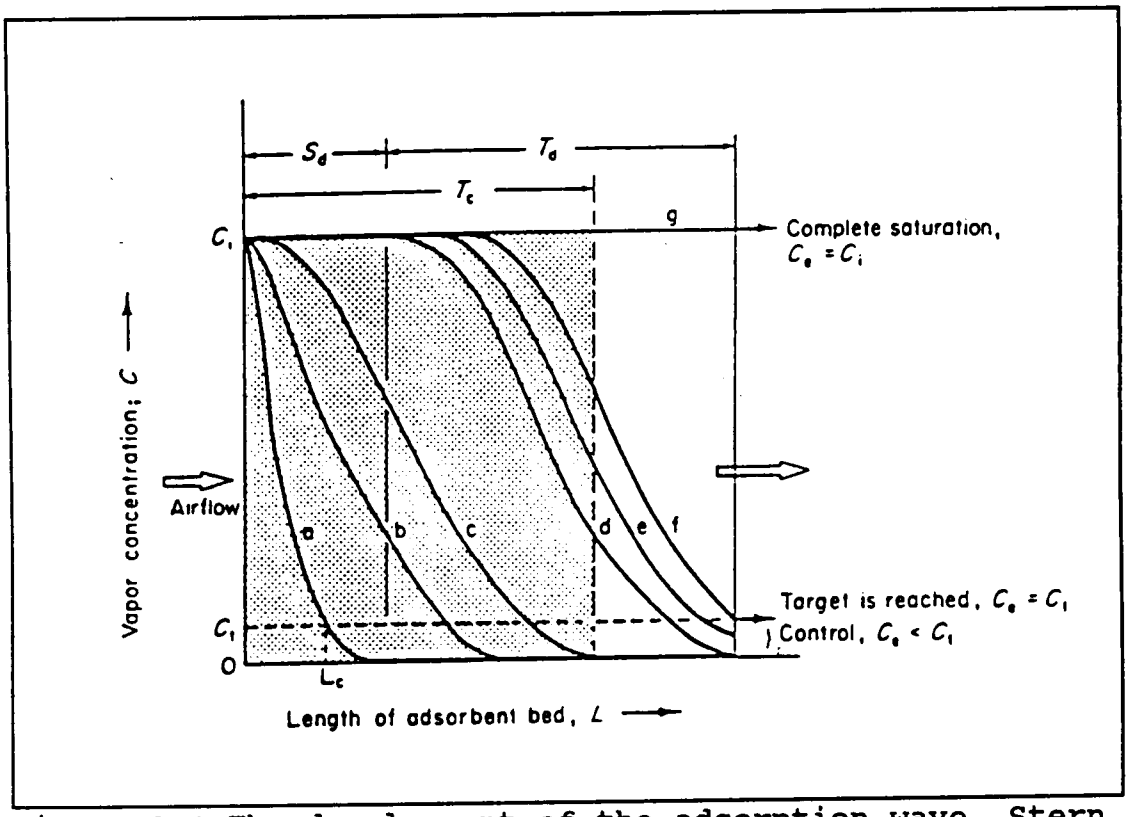


Figure 2-4 The development of the adsorption wave, Stern, Air Pollution 3rd version.

The concept of the adsorption line is furthered by Amos Turk in Air Pollution 3rd ed. Volume IV Engineering control of air pollution. Figure 2-5 illustrates the development of the adsorption wave for a steady-state system. Notice that the x-axis is defined as the length of the adsorbent bed. The bed is thick enough and has characteristics which allow the system to reach steady state. Once steady-state is achieved then the width of the adsorption zone remains constant and the system will breakthrough as predicted by conventional theory. It is important to recognize that the theory does not account for the development of the adsorption zone.

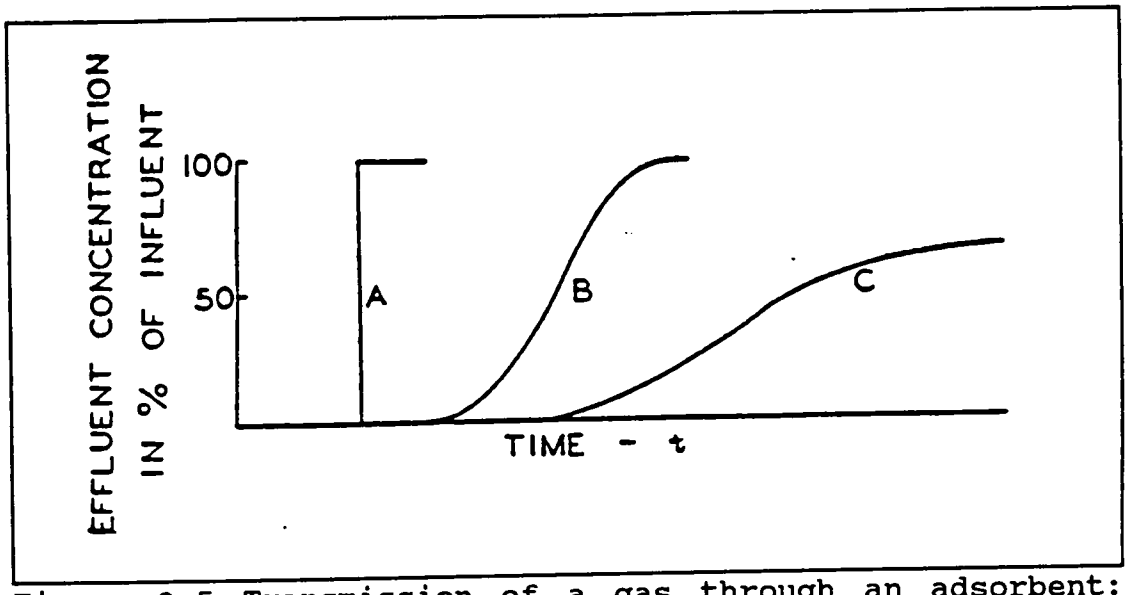


Figure 2-5 Transmission of a gas through an adsorbent: Klotz.

Perry's Chemical Engineering Handbook offers additional insight into the development of the adsorption wave. It suggests that the system represented in figure 2-6 is equilibrium-limited breakthrough. The "vertical projection to X versus time scales shows the proportionate pattern as it emerges through two successive cross sections at h_1 and h_2. Such curves cannot be sharpened by physical effects; if sharper breakthrough is wanted, the equilibrium must be changed by lowering the temperature or by adopting a different sorbent."[19] This type of isotherm is representative of activated carbon adsorption of an organic vapor.[3] In figure 2-7 the unsteady-state system is represented. In this system the development of the adsorption wave is different and it behaves more as an adsorption line for thin bed depths. It is clear in this illustration that the wave continues to expand as it travels through the bed with the first curve having a width of 4.3 units of length and the second with a width of 6.1 units of length.

Additional spreading of the adsorption zone may be attributed to the mass-transfer effects which are often small compared with those associated with equilibrium in the steady-

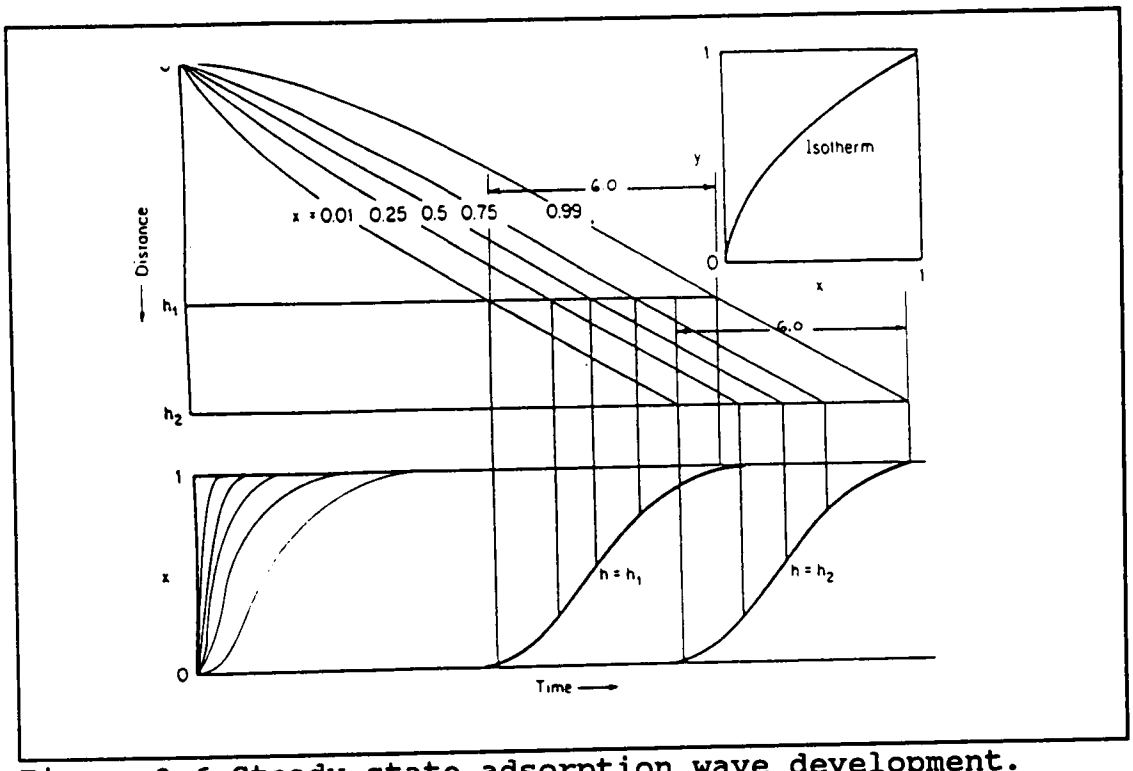


Figure 2-6 Steady-state adsorption wave development.

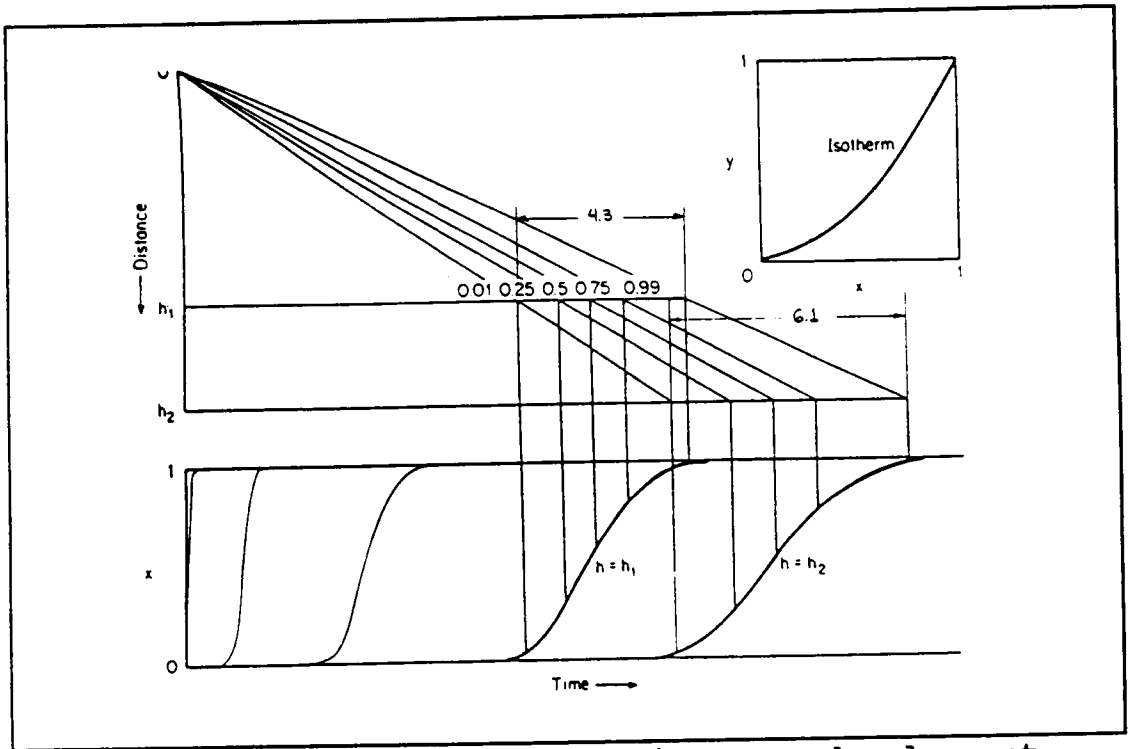


Figure 2-7 Unsteady-state adsorption wave development.

state situation. These mass-transfer effects may be a function of the variations in bed depth, adsorbent density and quantity of adsorbent. The resultant breakthrough curve may be empirically divided into nonsharpening, sharpening, intermediate and compound types. Gradual nonsharpening breakthrough curves are identified with unfavorable equilibrium. Simple and complex breakthrough curves are associated with favorable equilibrium.[19]

2.6.2.4 Adsorption zone and Critical bed depth

One must consider the width of the adsorption zone when evaluating adsorption systems. The critical bed depth is the primary reason for this consideration since, in the concept of thick bed theory, if the adsorption zone is larger than the critical bed depth, the system will start breaking through the instant that the adsorbate is present, although this is not physically possible. ASTM defines the critical bed depth as the minimum depth of an adsorbent bed required to contain the mass transfer zone.[18] This makes clear the importance of this parameter in the design of adsorption systems. Figure 4 (Klotz) illustrates the different development of the adsorption zone or breakthrough curve over time. Curve A is an idealized system where the wave is transmitted through the bed and remains unchanged by its characteristics. Curve B is more typical of a system which has reached equilibrium and is traveling through the bed. Curve C illustrates the system which may not have reached equilibrium and the adsorption wave becomes the breakthrough curve.[21]

2.6.3 Adsorption Isotherm

2.6.3.1 Definition

The standard definition of an isotherm is "a plot of quantity adsorbed per unit of adsorbent against equilibrium

concentration, or pressure, when temperature is held constant".[12] For an activated carbon adsorbent, there are several physical parameters which effect the adsorption isotherm. Kirk and Othmer suggest that the internal surface area, distribution size and shape of the pores, and surface chemistry all effect the capacity and rate of adsorption. In addition, the macropores of the carbon are important to the transfer of adsorbate to adsorption sites.[2]

2.6.3.2 Types of Isotherms

Most authors characterize isotherms as a plot of the adsorbate concentration verses the adsorbent concentration where the adsorbate is plotted on the y-axis and the adsorbent on the x. Figure 2-8 illustrates the types of isotherms which have been identified in the literature. Types I-V are Brunauer classification of isotherms. An additional isotherm, type VI, is introduced by Noll et. al.

In general, the isotherms for microporous adsorbent are type I(refer to figure 2-8); the more complex forms are associated with multilayer adsorption and capillary condensation.[2] "Curves that are convex upward throughout (type I) are designated as "favorable" to uptake of solute; those that are concave upward throughout (type III), as "unfavorable" to uptake of solute; and those that follow a rising diagonal (not shown), as "linear". The terms favorable and unfavorable refer to the uptake step. Other isotherms (types II, IV, and V) have one or more inflection points. In these plots, P is the vapor pressure, or condensation pressure, of the solute.

From Adsorption Technology for Air and Water Pollution Control by K.E. Noll, V. Gounaris, and W.S. Hou states that the majority of physical adsorption isotherms may be grouped into six types (see figure 2-8). All of these isotherms are reversible. The authors refer to the Type I isotherm as a

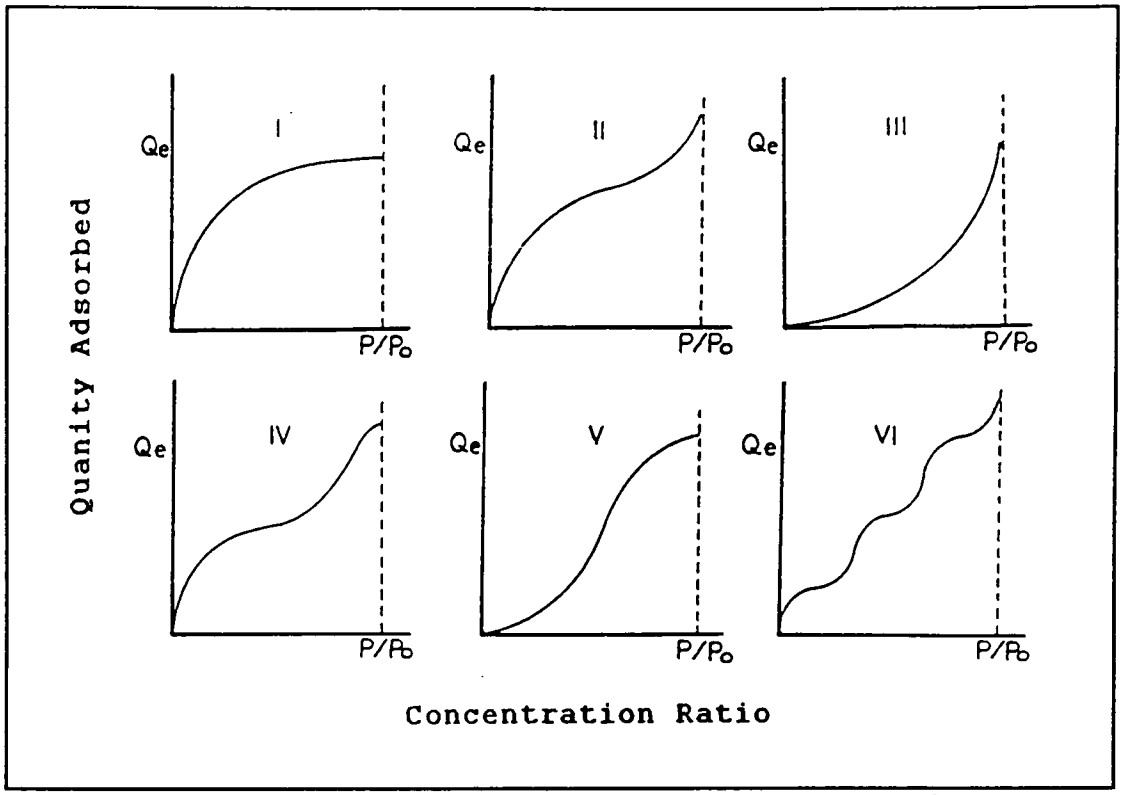


Figure 2-8 Types of Isotherms for Gaseous Adsorption: Noll.

Langmuir isotherm and it is reversible. This type of isotherm is typical of microporous solids having relatively small external surfaces (e.g., activated carbon, molecular sieves). For these microporous solids the internal surface area is less important than the governing micropore volume.

The Type II isotherm is the normal form of isotherm obtained with a nonporous or microporous adsorbent. The Type III isotherm are not common; however, is characteristic of water vapor adsorbed on pure nonporous carbon. The hysteresis loops identify the Type IV isotherm which is typical of mesoporous industrial adsorbents. The uncommon Type V isotherm is related to the Type III by the weak adsorbent-adsorbate interaction in certain porous media adsorbents. Finally, the Type VI isotherm represents stepwise multilayer adsorption on a uniform nonporous surface. It is commonly a result of the adsorption of argon or krypton on graphite carbon blacks at low temperatures.[22]

This isotherm information is very important when combined with the information on the breakthrough curve. It can be used to further characterize the adsorption zone, to determine the width of the zone, and the time to reach equilibrium. Referring back to figures 2-6 and 2-7, the two most common type of isotherms are evaluated and show the contrast as the favorable and unfavorable isotherms. It is important to recognize the changing shape of the adsorption zone in each and how the shape of the unfavorable isotherm mass transfer zone continues to widen regardless of bed depth.

2.6.3.3 Isotherm Mathematical Models

There are three major types of mathematical systems which have been developed to explain and model the behavior of isotherms. These models are the Brunauer, Emmett, and Teller (BET), Langmuir and Freundlich. A brief description is given in the following sections.

2.6.3.3.1 Brunauer, Emmett and Teller

In the 1930's, Brunauer, Emmett and Teller extended Langmuir's approach to multilayer adsorption. This extension was the BET equation. The following equation is the BET equation.

$$\frac{q}{Q_o} = \frac{bP/P_s}{(1-P/P_s)(1-P/P_s + bP/P_s)} \qquad (2\text{-}1)$$

P/P_s = the partial pressure inlet over the saturation vapor pressure
b = a temperature dependent equilibrium constant
$= b_o \exp(-\Delta H/RT)$
b_o = the nature of a frequency factor
ΔH = the heat of adsorption
R = ideal gas constant
T = temperature

Q_o = a temperature-independent constant which is supposed to represent a fixed number of surface sites

q = equilibrium adsorbed amount on the adsorbent.

This equation is not unit specific; however, one must make sure that they are consistent. They assumed that each of the molecules in the first layer adsorbed provided one site for the second and subsequent layers. As this secondary layer is filled the molecules are assumed to behave as a saturated liquid. This assumption is only valid while the equilibrium constant for the first layer of molecules is in contact with the surface of the adsorbent. In addition to assuming this type of adsorbate/adsorbent behavior, the expression has been found to be limited by p/p_s values. The p/p_s is the partial pressure of the contaminant over the saturation vapor pressure of the saturated liquid sorbate at the relevant temperature. For physical adsorption isotherms the range for which the equation is valid is from $0.35< p/p_s <0.5$.[22] This is a narrow range and should be considered when evaluating the system.

2.6.3.3.2 Langmuir

The second traditional approach which may be used to model isotherms is the Langmuir model. It was originally developed to represent chemisorption on a set of distinct localized adsorption sites. There are five assumptions which were used in the derivation of the Langmuir adsorption isotherm: "1-the adsorbed gas behaves ideally in the vapor phase; 2-the adsorption gas is confined to a monomolecular layer; 3-the surface is homogeneous, that is, the affinity of each binding site for gas molecules is the same; 4-there is no lateral interaction between adsorbate molecules; and 5-the adsorbed gas molecules are localized, that is, they do not move around on the surface."[22] The Langmuir equation is as follows:

$$q = \frac{Q_o bC}{1 + bC} \qquad (2\text{-}2)$$

Where C is the equilibrium concentration.

2.6.3.3.3 Freundlich

The final classical description of isotherms is based on the Freundlich relationship. There are two assumptions which are required for the system to be represented by this type of equilibrium relationship. The first is that there is no association or dissociation of the molecules after they are adsorbed on the surface. The second is that there is no chemisorption occurring in the system. This means the Freundlich equation is only valid for a purely physical adsorption process. This model may be developed for heterogeneous surface and assumes that each sites obeys the Langmuir equation.

The Freundlich equation does have limitations. The most important is the amount adsorbed increases infinitely with increasing concentration or pressure. This limitation causes the system to become inaccurate for high concentrations due to the over prediction of adsorbent coverage. At low concentrations the isotherm equation breaks down and will not reduce to a linear form. This leaves the middle concentration range for representation by the Freundlich equation. Noll states that "in general, a large number of the experimental results in the filed of van der Waals adsorption can be expressed by means of the Freundlich equation in the middle concentration range."[22]

Cooper and Alley in their text Air Pollution Control A Design Approach derive the Freundlich isotherm equation from the Langmuir equation. They then utilize this equation to represent the isotherm and show that it can be the best model for representing adsorption of organics on activated carbon.[23]

This is further confirmed by Kirk and Othmer in their statement "the isotherm for some systems, notably hydrocarbons on activated carbon, conform more closely to the Freundlich equation."[2]

Since this adsorption isotherm is commonly used to represent systems, ASTM has developed a standard definition. In ASTM D 2652-76, the Freundlich adsorption isotherm is defined as "a logarithmic plot of quantity of component adsorbed per unit of adsorbent verses concentration of that component at equilibrium and at constant temperature, which approximates the straight line postulated by the Freundlich adsorption equation:

$$\frac{x}{m} = kC^n \qquad (2\text{-}3)$$

x = ref quantity adsorbed,
m = quantity of adsorbent,
C = concentration,
k and n = constants."

This equation may also be expressed as:

$$C_e = \alpha\ (X_{sat})^{\beta} \qquad (2\text{-}4)$$

C_e = equilibrium concentration, $(1/k)^{1/n}(x/m)^{1/n}$
X_{sat} = weight of adsorbate/weight of adsorbent, x/m
α, β = constants, $(1/k)^{1/n}$ and 1/n, respectively. Note that α has units of concentration and β is a pure number.

These traditional equations have acted as a stepping stone for the development of other mathematical, empirical and statistical methods to characterize adsorption. Section VII addresses some of the new literature and associated research in the field of adsorption. This information is only a representive sample of the vast amount of research which has been done in the area of adsorption.

2.7 Modeling the Adsorption Mass Transfer Process

2.7.1 Introduction to theories

Covering all of the existing adsorption theories is beyond the scope of this thesis; therefore, an attempt has been made to present a representative sample of commonly used theory as a basis for the research effort. Adsorption theory has been identified as a mass transfer process since the turn of the century. Authors have many variations on the constants and other factors which influence the system but agree on the basic mass transfer operation; however, the three basic equations explained in the previous section act as a starting place for the development of most adsorption theories. It is important to remember that the majority of these theories are based on mass balances and mass transfer behavior for a specific adsorbent and adsorbate.

In the 1920's, Bohart and Adams developed their adsorption theory. This was followed by Mecklenburg's theory based on gas mask filtration. Later, Klotz modified the Mecklenburg theory to produce his own representation of the adsorption process. Other theories have been developed by Danby et al., Sille'n, Wheeler and Robell, Van Dongen and Stamperius, Nelson and Correia, and one based on statistical moments developed by Grubner.[16] Jonas and his coworkers have taken several of these approaches and developed their own explanation for specific adsorption processes. Dubinin and his co-workers have contributed to the analysis of adsorption and characterization of activated carbon by developing much of the "state-of-the-art" theory. Dubinin-Polanyi developed a relationship to calculate the mean capacity of microporous carbons adsorption.[20] Dubinin and Radushkevich developed a linear plot showing that micropore systems are not homogenous as previously thought.[24,25] Although all of these theories are applicable to varying extents, a theory following some of

Jonas' work has been selected to be used for modeling purposes. This theory is developed and discussed in the Theoretical Development Chapter 3.

2.7.2 Research Applications

Although a large amount of research has been conducted on the use of activated carbon as an adsorbent, much less has been reported on its characterization in thin beds. However, the term "thin bed" is vague and one may argue that there should be a comparison of the critical bed depth to actual bed depth as the descriptive parameter for an experimental situation. Even though there seems to be a small amount of information which is directly applicable to thin bed experiments, this section outlines some experiments which may provide useful information in their characterization.

David W. Jones and Peter Watts in their article "Kinetics of Vapor Sorption by Latex-Bonded Carbon Particles"[26], describe a system which is very similar to this thesis research. The adsorbate was isopropyl methylphosphonofluoridate vapor (IMPF) in concentrations ranging from 933 to 1,255 ppm. The adsorbent was a powdered activated carbon with a BET surface area of 1,500 m^2/g. In the experiment two different acrylic latex binders were used to attach the activated carbon to a fabric. The test conditions were performed under a linear flow velocity of 10.6 mm/s which converts to approximately 0.2 lpm when run through a 20 mm sample of the material. The outlet concentration was continuously monitored using a flame ionization detector. All of the "sorption" tests were performed at 30 °C.

The results of the testing were used to compare with a theoretical model which was developed for the system. The model was based on a Langmuir isotherm and used a continuous-feed stirred tank reactor to simulate the concentration distribution of the adsorbate as it was distributed in the

material. Before the breakthrough tests were performed, the "sorption" capacities of each of the individual materials were determined. For the activated carbon, "M_c, the mass of adsorbate taken up by the carbon when in equilibrium with the surrounding vapor concentration", was 0.32 g/g at 196 ppm (1,120 mg/m^3) and 0.58 g/g at 1,173 ppm (6,700 mg/m^3). The fabric and the latex did not adsorb any significant amount of the adsorbate and for the latex films a diffusion and permeability coefficient were determined.[26]

Combinations of the materials were evaluated in breakthrough testing. The ranges for complete breakthrough curves or adsorption capacity curves was 17 to 40 minutes. If the breakthrough is defined as 1 percent, as in the other literature, the breakthrough times ranged from instantaneous to 2 minutes. The experimental data was then compared to the results of the mathematical model that was based on a continuous stir feed reactor. The modelled and experimental results agreed very well.[26]

The system inputs and procedures used in this thesis research were very similar to those of Jones and Watts. However, one major difference between the two is that Jones and Watts required the adsorbate to penetrate the latex binder film before adsorption could take place. This requires diffusion to occur and it becomes the rate limiting step. The flow velocity was 1/5 that of the study performed in this thesis research and explains part of the reason the system did not breakthrough instantaneously in all cases.

Other experiments related to thin beds of carbon material were aimed at creating a material with specific characteristics. There were no actual adsorption tests performed on the materials. Since there is a limit to the "thin bed" research, one turns to research which has be performed on more conventional bed depths. Industrial hygienists have performed indepth studies on activated carbon canisters for gas masks. This research deals with the factors

of relative humidity, flow rate, breakthrough time and critical bed depth. Jonas and Rehrmann[20] developed a kinetic equation for the adsorption of benzene at various flow rates. They show that increasing the flow rate causes a decrease in both the breakthrough time and adsorption capacity for a fixed amount of activated carbon.

Nelson and Harder detailed the effect of the two flow conditions on breakthrough times. They made the generalized statement "cartridge life is inversely proportional to flowrate." In their experiment the flow ranged from 14 to 71.4 lpm utilizing a constant concentration of 1,000 ppm. The results of the study showed that if the flowrate is doubled, the breakthrough time will be halved with no significant difference being observed between pulsating and steady-state flow patterns.[14]

A third study performed by Ackley, followed the work of Jonas and determined that a respirator sorbent bed can be "overwhelmed" by excessive concentration and airflow rate. Figure 2-9 illustrates the effect of bed depth and superficial air flow velocities on breakthrough time. These results agreed with those of Nelson and Harder. It is important to realize the test is for sulfur dioxide and ASC I activated carbon; therefore, one cannot apply the information on the breakthrough times directly to other experimental situations.[17]

From these three studies it is clear that the flowrate directly effects the bed depth. This relationship was the motivation for Rehrmann and Jonas[27] to develop a plugged flow model to calculate the residence time to calculate critical bed depth. The adsorbent was a granular activated carbon provided by Pittsburgh Activated Carbon Co. mesh size 12-80 with a surface area of 1,000 m^2/g. The adsorbate was 96.5 percent pure dimethyl methylphosphonate (DMMP). In this representation, the bed is composed of many carbon granule layers. The thickness of a layer was limited to the diameter of a carbon granule, a mean time of travel through each layer

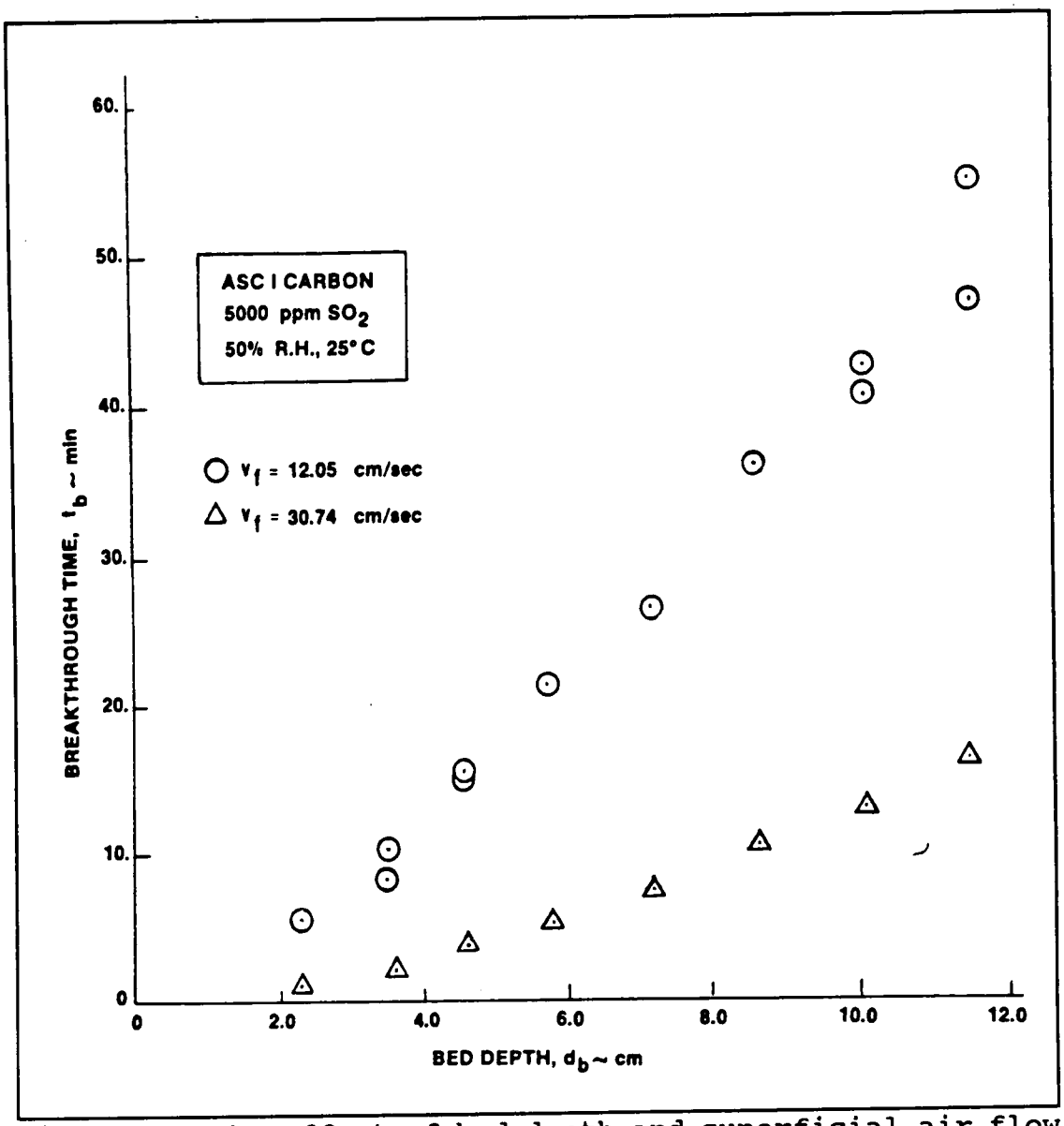


Figure 2-9 The effect of bed depth and superficial air flow velocity on breakthrough time.

can be calculated from the residence time of the vapor in the bed. As one can see the depth of the bed becomes dependent on the size of the activated carbon particles and the pores. The authors conclude with the statement that "...the smaller the carbon granules packed in a bed of fixed carbon weight the larger will be the number of pore mouths per unit bed area orthogonal to the flow of gas molecules."[27]

Another interesting result of this study was as the

volumetric flow rate was varied from 0.1 lpm to 3 lpm the critical weight of carbon changed from 0.0439 g to 0.3368 g with the adsorption capacity remaining constant. There were no tests at the 1 lpm condition but at 0.9 lpm and 1.2 lpm the critical bed weights were 0.148 and 0.183 g, respectively. The relationship shows the effect that flow has on the amount of adsorbent required in the bed.

This is further supported by another experiment reported by Jonas[20] that evaluated the effects of sorbent weight on breakthrough time. This study showed a linear relationship between gas breakthrough time and sorbent weight. Jonas et. al. modified the Wheeler equation to represent this breakthrough adsorbent weight relationship.

As discussed in the adsorbate section, concentration and type of vapor both influence the adsorption process. Nelson and Harder studied the effects of 131 different solvent vapors at a constant concentration of 1,000 ppm. A breakthrough curve was developed for each of the solvents. The experimenters concluded that "the service life cannot be attributed to a single solvent vapor property, but is a complex function of the nature of the solvent vapor and the adsorbing media as well as experimental conditions". They also confirmed the concept that the less volatile material are adsorbed to a greater degree than those with low boiling.[14] This information can be applied directly to the thin bed application since this relationship between an adsorbate and adsorbent is based on chemical characteristics. They followed this study with an experiment studying the effects of concentration. Finding that as concentration increased the adsorption capacity increased and the breakthrough time decreased. In this experiment the authors chose to represent breakthrough with a Freundlich type equation.

The results of the experiment showed that if the breakthrough percent was defined as 10 percent an average value for b was -0.67. This value for b seemed to be

independent of flow conditions; however, it was altered by relative humidity. Concentration influenced the performance of the respirator filters and resulted in a relationship where if concentration is reduced by a factor of 10, the service life was extended by a factor of 4 or 5. The Mecklenburg equation was used to calculate breakthrough times and agreed with experimental values below 20 percent breakthrough. There was no satisfactory method found to predict the entire breakthrough curve and effects of the relative humidity on the curve.[28]

The research on thick bed adsorption systems allows one to anticipate in part the behavior of a thin bed system. One of the most important concepts in comparing research related to the beds of adsorbents is the critical bed depth. Once determined it must be put into perspective with the actual width of the bed to allow for a relative comparison. By comparing the ratio of the critical bed depth over actual bed depth one may gain insight to the development of the adsorption zone and how the system will reach breakthrough and capacity.

CHAPTER 3

THEORETICAL DEVELOPMENT

The design of a theoretical model for this adsorption systems is based on the concept of knowing how much adsorbent is required to keep the adsorbate from breaking through the system at a specific point in time. In order to model, one must evaluate the quantity and thickness of adsorbent, concentration and type of adsorbate, and time to breakthrough. These parameters are represented by the mass balance equations developed in the text AIR POLLUTION ITS ORIGIN AND CONTROL by Wark and Warner.[29]

There are several assumptions which are made in order to develop this theory. Most significant is that the adsorbent / adsorbate isotherm is Freundlich in nature. Next, that the adsorbate and adsorbent are at equilibrium at the trailing edge of the mass transfer zone. Third, the constants in the Freundlich equation are developed based on experimental data for the specific adsorbent/adsorbate. An additional assumption is required for the development of the width of the mass transfer zone. If the pollutant concentration is sufficiently low then the mass flowrate of the carrier gas is approximately equal to the mass flowrate of the carrier gas and pollutant. Finally, the equation for the breakthrough time, requires one to assume that the mass transfer zone is fully establish at time equal zero. This latter assumption maybe a reasonable approximation for thick beds, however may not be true for thin beds as will be discussed later.

The development of the adsorption wave velocity is based on a simple mass balance between the inlet and the outlet of the adsorption system. The points which describe the inlet and outlet are functions of the concentration and represent the equilibrium point and the breakthrough point, respectively.

Equation 3-1 represents the basic mass balance for the system.

$$(m_g C_1)/\varrho_g = m_{ad} X_1 = \varrho_{ad} A V_{ad} X_{sat} \qquad (3\text{-}1)$$

For this equation the variables are defined as follows:

m_g = the mass flow rate of the gas phase entering
m_{ad} = the mass flow rate of the gas phase leaving
ϱ_g = the gas phase density
ϱ_{ad} = the apparent density of the granular bed
A = the cross-sectional area of the bed
V_{ad} = the velocity of the adsorption wave
C_1 = the gas-phase concentration of the pollutant (expressed as mass of pollutant/mass of adsorbent)
X_{sat} = the solid-phase concentration (expressed as mass of pollutant/mass of adsorbent)
X_1 = the solid-phase concentration (expressed as mass of pollutant/mass of adsorbent)
L = the total bed depth

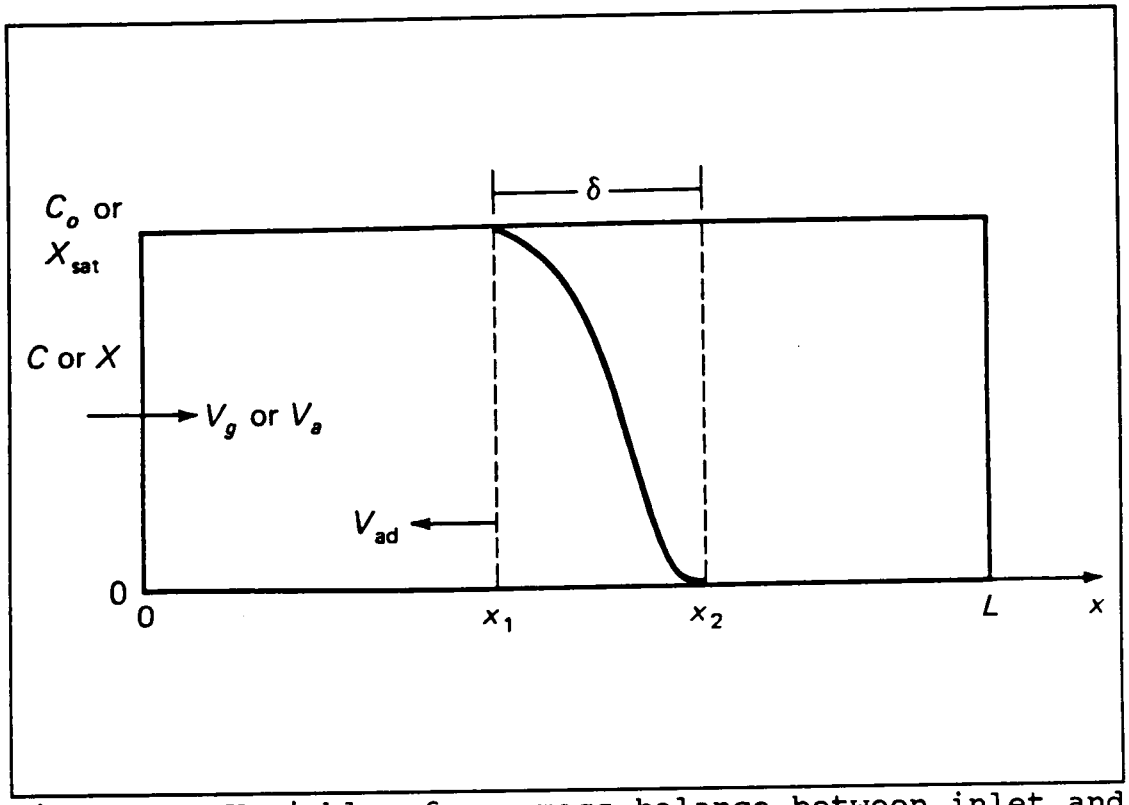


Figure 3-1 Variables for a mass balance between inlet and outlet of a thick bed adsorber.

As presented in section 3.6.3.3.3 of the Literature

Review, the Freundlich equation is a good approximation for the behavior of an organic compound adsorbed into an activated carbon. Equation 4-2 is the form which Wark and Warner use to develop their adsorption model. This equation is based on the equilibrium concentration for both the gas and solid phase.

$$C_e = \alpha (X_{sat})^{\beta} \qquad (3\text{-}2)$$

In this equation the variables are equal to:

C_e = gas phase equilibrium concentration
α = experimental constant with concentration units
β = constant based on experiment (pure number)
X_{sat} = equilibrium mass adsorbed (g/g).

Assuming that the trailing edge of the adsorption wave is at equilibrium one can conclude that at position 1 in Figure 3-1, $C_e = C_o = C_1$ and $X_1 = X_{sat}$. By making this assumption the two equations can be combined and solved for the adsorption wave velocity V_{ad}. Equation 3-3 is the expression for the adsorption wave velocity.

$$V_{ad} = \frac{V_g}{\varrho_{ad}} (\alpha)^{1/\beta} (C_o)^{(\beta-1)/\beta} \qquad (3\text{-}3)$$

In this equation V_g is the superficial velocity of the carrier gas. The adsorption wave velocity is important since it describes the movement of the adsorbate through the adsorbent. That information is used in turn to define the thickness of the mass transfer zone and the time to breakthrough for a given adsorber thickness.

The thickness of the mass transfer zone is based on two different mass transfer equations. Both equations describe the differential rate of mass transfer of the adsorbate gas onto the solid phase, dm_p. Equation 3-4 is based on developing a relationship between C and x in the adsorption zone. In this

equation dC is the differential change in concentration for some incremental distance dx.

$$dm_p = \frac{m_g}{\varrho_g} dC \qquad (3\text{-}4)$$

Equation 3-5 is the second representation of dm_p. In this equation the mass transfer rate depends on the volume of the adsorption bed, the mass flow rate, adsorbate concentration and a film transfer coefficient. This equation is:

$$dm_p = KA(C - C_e)dx \qquad (3\text{-}5)$$

where K = a film resistance coefficient. This film coefficient is defined by Jonas et.al (refer to Literature Review).
By combining these equation 3-4 and 3-5 and integrating between x_1 and x_2, an equation is developed to describe the position and width of the mass transfer zone (i.e. adsorption wave). The width of the mass transfer zone is called delta, δ, and is the resultant of $x_2 - x_1$.

The equation 3-6 describes the position in the adsorption zone as dependent on some concentration limits. For this development of the theory and model application, the limits placed on the system are from 1 percent to 99 percent of the inlet concentration. These limits can be adjusted by replacing the 0.99 values in equation 3-6 with the desired percent of the inlet concentration value. For example, if one was interested in defining breakthrough as 10 percent of the inlet concentration the 0.99 values are replaced with 0.90. On the other hand if one was interested in a more stringent breakthrough the 0.99 value can be replaced with 0.999. This allows for the breakthrough criteria to be set to 0.1 percent. It is important to remember that the curve is assumed to be symmetrical therefore the limits but be consistent with that

symmetry. The value of x is described as any position in the adsorption bed.

$$x = x_1 + \frac{m_a}{KA\varrho_g}\left[\ln 0.99\frac{C_o}{C} + \frac{1}{\beta-1}\ln\frac{1-(C/C_o)^{\beta-1}}{1-(0.99)^{\beta-1}}\right] \qquad (3\text{-}6)$$

Equations 3-1 - 3-6 are useful in providing a dynamic description of an adsorption system. However, when one is designing a system the time to breakthrough is the most important criteria. Equation 3-7 defines the breakthrough time, t_b:

$$t_b = \frac{L - \delta}{V_{ad}} \qquad (3\text{-}7)$$

In this equation one recognizes the importance of the velocity of the adsorption wave and width of the mass transfer zone. The variable L in the equation is equal to the thickness of the adsorbent bed. This equation defines the breakthrough time and is a function of equations 3-3 and 3-6. As discussed in the literature review this parameter is very important to the design of adsorption systems because it allows the designer to predict the time at which the pollutant breakthrough the bed.

A computer program was written in "Basic" to solve for the breakthrough time, the adsorption wave velocity, the width of delta, the concentration breakthrough curve profile and the incremental mass adsorbed. The solution required stepping through concentrations from 0.01 to 0.99 C/C_o. The computer code is found in Appendix A-2.

CHAPTER 4

EXPERIMENTAL METHOD

4.1 Test Materials

4.1.1 Description of untreated materials

The initial polymers considered as candidates for the MB material were nylon (N), polyethylene (PE), polyester (PET), and polypropylene (PP). Initial trial tests showed that powdered carbon did not stick to MB webs of N. PET and PP webs retained the carbon but, not as well as PE. Therefore, PE was selected as the polymer for the MB material. A 0.033 kg/m^2 PE MB web with an average fiber diameter of 7.53 $\pm$ 1.52 micrometers and a permeability of 77.9 cfm/ft^2 was used throughout the study.

PP was selected as the polymer for the spunbond (SB) material used on the calendared laminates due to process limitations at The University of Tennessee. A 0.00075 kg/m^2 PP SB nonwoven material was used on either side of the activated carbon-loaded MB material for strength. The SB web had an average fiber diameter of 30.88 $\pm$ 0.31 micrometers, and a permeability of 173.8 cfm/ft^2. The characteristics of the MB and SB webs are included in Table 4-1.

The fiber diameters were determined by Scanning Electron Microscope (SEM) analysis. Samples of the MB and SB materials were sputter coated for two minute with gold using a Technics Hummer II (Alexandria, VA). The temperature rise during sputter coating was less than 10°C/min. Silver paint was used to ground the edges of the material to the stub to reduce charging during SEM evaluation. Three photomicrographs of each type of material were taken using an ETEC Auto-scan SEM (Hayward, CA). A line was drawn on the photomicrograph from

Table 4-1. Laminate characteristics.

LAMINATE	AIR PERMEABILITY (CFM/FT^2)	LAMINATE WEIGHT (KG)	CARBON LOADING (KG/M^2)	THICKNESS (M)
RAW MELT BLOWN	492.2	0.00016	NA	0.00004
RAW SPUNBOND	1182.38	0.00003	NA	0.00002
HSA NON-CALENDERED				
NG4-40	60.4	0.0022	0.039	0.0017
NG5-40	64.5	0.0024	0.026	0.0012
NG6-40	58	0.0022	0.039	0.0015
NG7-80	26.9	0.0041	0.072	0.0023
NG8-80	26.9	0.0038	0.085	0.0014
NG9-80	47.9	0.0042	0.078	0.0017
NG10-120	34.8	0.0039	0.091	0.0020
NG11-120	14.8	0.0046	0.104	0.0021
NG12-120	31.9	0.0052	0.144	0.0021
HSA CALENDERED				
C1A40	19.4	0.0035	0.04	0.0013
C2A40	14.2	0.0035	0.04	0.0013
C3A40	68.7	0.0037	0.04	0.0020
C4A80	11.9	0.0043	0.08	0.0013
C5A80	4.98	0.0050	0.08	0.0012
C6A80	8.16	0.0048	0.08	0.0013
C7A120	4.98	0.0052	0.12	0.0013
C8A120	3.42	0.0054	0.12	0.0012
C9A120	7.23	0.0049	0.12	0.0013
STD NON-CALENDERED				
NG13F40	140	0.0024	0.039	0.0008
NG14F40	149	0.0026	0.052	0.0010
NG15F40	153	0.0024	0.039	0.0010
NG16F80	117	0.0038	0.091	0.0013
NG17F80	89.9	0.0044	0.13	0.0022
NG18F80	104	0.0043	0.124	0.0014
STD CALENDERED				
C10F120	15.8	0.0079	0.120	0.0013
C11F120	9.79	0.0077	0.12	0.0014

opposite corners resulting in a large "X". Fiber diameters of fibers that the "X" intersected were measured. The average fiber diameter was determined.

4.1.2 Treatment of materials

4.1.2.1 Application of carbons

The activated carbon was applied to the MB material in an apparatus which utilized a fluidized bed spray. The carbon was entrained within the fluidized bed and then sprayed on to the MB web. It was necessary to layer the MB material in order to retain the desired amount of activated carbon per unit area of web. The nominal loadings of activated carbon were 40, 80 and 120 g/m^2 of web. The webs were weighed gravimetrically to determine the approximate amount of activated carbon applied. Approximately 1 layer of MB web was required for each 40 g/m^2 of activated carbon applied. After application of the carbon to the MB PE web(s), the web(s) were then sandwiched between two MB PE webs (in the case of the non-calendared samples) or between two SB PP webs (in the case of the calendared samples). The physical characteristics of the laminates are summarized in Table 4-1. In general, samples were prepared in triplicate for each activated carbon loading as shown in the table.

4.1.2.2 Measurement techniques

A thickness gage as specified in Fed. Std. No. 191 Method 5030.2 and ASTM D 1777-64 (Reapproved 1975) was used to determine the thickness of the final laminated samples.

A High Pressure Differential Air Permeability Machine manufactured by the Frazier Precision Instruments Company (Gaithersburg, MD) was used to determine the permeability of the final laminates, measured in cfm/ft^2 at 0.5 inches of

water according to the ASTM Test Method D737-75 (Reapproved 1980): Standard Test Method for Air Permeability of Textile Fabrics.

A Mettler analytical balance, as specified by ASTM Test Method D3776-85, was used to determine the weight per unit area of the webs, laminates and activated carbon loadings. In addition, a weighing procedure was developed to double check the quantities of challenge gas adsorbed by the activated carbon loaded laminates during testing. This included weighing the filters before and after testing.

4.1.2.3 Calendering of samples

A set of the carbon loaded laminates was thermally calendared using a one-meter wide Kuester calender. The laminates were processed at 91°C (195°F) at 8.6 m/min between a smooth and 15 percent pattern surface area roll at a nip pressure of 385 pounds/linear inch in an effort to provide a stronger material. The characteristics of these materials are also presented in Table 4-1. Figure 4-1 and 4-2 are photographs of the calendered and non-calendered laminates.

4.2 Test Carbons

Three different activated carbons were analyzed with the Micromeretics ASAP 2000 automated surface area and pore size analyzer. Two samples of each of the carbons were analyzed to determine variability and to calculated the BET surface area, pore area and pore volume analyses. The system operates by degassing the sample, then develops an adsorption isotherm for nitrogen at incremental partial pressures and constant temperature. Once the adsorption phase of the analysis is complete the system desorbs the nitrogen and records the results automatically. Both the adsorption and desorption isotherms are used to determine the surface area, pore size,

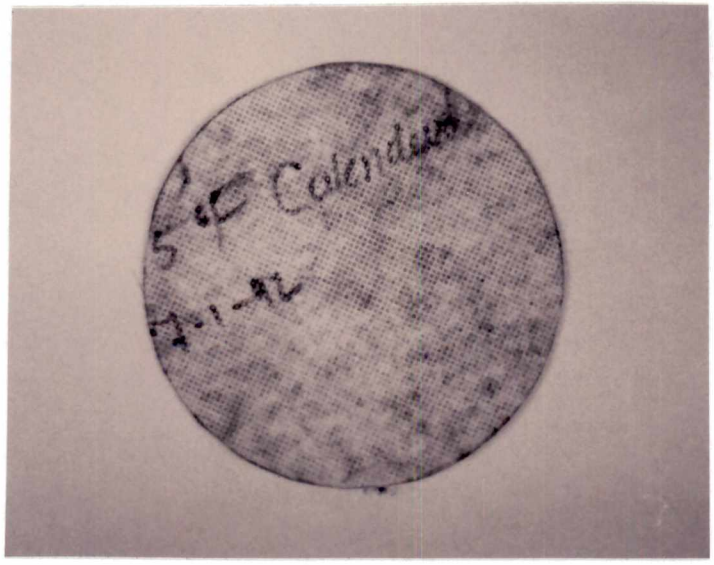


Figure 4-1 Photograph of calendered laminate.

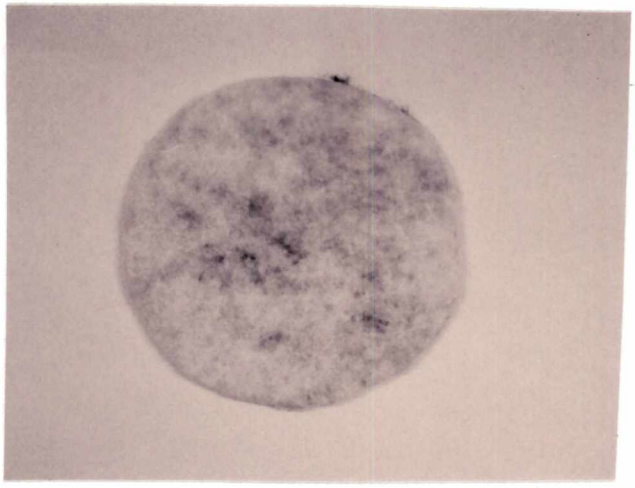


Figure 4-2 Photograph of non-calendered laminate.

pore area and pore volume.

Due to the application procedure for the activated carbon only the two types of powdered activated carbon were used in the laminates. The first was a high surface area activated carbon® (HSA) manufactured by the Kansai Coke and Chemicals Company, Limited, 5 Misono-cho, Amagaski City, Japan 660). The HSA carbon had a pore volume of 0.776 to 0.855 cm^3/g and a surface area of 2,812 m^2/g. The second was a standard 200-mesh activated carbon, referred to herein as STD carbon, obtained from Fisher Scientific (Pittsburgh, PA) with a pore volume of 0.066 to 0.073 cm^3/g and a surface area of 829 m^2/g. The detailed results of the analysis are found in Appendix A-3.

4.3 Test Gas

Trichloroethylene (TCE) was used as the challenge gas adsorbate for all of the tests. The mixture of 1,700 ppm of TCE in Nitrogen was purchased from National Specialty Gases (Durham, NC) and was certified by the vendor using a gas chromatograph. This mixture was used for the breakthrough testing. Three additional concentrations were purchased from the same vendor and certified in the same manner. These three mixtures of 2,125, 829 and 174 ppm were used in conjunction with the 1,700 ppm mixture to develop the adsorption isotherm. Due to availability both laboratory grade nitrogen or laboratory air was used to purge the system after each test.

4.4 Test Apparatus

A bench-scale dynamic adsorption system was constructed to allow the experimental determination of the ability of the activated carbon loaded media to serve as a protective barrier to specific challenge gases. The experimental set-up utilized a modified Dawson cup filter holder as shown in Figure 4-3.

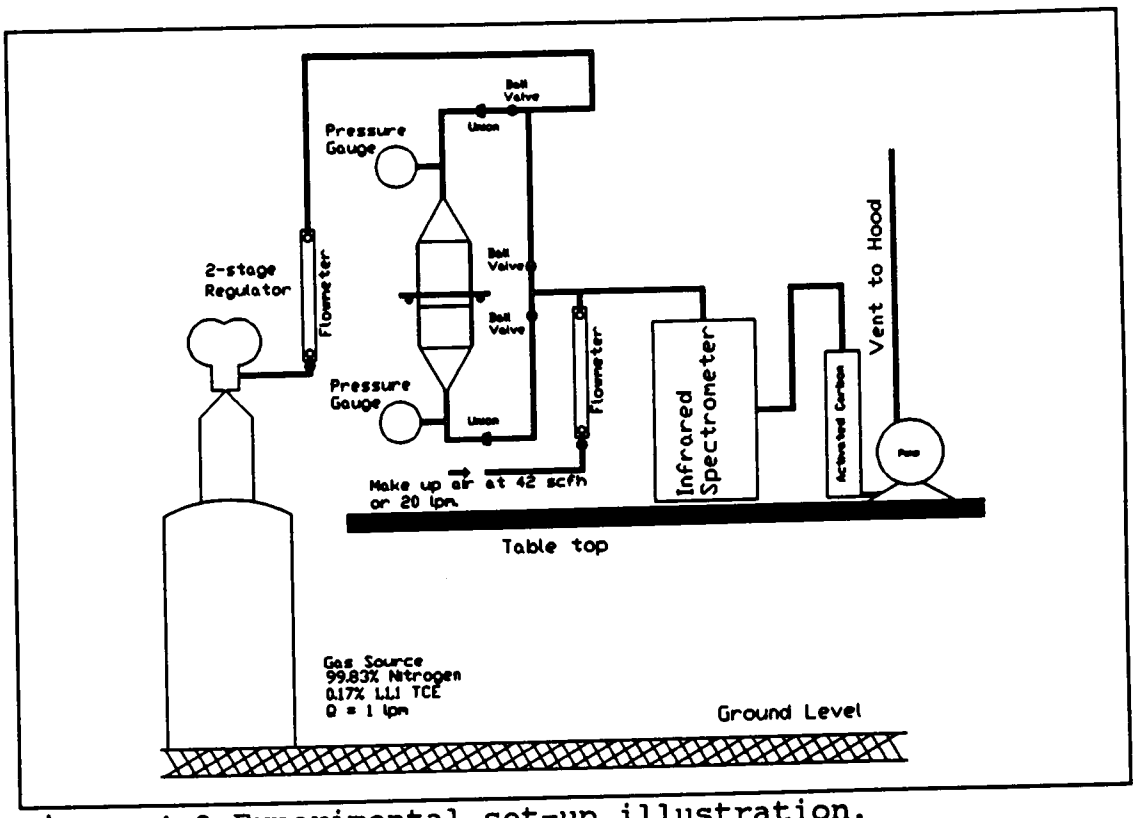


Figure 4-3 Experimental set-up illustration.

The diameter of the laminate exposed to the flow was 0.114 m (4.5 inches) with a filter area of 0.0103 m^2. Nitrogen gas containing a certified concentration of the challenge gas was delivered from a compressed gas tank through a two stage regulator and a rotameter to the filter holder at a constant flowrate of one liter per minute. From the flowmeter the gas passed through a "T" fitting with ball valves in each line. This allowed the operator to by-pass the Dawson cup before or after the dynamic adsorption test and route the gas directly to the challenge gas detector to measure the inlet concentration. During the adsorption test, the gas was passed through the Dawson cup assembly and then to the detector to measure the outlet concentration. In either case, the gas then passed from the detector through a final activated carbon column to capture any challenge gas not adsorbed in the filter. The flow was then vented into a laboratory exhaust hood.

All of the piping, fittings, and the filter holder used in the test assembly were made of stainless steel to ensure that there was no interaction between the test assembly and the challenge gas.

4.5 Detector

A Foxboro MIRAN 1A infrared spectrometer was used to continuously monitor the concentration of the challenge gas. At the beginning of each test the instrument was calibrated by diverting the gas directly to the detector. The detector is a variable wavelength, variable pathlength spectrometer capable of measuring a wide variety of gases which have infrared absorption spectra. The output of the spectrometer is the dimensionless absorption unit (AU) which is converted to parts per million (ppm). The test settings for the MIRAN 1A detector are listed in Table 4-2. Information on the use of the MIRAN 1A and its characteristics can be found in Appendix A-4.

Table 4-2. MIRAN 1A Detector Settings

Characteristic	Detector Setting
Wavelength (microns)	10.7
Path length (meters)	2.25
Function Switch (AUs fullscale)	0.1-1.0
Response Time	1 s
Minimum Detectable Concentration	0.4 ppm

The response of the MIRAN 1A was continuously recorded on a strip chart recorder which was calibrated in ppm and calibrated for 0-1,700 ppm. Once calibrated, the analyzer was shifted between the 0.1 (0-170 ppm) to determine the initial breakthrough of the TCE and to the 1.0 AU scale (0-1,700 ppm) during the later portion of the adsorption test as the concentration exceeded 170 ppm. This same procedure was used

during the adsorption isotherm testing.

4.6 Testing Procedure

The procedure used during the adsorption tests was as follows. The MIRAN detector was allowed to warm up for five minutes prior to testing. The warm up utilized ambient air and allowed the system to come to equilibrium and be zeroed. No difference was found between zeroing the instrument with ambient air or nitrogen.

A system calibration was performed at the beginning of each test run by by-passing the Dawson cup. After completing the calibration, the system was flushed with pure nitrogen gas to purge the detector of the TCE. The challenge gas was then passed through the filter holder containing the activated carbon loaded laminate and the outlet concentration was monitored. The breakthrough time was defined to be the elapsed time between initial contact of the TCE with the laminate and the time at which 1.0 percent of the inlet gas concentration (17 ppm) appeared in the outlet. For tests in which the breakthrough time was the primary parameter of interest, the outlet concentration was monitored and recorded until the outlet concentration was significantly higher than the 1 percent breakthrough concentration. A limited number of adsorption isotherm tests were conducted to monitor the entire breakthrough curve in an effort to determine the total adsorption capacity. At the end of the test, the by-pass valve was again switched to allow the inlet concentration to go directly to the detector, after which the detector calibration was rechecked. The span values obtained before and after the test were averaged to obtain the final calibration value used in the analysis of the breakthrough curves.

The non-calendared and calendared activated carbon loaded laminates which had been prepared with carbon loadings of

nominally 40, 80, and 120 g/m^2 using the HSA and STD carbons were cut to fit the circular filter holder. Each laminate was tested for breakthrough time a minimum of two times. After testing the laminate, it was weighed and then regenerated. Regeneration consisted of placing the laminates in a forced draft oven at 65°C for 24 hours. Air flow was induced by a pump which was external to the oven. All of the laminates were placed through the regeneration step prior to conducting the first adsorption test. This ensured that any gases that may have been adsorbed prior to receipt of the carbons, during construction of the laminates or during the carbon loading procedures were desorbed.

4.7 Data Analysis Process

Fundamental to the data analysis process was the requirement of a continuous monitoring system. The use of the Miran 1A with the output recorded on a strip chart recorder provided a measure of outlet concentration at any time interval desired. The recorder speed was set so that one could easily measure the concentration in 6 second intervals if desired. Due to test duration time and the relatively flat slope of the adsorption wave a 24 second time interval was selected to read concentration values.

Once a test was completed, the average value for each 24 second interval was input into a spreadsheet where a simple mass balance was performed to determine the amount adsorbed at any given interval in time and plot the breakthrough curve. Appendix A-5 details the operations which were used in the spreadsheet analysis of the outlet concentration values. These calculated values of grams of TCE/gram of activated carbon were compared to the gravimetric values which were determined by weighing the laminates before and after each test. This comparison is illustrated in figure 4-4. Although there is some scatter, there is general agreement between the

adsorption values obtained by gravimetric analysis and by integrating the outlet concentration with time. The regression coefficient, R^2, is 0.6.

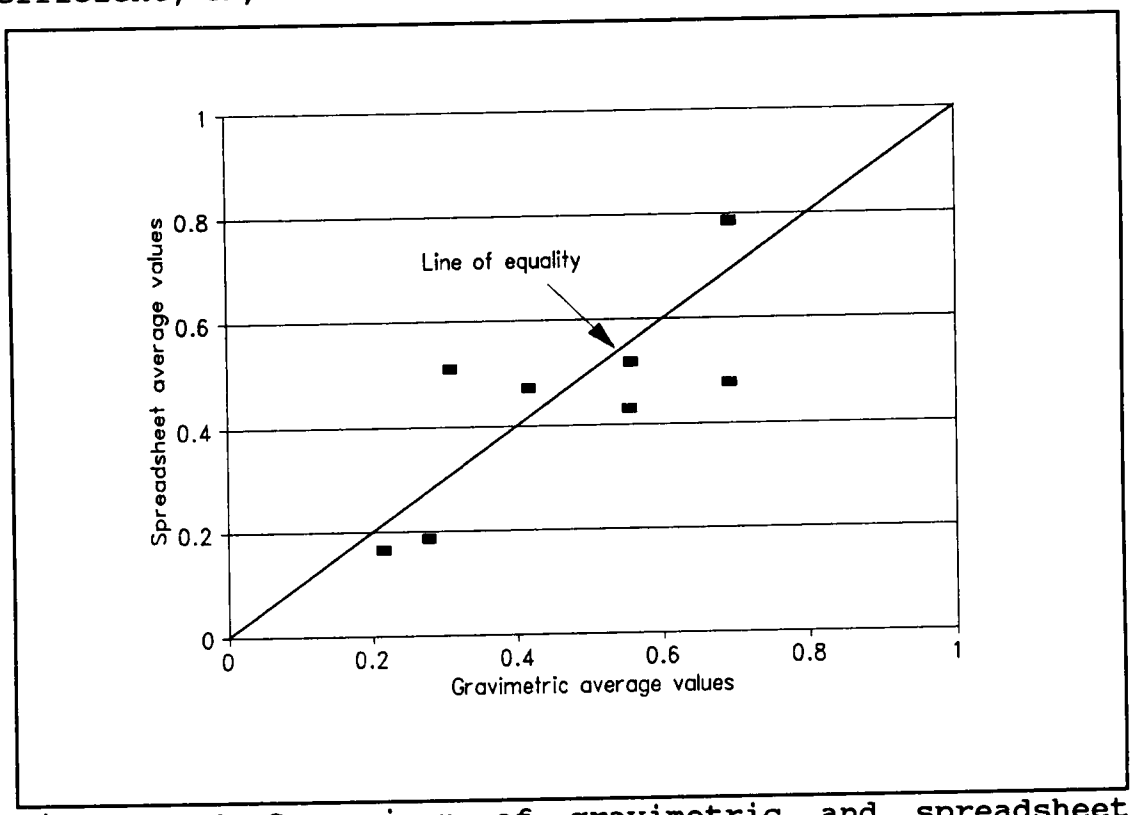


Figure 4-4 Comparison of gravimetric and spreadsheet values.

CHAPTER 5

RESULTS

5.1 Experimental Results

The experimental results include three areas: breakthrough testing, capacity isotherm testing and theoretical modeling. The information gathered from the breakthrough testing and the isotherm testing are used as a basis for comparison in the application of the theoretical thick bed model. This chapter details the experimental results and discusses their significance to adsorption research.

5.1.1 Breakthrough Time Testing

5.1.1.1 Typical Breakthrough Curve

While the primary objective of the testing was to determine the breakthrough time for each of the laminates, it is worthwhile to first present a typical breakthrough curve to illustrate the overall behavior of a laminate during the adsorption test. For comparison purposes, this test was also conducted using the current issue Battle Dress Overgarment liner (BDO). This material consisted of a polyurethane non-woven fabric impregnated with a slurry of latex binder and activated carbon and a 0.0678 kg/m^2 nylon tricot knit that was flame bonded to one side. The material was 0.0023 m thick with approximately 120 g/m^2 of superactivated carbon. The outer layer was a 50/50 nylon/cotton 0.2374 kg/m^2 twill treated with a water repellent finish. The air permeabilities of the BDO was 48 - 53 cfm/ft^2 at 0.5 inches of water.

Figure 5-1 illustrates the overall breakthrough curve obtained for three samples. The two curves which are

represented by squares are for current issue BDO liners. The triangles represent the total breakthrough curve for the experimental laminate NG7-72. These results were obtained using the test assembly and the same test conditions used to test the laminates. The gas concentration was 1,700 ppm of TCE at a flowrate of one liter per minute. Breakthrough was defined as the occurrence of 1 percent of the inlet concentration (17 ppm). The breakthrough point is shown more clearly in the insert found in figure 5-2. Table 5-1 details the times at which each of the samples reached breakthrough. Following breakthrough, a very slow but steady increase in the outlet concentration was observed. Total breakthrough, defined as the point at which the inlet concentration is equal to the outlet concentration, occurred at approximately 2,500 seconds for the current issue BDO liners. The experimental laminate reached total breakthrough at approximately 3,500 seconds. In contrast, thick bed adsorbers typically have breakthrough times on the order of hours or days, and the time between the breakthrough and the total capacity is small relative to the time to breakthrough.

Table 5-1. Characteristic Breakthrough Curve Time and Adsorption Capacity.

Parameter	**BDO-1**	**BDO-2**	**NG7-72**
Carbon Loading, g/m^2	120	120	72
Breakthrough Time, sec	200	350	875
Capacity Time, sec	2500	2500	3500
Breakthrough Adsorbed, g/g	0.0412	0.0711	0.126
Capacity Adsorbed, g/g	0.1726	0.1985	0.265

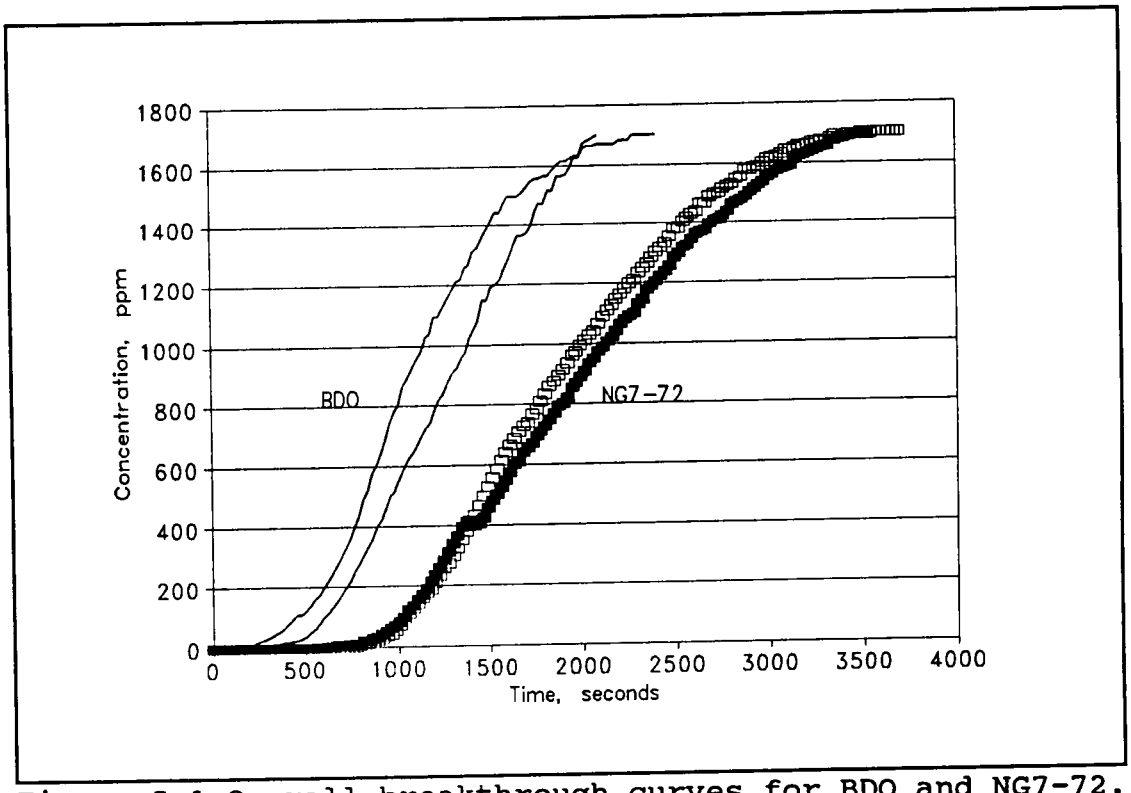


Figure 5-1 Overall breakthrough curves for BDO and NG7-72.

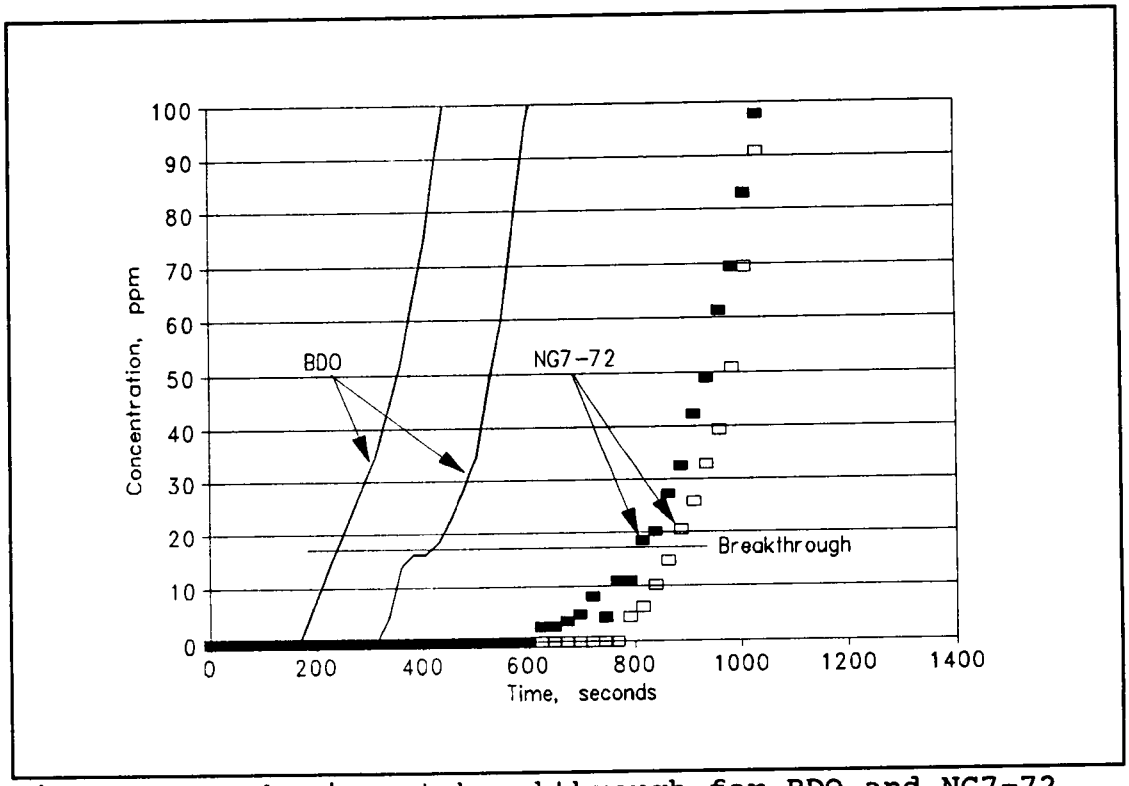


Figure 5-2 Behavior at breakthrough for BDO and NG7-72.

Not only did the time to breakthrough and capacity change, but so did the amount of TCE adsorbed. Table 5-1 details the magnitude of the differences. The experimental laminate was able to adsorb two to three times more than the current issue BDO liner at the point of breakthrough. In addition, the experimental laminate had adsorbed 25 to 35 percent more than the current issue BDO when capacity was reached. The following sections detail the laminate characteristics and their performance effects on breakthrough.

5.1.1.2 Carbon Loading

The carbon loading on the laminates is an important parameter because it directly affects the thickness of the laminate. As the amount of carbon increases the thickness of the laminate increases. The motivation for evaluating the different loadings was to determine how thin of a laminate could be developed and still achieve a reasonable breakthrough time. The capacity was the only criterion which was set forth by the Army; however, the time to breakthrough was also evaluated as described in the experimental methods section.

Figure 5-3 is a graph of the breakthrough time (in seconds) versus the areal density (carbon loading) of the HSA and STD carbons in g/m^2. This figure shows the dependence of the breakthrough time on the amount of carbon present. In the case of the HSA carbon, there was an obvious linear increase in the breakthrough time as the areal density increased, ranging from approximately 400 seconds at the 40 g/m^2 carbon loading to 1,200 seconds for the 120 g/m^2 carbon loading. There was more scatter in the case of the STD carbon; however, the increase was still apparent. The data were evaluated and the lines on the figure are the least squares linear fit of that data. For the HSA carbon the line is $y = 10.0x + 50$ and for the STD carbon the line is $y = 5.9x - 61.6$ with R^2 of 0.7998 and 0.4988 respectively.

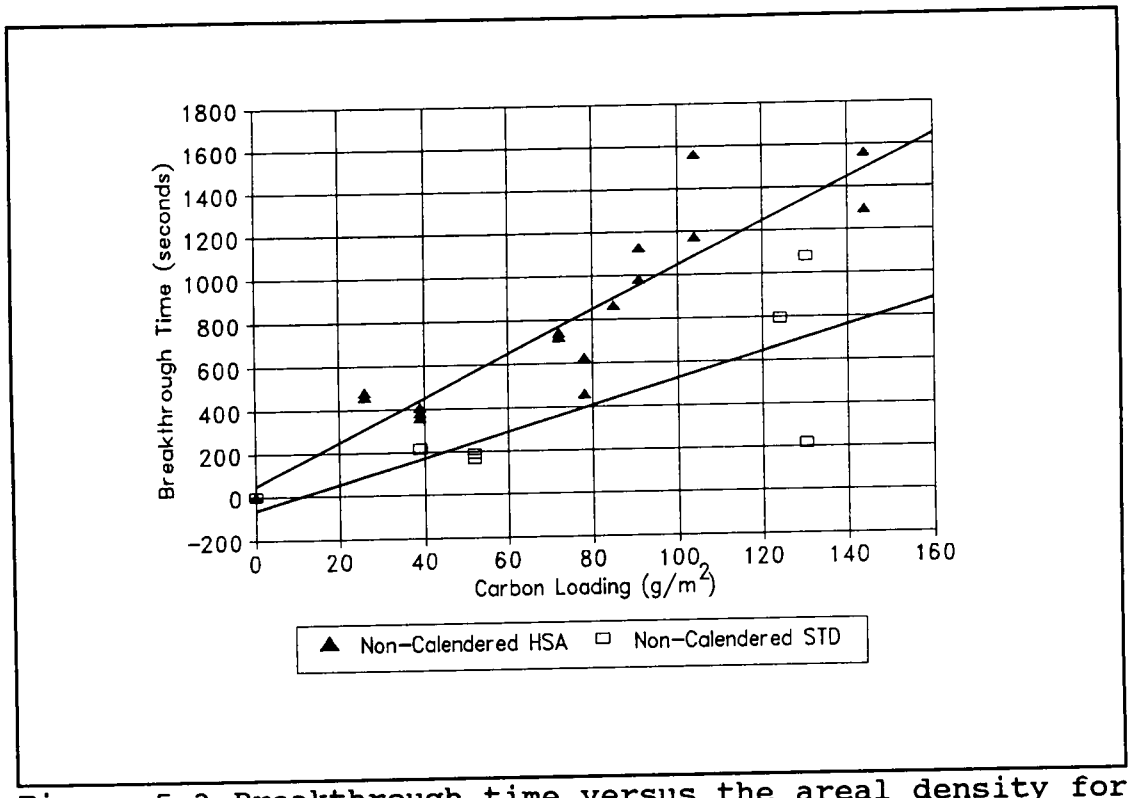


Figure 5-3 Breakthrough time versus the areal density for HSA and STD carbons.

The two lines should intersect at the origin of the graph since there would be no carbon present. One explanation why this did not occur is that the distribution of the filter was not uniform. This non-uniformity is shown by the scatter in the data. A secondary observation is that the upper portion of the scatter may provide a baseline adsorption maximum for each laminate. Then the variation from the maximum condition could be linked to the non-uniformity of the carbon distribution.

5.1.1.3. Different Carbons

The increased breakthrough time for the HSA carbon as compared to the STD carbon is evident, and was expected, since the surface area of the HSA carbon was nearly three times that of the STD carbon. Appendix A-3 provides detailed information on the surface area of the carbons.

The decreases in the breakthrough times and the adsorption capacities of the STD carbon were a combination of several factors. First, surface area of the STD carbon was considerably less that of the HSA carbon. Another factor was the non-uniformity of the larger mesh commercial grade carbon when it was applied to the surface of the MB web. This non-uniform distribution is illustrated in figure 5-4 for laminate number NG13F-40 which shows a photograph of the carbon loaded laminate which was made on a light table. The uneven distribution of the carbon is evident and was observed to be the greatest in those laminates with the lower carbon loadings. The flowrate through the lighter areas will increase due to the increased permeability causing these areas to reach capacity earlier, giving rise to premature breakthrough when compared to more uniformly distributed carbon loadings. In addition, reproducibility of the laminates at a given carbon loading deteriorated. The weight between samples varied and the larger diameter 50-200 mesh commercial carbon particles where loosely held on the surface of the MB web with a tendency for the carbon to shift around on the web. Not only did this cause a problem of inconsistent carbon weights between samples, it also contributed to the variation in the distribution of the carbon on the laminates.

5.1.1.4 Calendered Laminates

The calendering process had a negative effect on the breakthrough time of the laminates. Figure 5-5 shows the results of the tests conducted on the calendered samples for the HSA and STD carbons. The relative behavior of the calendered samples was similar to that for the non-calendered samples in that the HSA carbon was consistently more adsorptive that the STD carbon. The STD carbon samples were only tested at the 120 g/m^2 loading due to the difficulties related to poor coverage of the material. However, it is

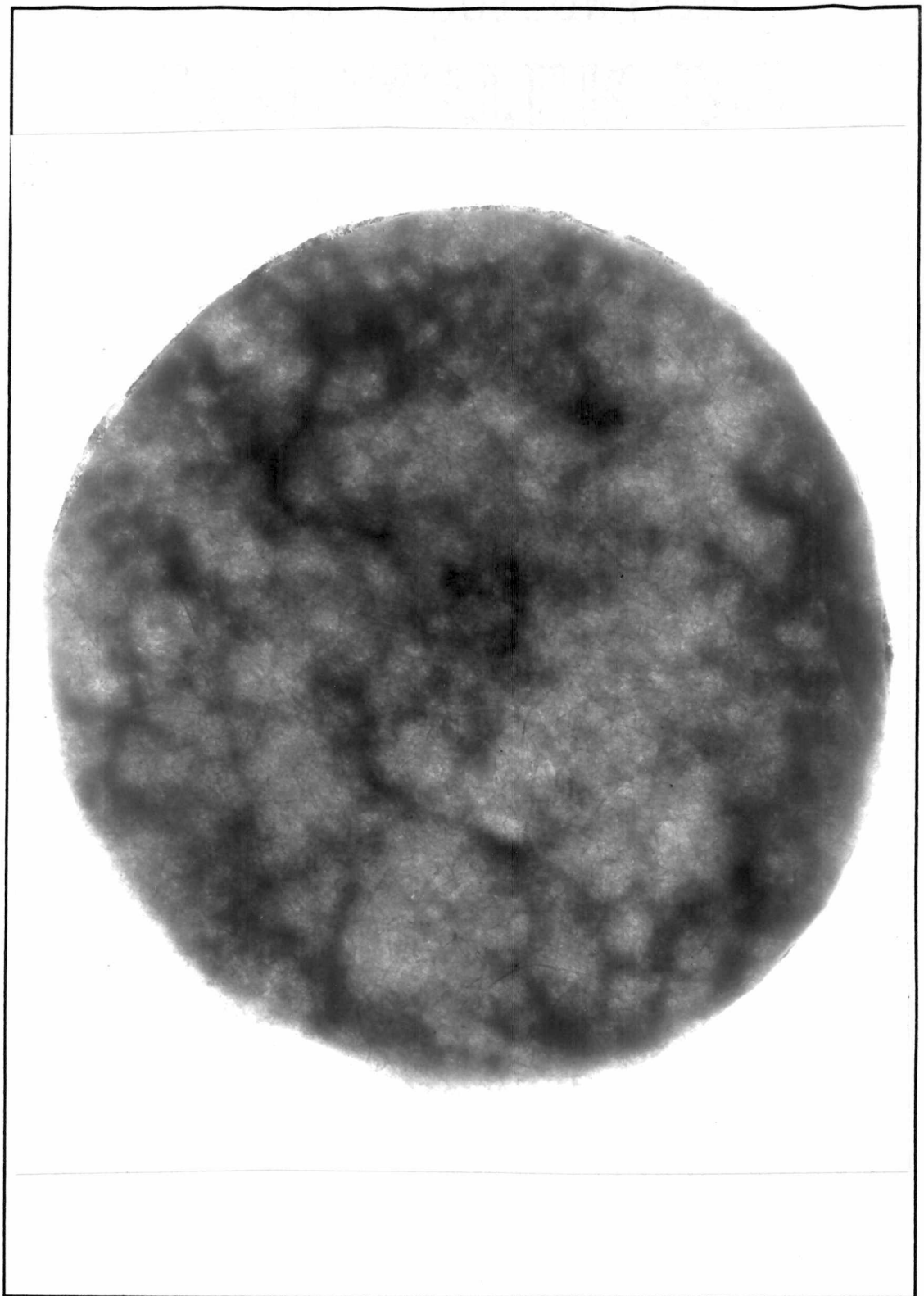


Figure 5-4 Photograph of NG13F-40: poor distribution of STD carbon.

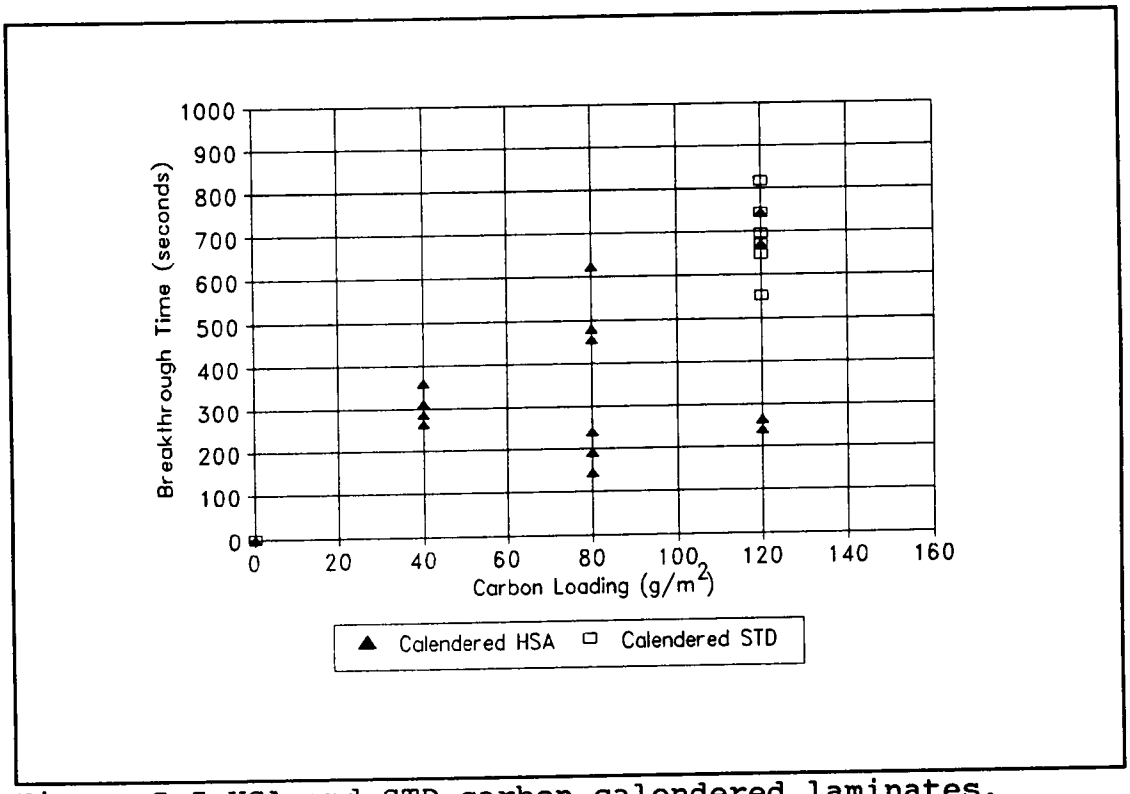


Figure 5-5 HSA and STD carbon calendered laminates.

important to note that the scatter of the data is considerably greater than that of the non-calendered samples and the breakthrough times were significantly less than those for the non-calendered samples. Figure 5-6 compares the breakthrough times for the non-calendered and calendered HSA samples showing that the time to breakthrough for the calendered samples was only about 40 percent of that of the non-calendered laminates.

The decreased breakthrough times and adsorption capacities of the calendered laminates as compared to non-calendered laminates were attributed partially to the 15 percent thermally bonded areas which caused a reduction in the available activated carbon. It is likely that the calendering also partially encapsulated the carbon thus decreasing the available number of adsorption sites. While the calender only produced a 15 percent calendered area, the percentage of fused area was considerably greater as suggested by the decreased

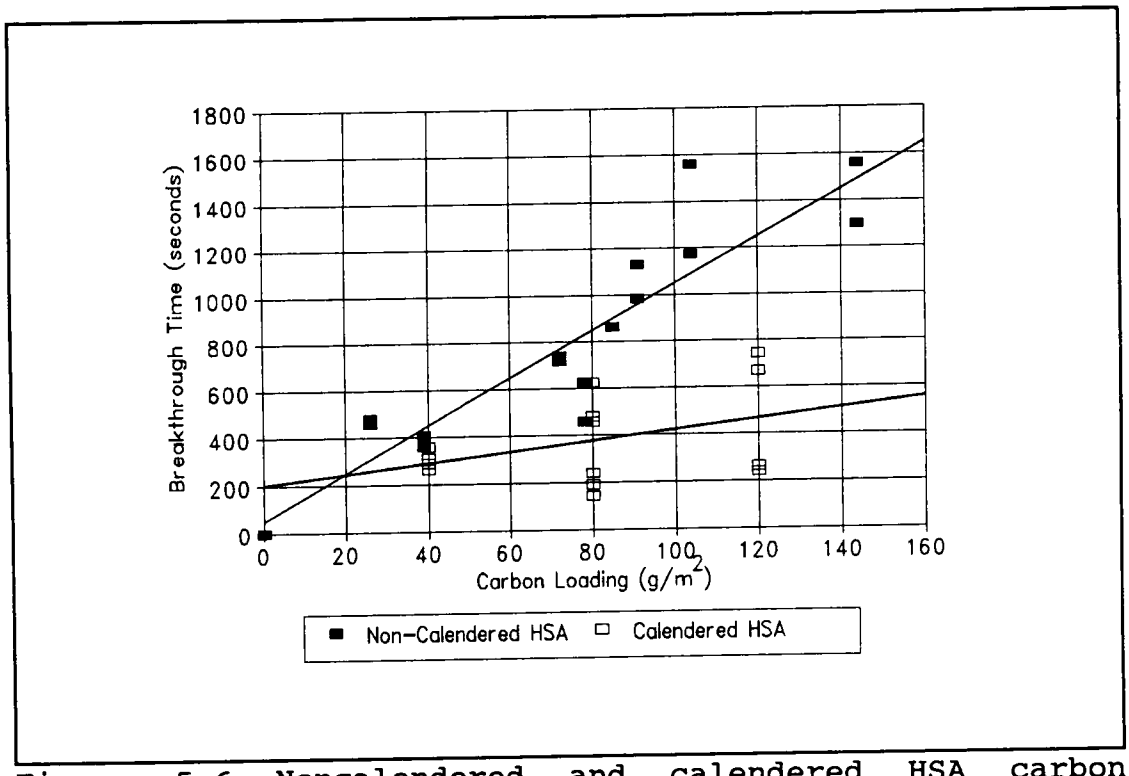


Figure 5-6 Noncalendered and calendered HSA carbon laminates.

air permeability of the calendered samples. Based on the addition of the two layers of the SB web to the MD laminate prior to calendering and the 15 percent loss in area due to calendering, it was estimated that the permeability should have decreased by approximately 40 percent. As shown in table 4-1, the permeabilities of the calendered samples were generally reduced by 50-75 percent.

In addition to evaluating the time, the total adsorption capacity was evaluated. The actual adsorption capacity (g/g) at the time of 1 percent breakthrough, referred to herein as then breakthrough capacity, is shown in figure 5-7 for all of the samples. The non-calendered HSA carbon had an average capacity of 0.172 g/g, whereas the non-calendered STD carbon had a capacity of 0.083 g/g. For the calendered samples the average capacity was 0.0779 g/g for the HSA carbon and 0.0870 g/g for the STD carbon.

5.1.2 Adsorption Isotherm Tests

Modeling of the adsorption system at capacity is advantageous since it allows one to predict, at least for a theoretical thick bed situation, how the adsorbate will behave and the effects of each of the bed characteristics. The modeling requires specific information on the adsorbate and adsorbent. That information is obtained by developing an adsorption isotherm.

The development of an adsorption isotherm requires a minimum of three points or concentrations. Four certified bottles of TCE were used to test the laminates for this experimental development of an adsorption isotherm. The concentrations were 2,125, 1,700, 829, and 174 ppm. Figure 5-8 shows the results of these tests which were conducted on laminate NG7-80 with a carbon loading of 72 g/m^2. All of the tests were conducted to the point of total capacity with the exception of the 829 ppm test which was only tested to 36% of the inlet concentration. While the 174 ppm test was conducted to completion, a recorder malfunction resulted in the loss of the data concentration data during the first part of the capacity test.

Utilizing the theory developed in Section 4, Theoretical Development, one can determine the characteristic Freundlich isotherm for the given test conditions. The isotherm equation takes a linear form when the natural log is applied to both sides of the equation, then the coefficients alpha and beta become the y-intercept and slope, respectively. Because of the exponential form of the equation the isotherm plots as a straight line on a log/log plot. Figure 5-9 shows a plot of the concentration of TCE ppm versus the adsorption capacity in grams of TCE per gram of HSA carbon. This plot shows the data with a least squares regression applied to the data points for both the breakthrough and total capacities. The two equations are as follows:

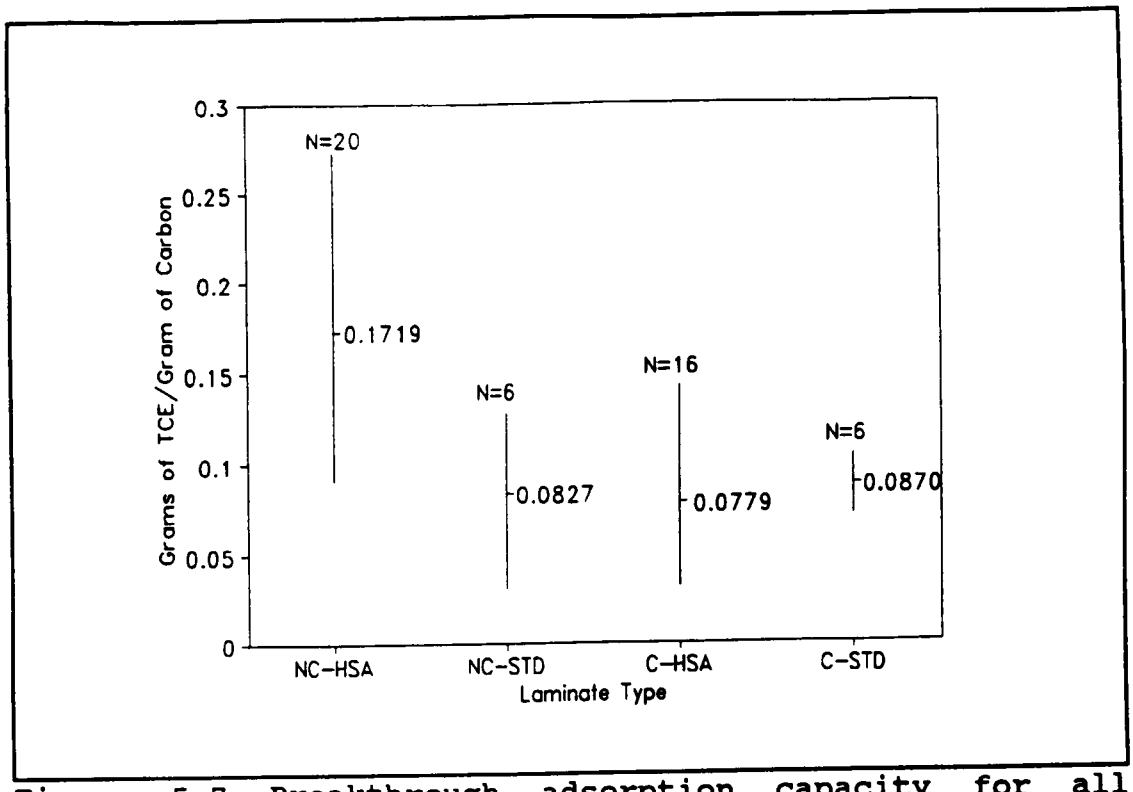


Figure 5-7 Breakthrough adsorption capacity for all laminates.

Breakthrough capacity: $C = 33,860\ X^{1.46}$, $R^2 = 0.86$

Total Capacity: $C = 42,192\ X^{2.47}$, $R^2 = 0.99$.

There is a significant difference between the total adsorption capacity and the capacity at the breakthrough point (in contrast to thick bed systems). The units on C and alpha are ppm. The value of beta is a pure number and is unaffected by the units of the system. The alpha values, in kg/m^3, are 0.1882 and 0.2266 for breakthrough and capacity, respectively.

5.1.2.1. Breakthrough Time

In addition to the development of the isotherm this portion of the laminate testing provided useful information on the laminate performance under different concentration conditions. Several points are worth noting. First, the

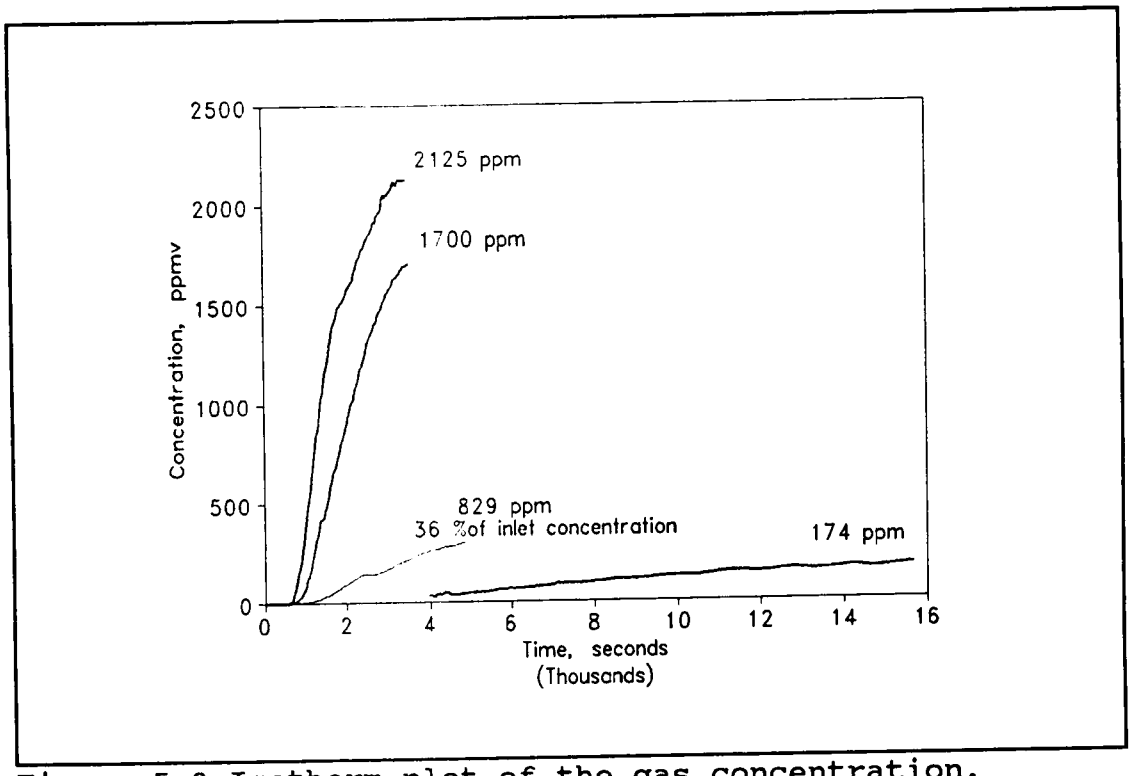


Figure 5-8 Isotherm plot of the gas concentration.

breakthrough time increased as the concentration of TCE was decreased. Referring back to figure 5-8, one can readily see the shift in the breakthrough times as the concentration decreases for this test laminate. Second, the time required to reach total capacity increased dramatically as the concentration was decreased. At 2,125 ppm the total capacity was reached in approximately 3,000 seconds, whereas the 174 ppm test required 16,000 seconds.

5.1.2.2. Capacity Adsorbed

The actual adsorption capacity in grams of TCE per gram of carbon at the time of 1 percent breakthrough, referred to herein as the breakthrough capacity is shown in figure 5-9 for each of the samples. For the non-calendered samples, the HSA carbon had an average breakthrough capacity of 0.172 g TCE/g of carbon, whereas the STD carbon had an average of 0.083 g/g.

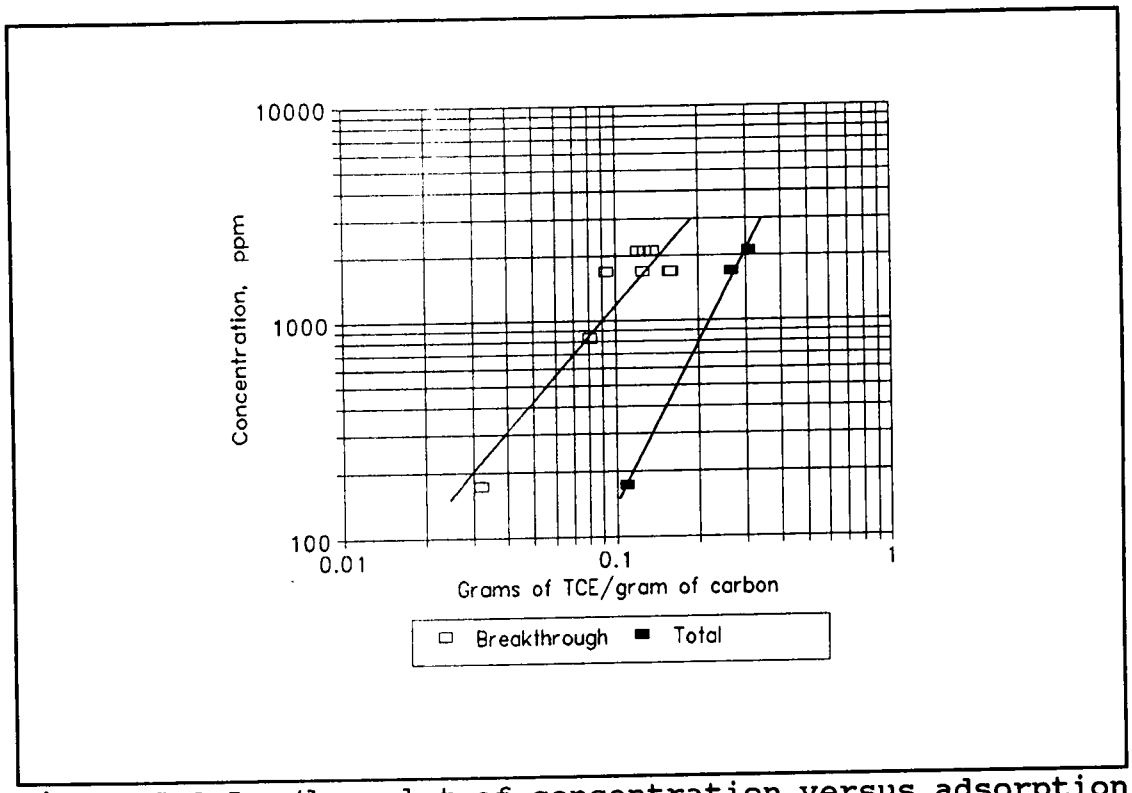


Figure 5-9 Log/log plot of concentration versus adsorption capacity.

The calendered samples had an average breakthrough capacity of 0.078 g/g for the HSA carbon and 0.087 g/g for the STD carbon. These values were greater than the breakthrough capacities of the existing BDO which was tested as shown in Figure 5-1.

The total adsorption capacity ranged from 0.11 g/g at 174 ppm to 0.3 g/g at 2125, nearly a three-fold increase, indicating the importance of the adsorbate concentration. Even more important is the fact that the real operating capacity, as expressed by the breakthrough capacity, was only 0.03 g/g for 174 ppm and 0.14 g/g at 2125 ppm, or 27 percent to 46 percent of the total capacity.

5.1.3. Experimental Challenges and Developments

The original test matrix was designed for each of the laminates to be tested in triplicate. However, a problem was

encountered during the regeneration process. Although, the average regeneration temperature of 65 °C was well below the melting temperature of the PEMB (T_m = 130 °C), some of the laminates shrank and could not be retested after regeneration. figure 5-10 illustrates the shrinkage of the NG4-40 laminate after three regenerations. Shrinkage was attributed to the resin, non-uniform temperature distribution in the oven, and inherent characteristics of the MB wed. The glass transition temperature (T_g) of the PE resin is -80 °C. Shrinkage could be minimized using a resin with a higher T_g and an oven with better internal circulation.

Another deficiency was cited during the dynamic adsorption tests and was related to both the calendering process and the carbon distribution. While all of the calendered laminates had a finite breakthrough time (defined as 1 percent of the inlet concentration or 17 ppm), several of the samples exhibited a small, but observable penetration of TCE from the start of the test. The concentration remained relatively constant until breakthrough began. This penetration or "bleeding" of the TCE suggests that there may have been some small holes or imperfections in the calendered laminates resulting in areas without activated carbon. Figure 5-11 illustrates bleedthrough in one of the calendered laminates. Like the calendered samples the filters with poor distribution of the carbon experienced saturation in the thinner areas earlier. As these areas reached saturation the adsorbate began to breakthrough in small quantities. This concentration did not always reach the 1 percent threshold which defines breakthrough and depends entirely on the amount of area which was thinly covered by the activated carbon. This poor distribution of the activated carbon is undesirable since the objective is to have no measurable penetration up to or near the time of breakthrough. Depending on the sensitivity of the analytical technique used, this premature "bleeding" may or may not be detected. Further study is on-going at TANDEC to

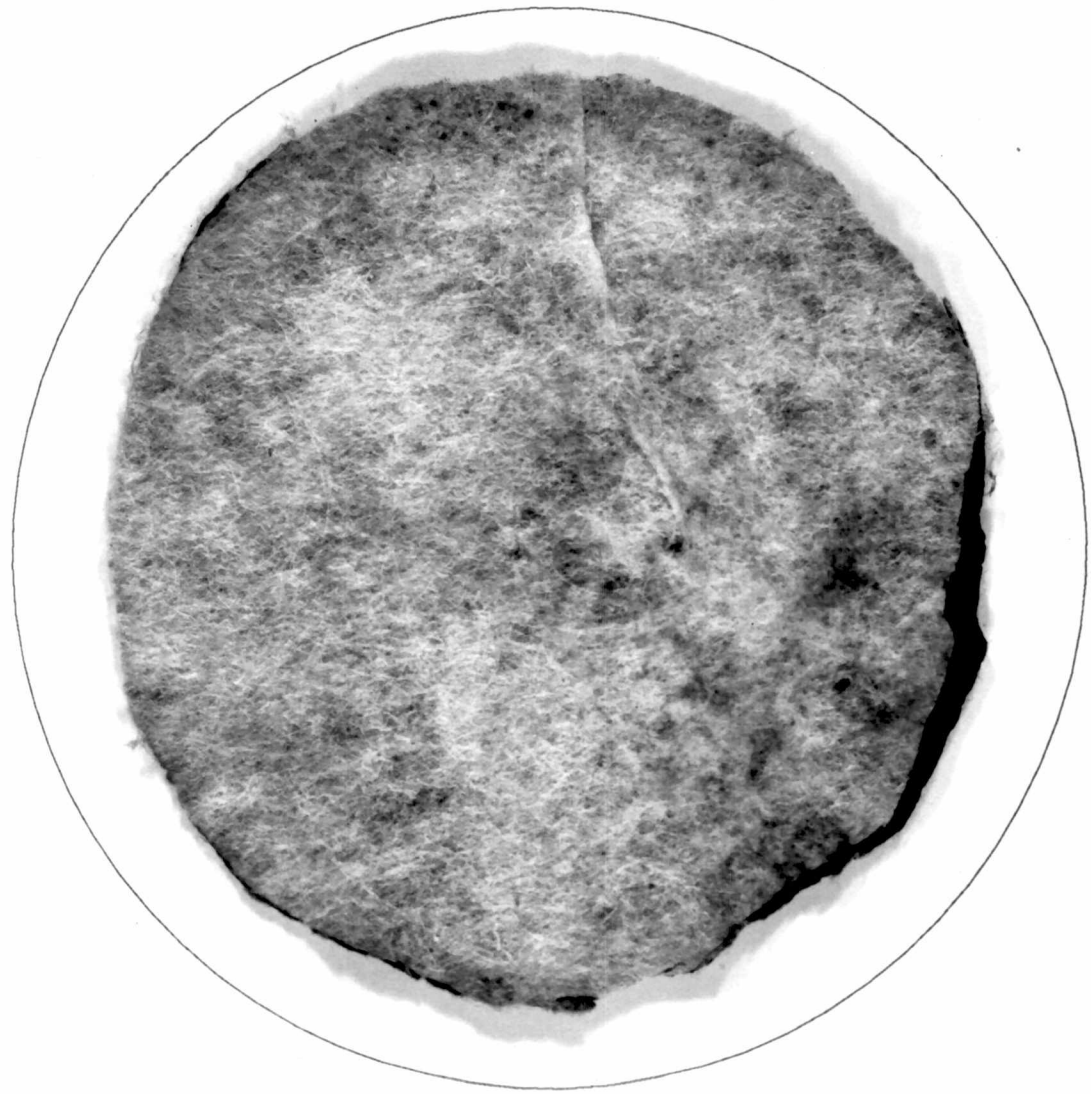


Figure 5-10 Photograph of laminate shrinkage.

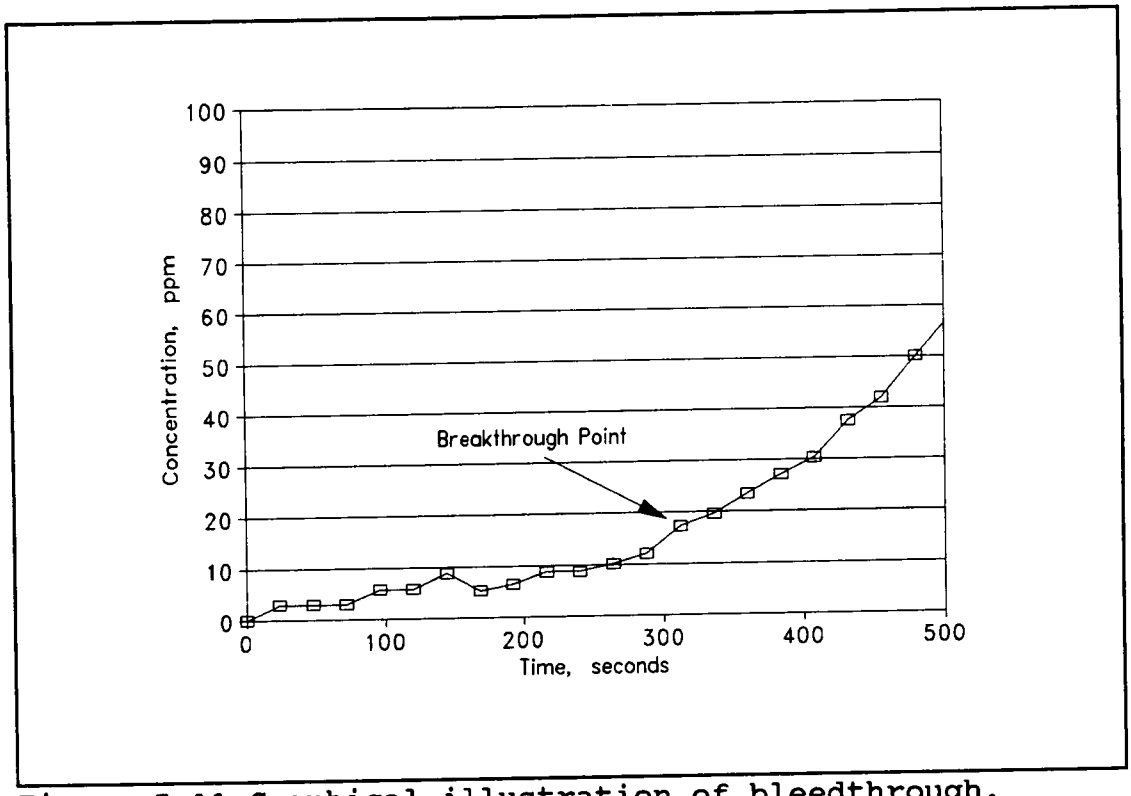


Figure 5-11 Graphical illustration of bleedthrough.

quantify the cause of bleedthrough created by the calendering process and to identify calender operating characteristics required to eliminate this problem.

5.2 Theoretical Model

The process of theoretically modelling may be described as a set of steps. These steps are selection, formulation, testing and application. The process of model selection requires one to identify the questions to be answered and the information required to answer those questions.

The formulation of the model is putting the pieces together for answering the questions identified in the selection. Equations 3-3, 3-6, and 3-7 are the basic governing equations for the selected model. These equations were developed and discussed in Chapter 3. Since the equations are interdependent, the computer code was written to solve them in

the order that they are presented in that section.

Once the program was debugged and running, it was tested. The initial test was to model a conventual thick bed adsorber. For this solution the adsorption wave velocity, delta and the time to reach breakthrough were calculated. The results agreed with an independent solution determined by "hand" calculation.

After determining the accuracy of the program against the existing solution, the model was ready for application. The application requires the user to determine the effects of input parameter variations (i.e. sensitivity analysis). Each of the inputs was varied over two to three orders of magnitude. In addition, the inputs were varied over range close to mean parameter value defining the baseline condition (see Table 5-2). The base condition values were used for the sensitivity analysis to reduce the possible number of combinations. They were based on the average laminate density, thickness and carbon loading. The flow, gas concentration, alpha and beta were set based on experimental conditions and isotherm capacity calculations. The sensitivity analysis procedure required all of the base conditions to be held constant while each of the individual parameters was evaluated.

These parameters had slightly different effects; however, there were two distinct groups. The first group shifted the breakthrough time and the second changed the shape of the adsorption wave. Bed depth, velocity and beta shifted the breakthrough time whereas beta, alpha, inlet concentration, film coefficient and density changed the shape of the adsorption wave.

Figure 5-12 illustrates the bed depth sensitivity analysis. Changing the bed depth results in moving the breakthrough time from a premature to a finite value. From the

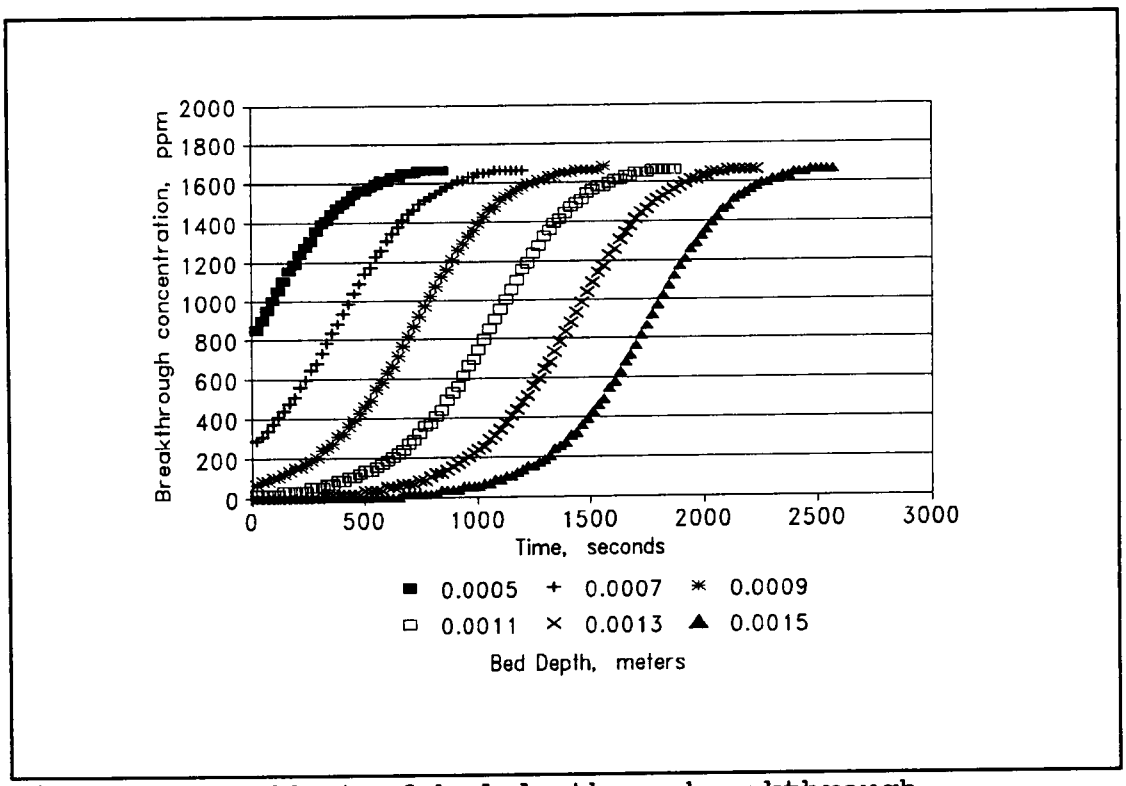


Figure 5-12 Effect of bed depth on breakthrough.

Table 5-2. Adsorption model sensitivity analysis.

α,kg/m^3	β	ρ_{ad} kg/m^3	V,m/s	K,s^{-1}	C_o,kg/m^3	L,m
0.01	1.0	1	0.0001	5	0.00009	0.00009
0.10	1.4	10	0.001	10	0.0009	0.0005
0.13	1.8	50	0.0015	20	0.0044	0.0007
0.16	2.2	100	0.002	30	0.0091	0.0009
0.19	2.6	150	0.0025	40	0.0114	0.0011
0.21	3.0	200	0.003	50	0.091	0.0013
0.24	3.4	250	0.004		0.91	0.0015
0.27	10	1000	0.01			0.009
1.0	100					0.09
10						0.9
Constants						
0.2266	2.47	115	0.002	13.3	0.0091	0.0008

graph the critical bed depth is between 0.0009 m and 0.0011 m. As the bed depth increased beyond 0.0011 m the breakthrough

time increased. Evaluating the effect of an order of magnitude one gains additional perspective. For example, at a bed depth of 0.0009 m breakthrough occurs at t = 0. If one increases the bed depth to 0.009 m breakthrough occurs at t = 13,560 seconds. The shape of the adsorption wave did not change as a function of bed depth.

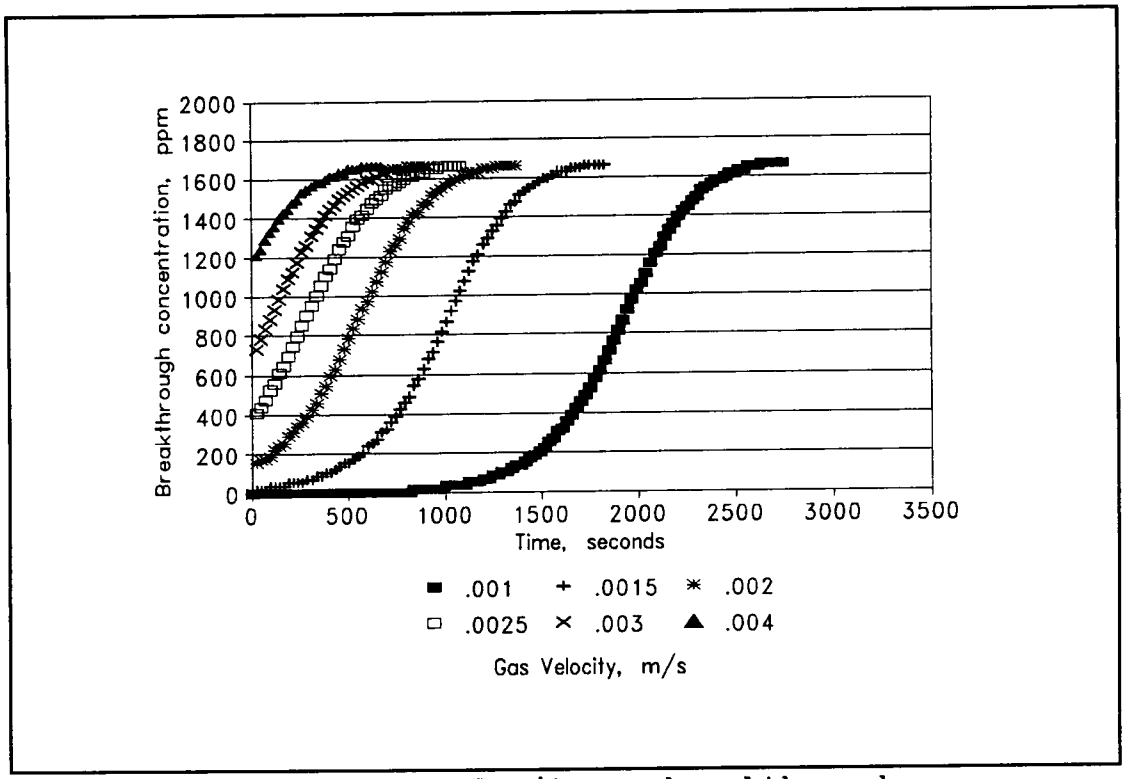


Figure 5-13 Effect of velocity on breakthrough.

Similar to bed depth, the velocity of the carrier gas did not change the shape of the adsorption wave. As the velocity increased the time to breakthrough moved toward zero. This indicated that for any system there is a critical carrier gas velocity that will produce almost immediate breakthrough. As one would expect, changes in the carrier gas velocity change the adsorption wave velocity. This change in adsorption wave velocity explains reduced time to breakthrough. As the velocity varied from 0.0001 m/s (meters per second) to 0.001 m/s, the breakthrough time went from more than 24,000 seconds to t = 0. As the velocity increased to 0.004 m/s the model

predicted that the system would breakthrough at 1,200 ppm at time = 0. It is actually impossible for this condition to exist where the curve is instantaneously 71 percent through the adsorption bed; therefore, the reliability of the model must be questioned when predicting premature breakthrough. Figure 5-13 illustrates the changing point of breakthrough. The order of magnitude effect of velocity is drastic. If the velocity is set at 0.01 m/s the bed reaches 96 percent of capacity at 24 seconds. Shifting two orders of magnitude to a velocity of 0.0001 m/s, the bed requires more than 24,000 seconds before any traces of the inlet concentration penetrate the bed completely.

Beta variation exhibited a set of interesting characteristics since it shifts the breakthrough time and changes the adsorption wave shape. Figure 5-14 shows the sensitivity analysis for beta. Large values of beta increase the time to breakthrough. These values flatten the portion of the adsorption wave so that a "bleedthrough" type of condition is observed. The shape of the adsorption wave seems to remain relative constant for the intermediate values of beta. As the values become small the system begins to change the shape of the adsorption wave by stretching the capacity portion of the curve. One has to be skeptical of the lower values of beta which predict the premature breakthroughs. When comparing the effects of order of magnitude tests the breakthrough differences between a beta of 1.01 and 10 are t = 0 and 350 seconds, respectively. Although the results from the order of magnitude tests are interesting they may be unrealistic since beta typically varies only slightly.

Similar to beta the variation in the parameter alpha was relatively insignificant. Alpha variations did not change the time to breakthrough but changed the shape of the wave. When varied from .13 to .27 kg/m^3 or 2,425 to 5,040 ppm of TCE, the variation in the width of the adsorption wave was minimal. Figure 5-15 illustrates the effect of the change in alpha

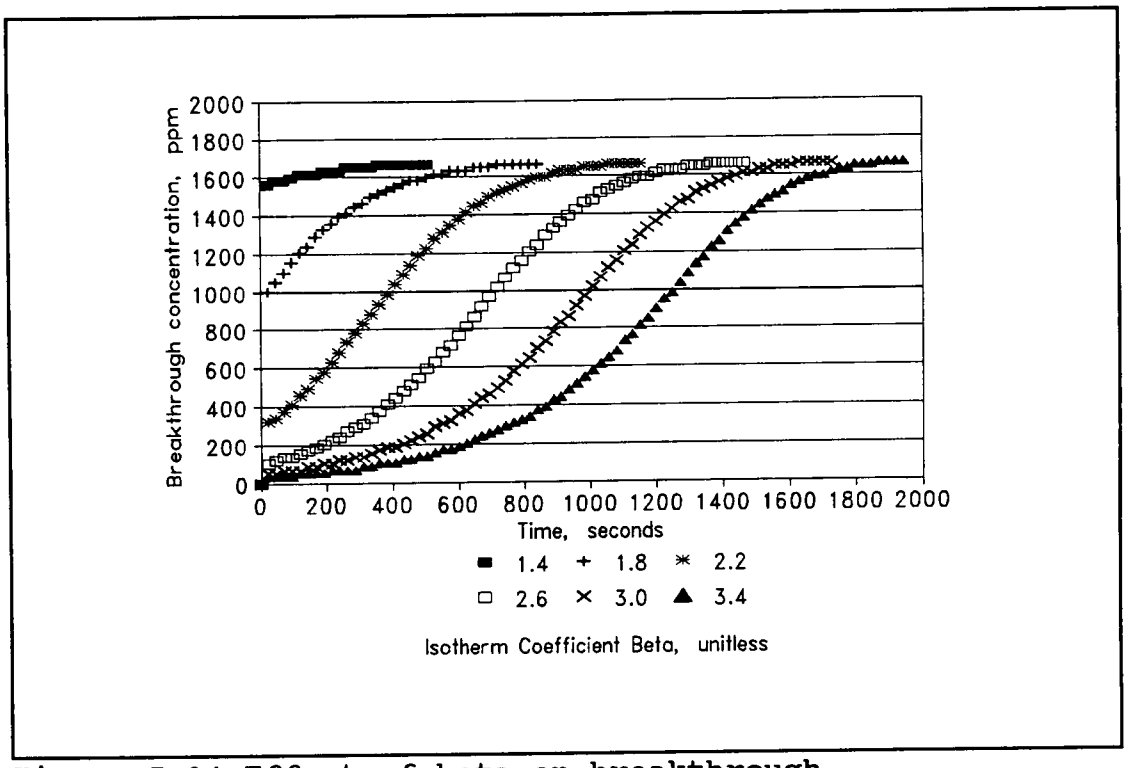


Figure 5-14 Effect of beta on breakthrough.

values. There seems to be little difference in the time to capacity and the point at which breakthrough occurs. In general, as the value of alpha decreases the adsorption wave becomes flatter.

Variation in the inlet concentration followed the same trend as alpha. Figure 5-16 illustrates the decrease in inlet concentration dramatically flattens the adsorption wave. As the concentration of the adsorbate increases the time for the bed to become saturated is reduced. This is obvious if one realizes that for a given ρ the inlet concentration is beta times alpha. The middle four curves in figure 5-16 represent a model prediction of the experimental isotherm test concentrations. The range of concentrations span two orders of magnitude without having a profound impact on the results. It is important to note that even for very low concentrations the system will start breaking through at $t = 0$ for a combination of inputs which were used to perform the sensitivity analysis.

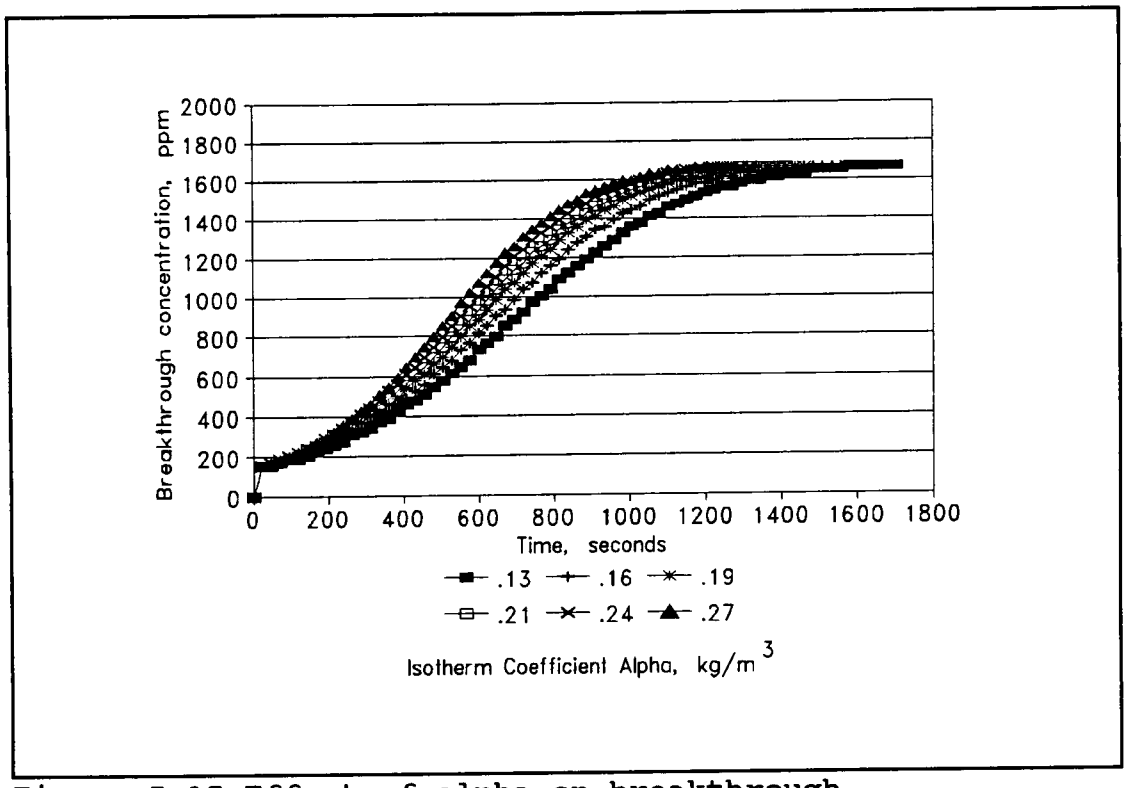


Figure 5-15 Effect of alpha on breakthrough.

Film coefficient variations, K, caused a response which was different than all of the other variations. Although it can be classified as a breakthrough shifting parameter, the variation caused the curve to compress a great deal over one order of magnitude. The limits for the sensitivity analysis for the film coefficient were set between 5 and 50 and there seemed to be no reason for evaluation beyond this range since the calculated value for the system fell well within this range.[31] As figure 5-17 illustrates as the value of K increases the curves become increasingly closer together. As K approaches infinity the curve would theoretically approach a step function. The greatest variation occurs between the values of 5 and 20. In this range the breakthrough changes from almost complete breakthrough to a point where there is a finite time to breakthrough. At the upper end of the range for K, between 40 and 50, the system seems to have reached steady state. One should realize that the film coefficient is a

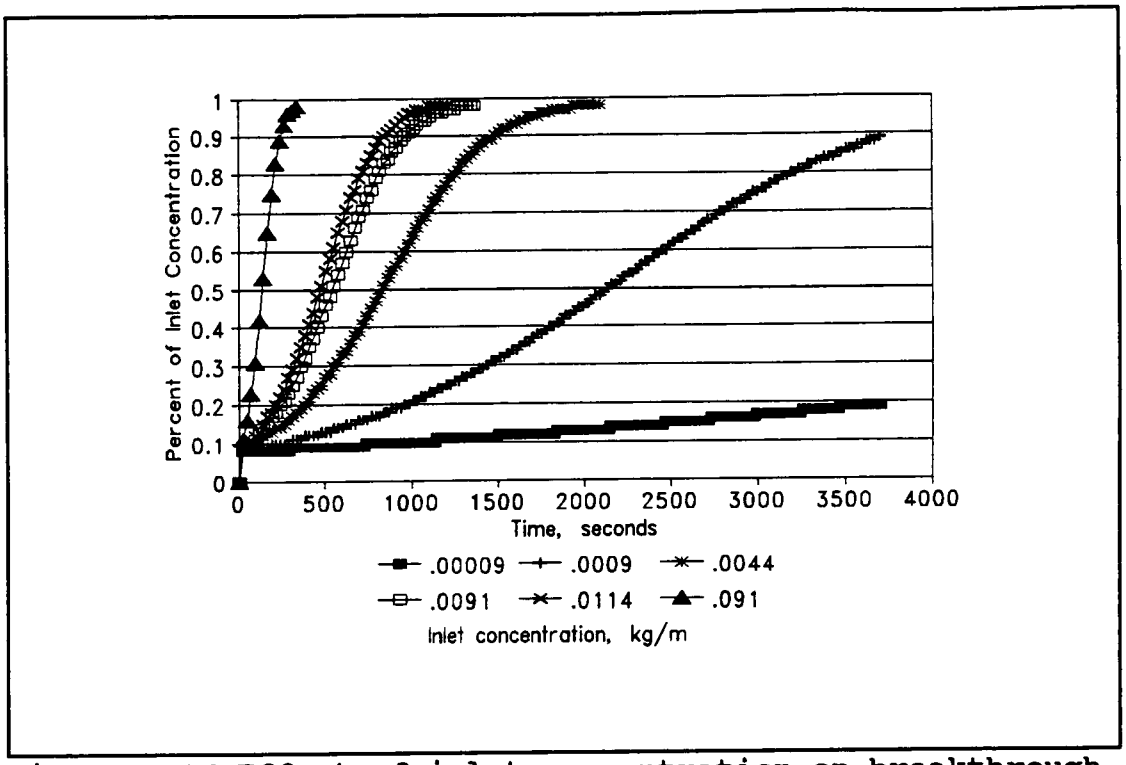


Figure 5-16 Effect of inlet concentration on breakthrough.

function of a experimentally derived number based on the molecular weight. Table 5-3 gives insight to the affect that the adsorbates molecular weight has on the film coefficient.

Table 5-3. Film coefficient and molecular weight relationship.

Film Coefficient, K	Molecular Weight
5	925
10	231
20	58
30	26
40	14
50	9

The density of the adsorbent bed did not change the point at which breakthrough occurred but it did change the shape of the adsorption wave. The width of the adsorption wave (i.e. delta) increases dramatically for beds which have low densities. For example, a bed with a density of 1 kg/m^3 the calculated value of delta is 0.0013 m. As the density

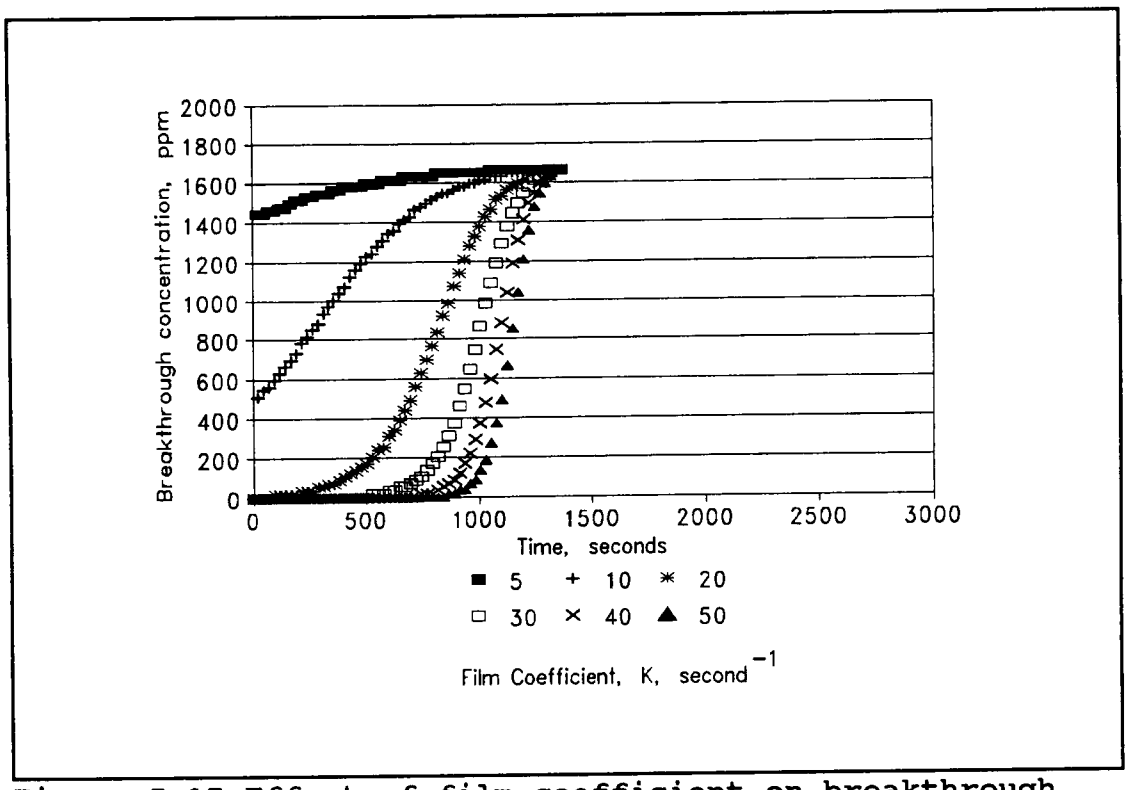


Figure 5-17 Effect of film coefficient on breakthrough.

increases the width of delta is reduced. Figure 5-18 illustrates the effect of density on the breakthrough time. It shows that as the density is increased the time required to travel through the bed increases. For a bed density of 10 kg/m^3 the adsorption wave travels completely through the bed in approximately 100 second. Increasing the bed density an order of magnitude results in an increase of 900 seconds (total of 1,000 seconds) for the wave to travel completely through the bed. By doubling the density to 200 kg/m^3 the adsorption wave requires 2,400 seconds to reach capacity. The variation of the density is important to evaluate since the density of the experimental laminates ranged from approximately 50 to 200 kg/m^3.

The sensitivity analysis provided useful information which aided in understanding the effects of variations in the input parameters. The next step was to compare the modeled

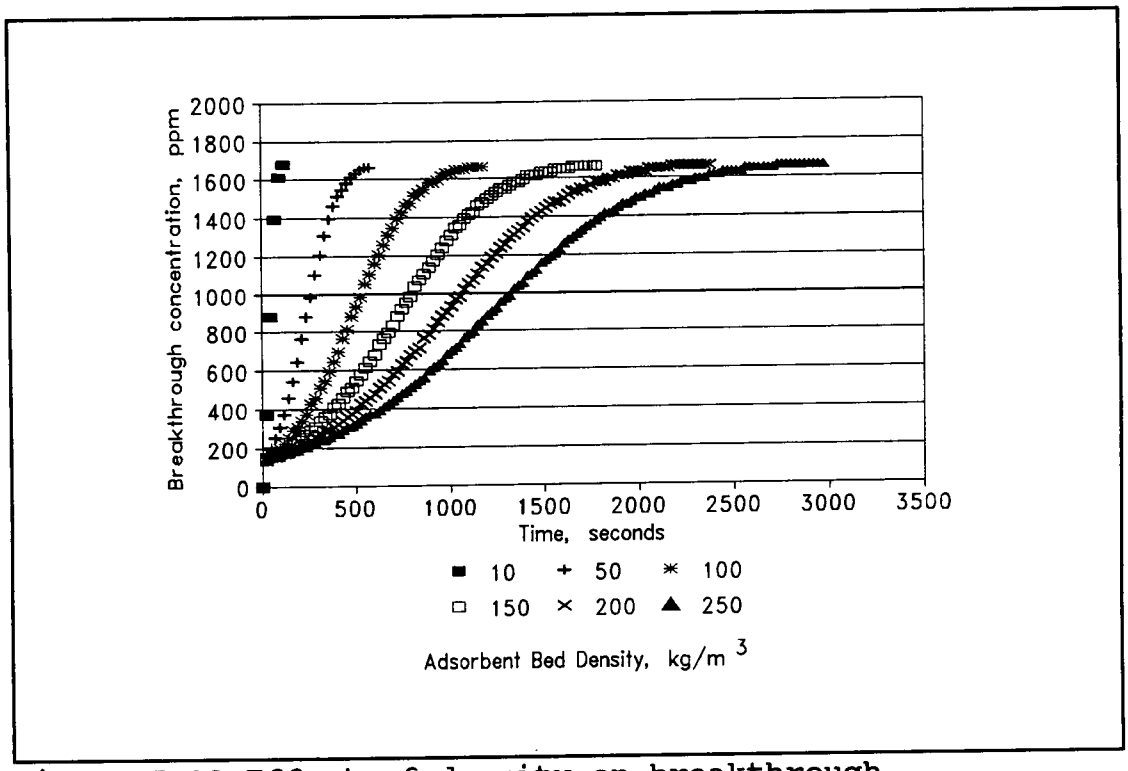


Figure 5-18 Effect of density on breakthrough.

results with the observed experimental results. Figure 5-8 and Figure 5-19 illustrate the experimental isotherm data and the theoretical model isotherm data. Both of these are plotted on the same scale to allow for a direct comparison of the data. It is clear that there is little agreement between the two. As a result, one has to ask the question if the quantity of adsorbent and isotherm constants are the same why are the values predicted by the model not closer to the experimental values?

This question is answered by looking at the assumptions of the model. In order to calculate delta the model assumes that the adsorption wave was fully developed at time equal to zero. This assumption is approximately correct for thick bed systems since for a thick bed the width consumed by delta is only a small fraction of the total bed depth. However, this causes a significant problem as the width of delta becomes closer and closer to the width of the bed. In order to illustrate this point the independent solution for the thick

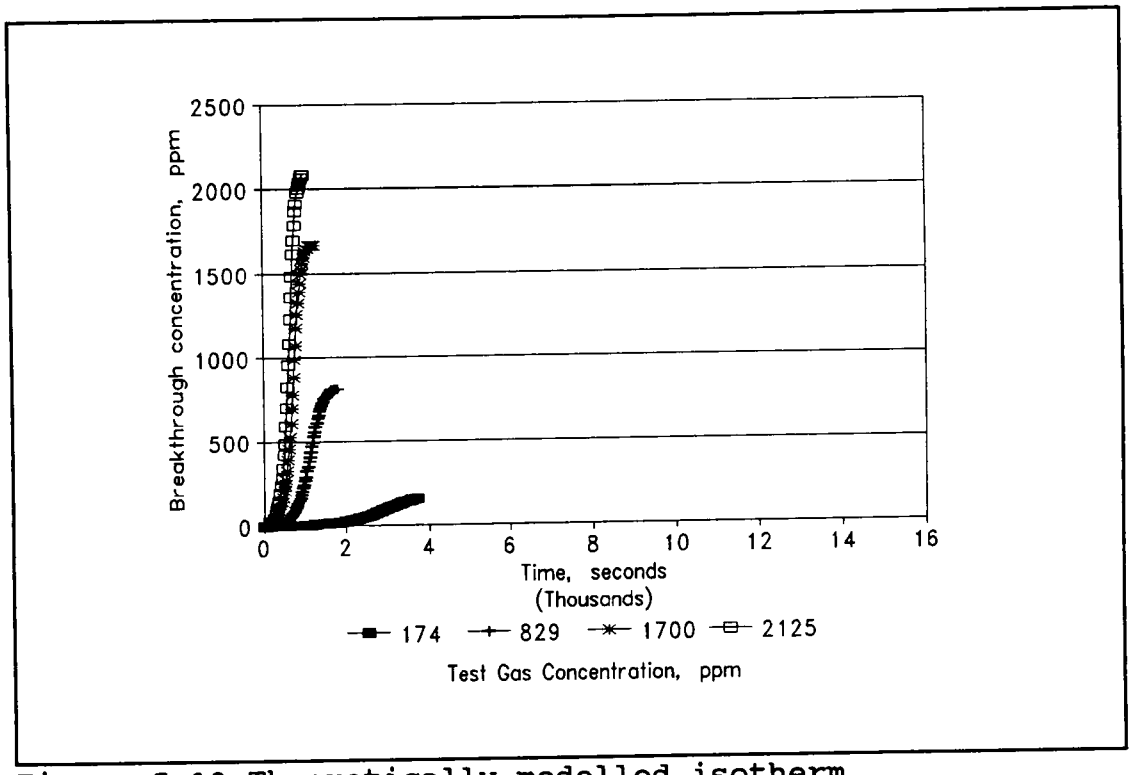


Figure 5-19 Theoretically modelled isotherm.

bed adsorber was used. For this solution only the density and bed depth were varied producing four different bed conditions that had the same quantity of adsorbent.

This modeling exercise initially evaluated the effect of the changing density and bed depth on the breakthrough time. As the bed depth decreased the time to reach breakthrough decreased. Even though the change in the adsorption wave velocity was reduced in proportion to the density of the bed. The width of the adsorption wave, delta, is not changed by the depth / density variation. Therefore, for a system which is 1 meter thick the delta is the same as for a system which is 0.01 meters thick. Figure 5-20 illustrates two beds. The first has a bed depth of 1, bed density of 2, adsorption wave velocity of 1, and width of delta of 0.5. In the second bed, depth is 2, density is 1, adsorption wave velocity is 2 and delta is 0.5 (refer back to equation 4-6 in the theoretical development for calculation of delta). When this equation is applied to Bed 1 the breakthrough time calculated is 0.5 time

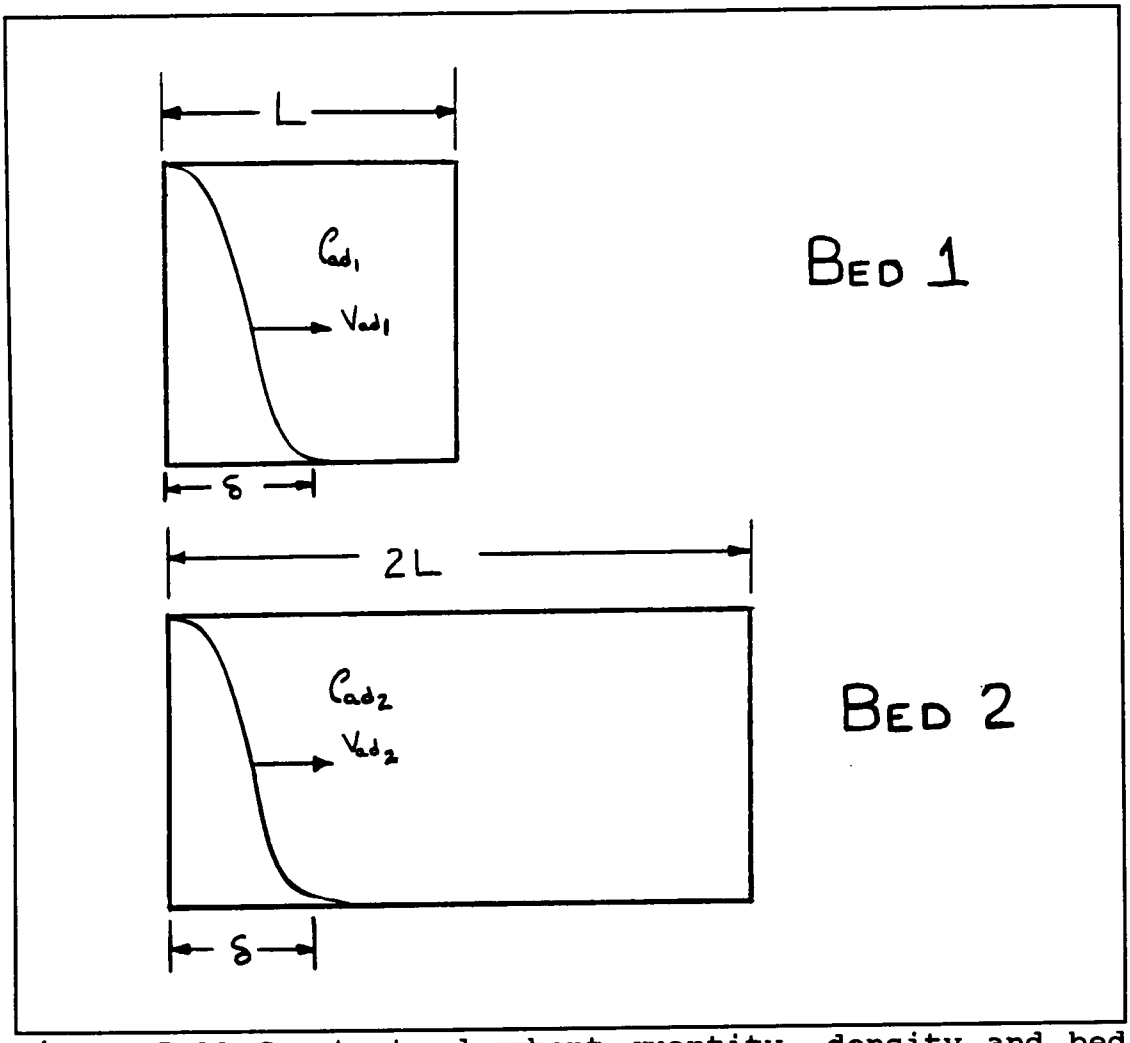


Figure 5-20 Constant adsorbent quantity, density and bed depth variation.

units for Bed 1 and 0.75 time units for Bed 2. This figure shows that the increased depth causes the system to require more time to reach breakthrough. It is important to note that the amount of adsorbent present has not changed. This also produced an interesting effect on the breakthrough curve. Although the time to reach breakthrough for each of the beds was different, the time to capacity was the same. As a result, the breakthrough curve for Bed 1 was much wider than that of Bed 2 (i.e. the concentration profile took longer to exit the bed). This phenomena of the two beds reaching capacity at the same time inspired the next portion of the analysis.

By dividing the system into three sections one can analyze the mass adsorbed by each section. Figure 5-21 illustrates the three sections of an adsorption unit. The mass adsorbed in section A is not accounted for in the thick bed theory. The reason for this is the assumption of the delta being fully established. However, this value was calculated to prove that the theory could be forced to account for all of the mass in the system. The mass adsorbed in section B is the amount before the system reaches breakthrough. Section C represents the mass adsorbed from the point of breakthrough to the time the bed reaches capacity. The resultant wave is the breakthrough curve.

For thick beds the mass of section A is only a fraction of the total mass adsorbed in the system. Table 5-4 lists the masses adsorbed for each of the sections. It is clear that the difference between the 5.6 m bed and the 0.0875 m bed is significant since the mass adsorbed in the "thin" bed is approximately 30 percent of the total mass adsorbed by the system and for the thick bed is only 1 percent.

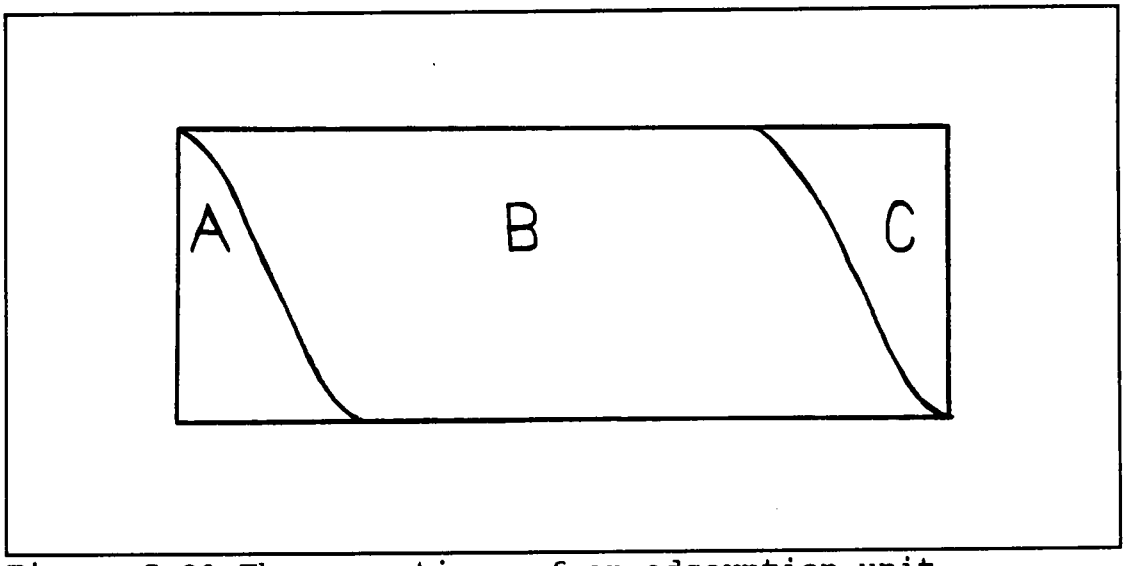


Figure 5-21 Three sections of an adsorption unit.

The mass percent adsorbed is proportional to the percent of the bed depth occupied by delta. This difference in percent

of the bed occupied by delta is the most significant problem with using the existing thick bed theory to predict the performance of thin bed adsorbers. This problem is complicated by the fact that the adsorption wave is dynamic until it reaches a steady-state width of delta. One knows that from physics the wave can not be established instanteously (refer to figure 2-6 and figure 2-7). Therefore as the adsorption wave begins to develop one must create a relationship for it in distance and time. The development of this relationship require further research and is beyond the scope of this thesis.

Table 5-4. Effect of bed depth and density variation.

Bed Density, kg/m^3	43.75	350	700	2800
Bed Depth, m	5.6	0.7	0.35	0.0875
Mass Carbon, kg	2940	2940	2940	2940
Mass section A, kg	0.158	1.263	2.527	10.106
Mass section B, kg	32.441	30.116	27.527	11.518
Mass section C, kg	0.174	1.395	2.787	11.148
Total Mass Adsorbed, kg	32.773	32.773	32.773	32.773

5.3 Conclusions

The research showed that a "thin" laminate could be created that has a finite breakthrough time. In addition, these laminates out performed the existing BDO materials. When the test laminates were calendered their durability improved; however, their ability to adsorb was reduced. The isotherm tests provided insight into the performance of thin bed adsorbers.

The most significant difference which was illustrated is the requirement to use the adsorption coefficient generated at breakthrough rather than those at capacity. For a thick bed system these values are very close and make little difference

in the design of the adsorber. This is not true for the thin bed system due to the relative width of delta. Figure 5-9 is a illustration of the experimental adsorption isotherm. It is clear that as the bed thickness increases the breakthrough and capacity values become closer.

CHAPTER 6

FUTURE WORK

The results of this thesis illustrate how bed characteristics affect adsorption systems. The most important of these is the formation of the adsorption wave. As the width of the adsorption wave increases, the assumption of it being fully established is no longer valid. There is a need for research to understand the relationship between bed thickness, size of delta, critical bed depth, and how steady state delta is established. In the ASTM standard definition of the critical bed depth, there is no mention of the development of the adsorption wave. It is assumed that it is already at an equilibrium or constant value.

To develop a theoretical model for the thin bed system a relationship between the bed depth and the width of delta is required. The test matrix would have to examine multiple bed depths, at multiple concentrations and measure the associated values of delta. Once this information was gathered, one could plot the relationship of delta versus bed depth. From this plot a mathematical relationship could be developed and applied to the existing theory to predict the initial formation of the adsorption wave.

In addition to evaluating the effect of thickness, a second set of experiments could evaluate the effect of bed uniformity on the formation of the adsorption wave. This set of experiments would test beds with varying thickness deviation. One would expect that the thinner sections of the bed would reach breakthrough first. As the deviations increased the width of delta would be expected to increase and as the deviation decreases the width of delta would decrease. One could potentially cause delta to become a step function if the deviations increased to extremes. In this case sections of the bed would perform as individual beds within a single bed.

This information could then be combined with the first series of experiments to supplement the existing theory and potentially model systems with varying degrees of non-uniformity.

By performing these experiments, one would obtain a greater understanding of the development of the adsorption wave. This will allow for the elimination of the assumption that the width of the adsorption wave is fully established at time equal zero. The theory would then be supplemented with the relationship that describes the development of delta as a function of time and mass. At that point, the model would be applicable to thin bed simulations. This research effort could be further strengthened by evaluating different compounds to determine their effects on the development of the adsorption wave.

LIST OF REFERENCES

LIST OF REFERENCES

[1] Buonicore, A. J. & Davis, W. T. (1992). Air Pollution Engineering Manual. New York: Van Nostrand Reinhold.

[2] Kirk-Othmer. (1992). Encyclopedia of Chemical Technology, Fourth Edition. 1, New York: John Wiley & Sons.

[3] Kirk-Othmer. (1992). Encyclopedia of Chemical Technology, Fourth Edition, 4, New York: John Wiley & Sons.

[4] American Society of Testing Materials. (1991). D 2652-76 (Reapproved 1987) Standard Definitions of Terms Relating to Activated Carbon. Annual Book of ASTM Standards. Philadelphia: American Society For Testing and Materials.

[5] Sing, K. S. W. (1985). Pure Applied Chemistry. 57, 603-619.

[6] Innes, R. W., Fryer, J. R. & Stoeckli, H. F. (1989). On the correlation between micropore distribution obtained from molecular probes and from high resolution electron microscopy. Carbon. 27 (1), 71-76.

[7] Jaroniec, M., Madey, R., Choma, J., McEnaney, B. & Mays, T. J. (1989). Comparison of Adsorption methods for characterizing the microporosity of activated carbons, Carbon. 27 (1), 77-83.

[8] Innes, R. W., Fryer, J. R. & Stoeckli, H. F. (1989). On the correlation between micropore distribution obtained from molecular probes and from high resolution electron microscopy." Carbon. 27 (1), 74.

[9] Dubinin, M. M. (1989). Fundamentals of the theory of

adsorption in micropores of carbon adsorbents: Characteristics of their adsorption properties and microporous structures. Carbon. 27 (3), 457-467.

[10] Stoeckli, H. Fritz. (1990). Microporous carbon and their characterization: The present state of the art. Carbon. 28 (1), 1-6.

[11] Seaton, N. A., Walton, J. P. R. B. & Quirke, N. (1989). A new analysis method for the determination of the pore size distribution of porous carbons from nitrogen adsorption measurements. Carbon. 27 (6), 853-861.

[12] ASTM. (1991). Annual Book of ASTM Standards. 15.01: Refractories; Carbon and Graphite Products; Activated Carbon D-28. Determination of Particle Size of Powder Activated Carbon. Philadelphia: American Society For Testing and Materials.Test Method: D 5158-91.

[13] Treybal, R.E. (1980). Mass Transfer Operations 3rd ed. NY: McGraw Hill.

[14] Nelson, G. O. & Harder, C. A. (1974). Respirator Cartridge Efficiency Studies: V. Effects of Solvent Vapor. American Industrial Hygienest Association Journal. 35, 391.

[15] Weissenhorn, F. J. (1989). Activated carbon: porosity and surface or capacity and free energy?. Carbon. 27 (1), 129-133.

[16] Wood, G. O. & Moyer, E. S. (1989). A review of the Wheeler Equation and Comparison of Its Applications to Organic Vapor Respirator Cartridge Breakthrough Data. American Industrial Hygiene Association Journal. 50 (8),

400-406.

[17] Ackley, M. W. (1985). Residence time model for respirator sorbent bed. American Industrial Hygiene Association Journal. 46 (11).

[18] American Society of Testing Materials. (1992).D 5160-91, Standard Guide for Gas-Phase Adsorption Testing of Activated Carbon. Annual Book of ASTM Standards. Philadelphia: American Society For Testing and Materials.

[19] Crawford, H. B. & Eckes, B. E. (1984). Perry's Chemical Engineers' Handbook. NY: McGraw-Hill.

[20] Jonas, L. A. & Rehrmann, J. A. (1974). The rate of gas adsorption by activated carbon. Carbon. 12, 95-101.

[21] Klotz, I. M. (1946). The Adsorption Wave. Chemical Reviews. Vol. 39.

[22] Noll, K. E., Gounaris, V. & Hou, W. (1992). Adsorption Technology for Air and Water Pollution Control. Lewis Publishers.

[23] Cooper, C.D. & Alley, F.C. (1986). Air Pollution Control A Design Approach. Chicago: Waveland Press.

[24] Stoeckli, H. F. (1990). Microporous carbon and their characterization: The present state of the art. Carbon, 28 (1), 1-6.

[25] Kraehenbuehl, F., Stoeckli, H. F., Addoun A., Ehrburger P., Donnet T.B. (1986). The use of immersion calorimetry in the determination of micropore distribution of carbons in the cours of activation. Carbon. 24.

[26] Jones, D. W. & Watts, P. (1988). Kinetics of Vapor Sorption by Latex-Bonded Carbon Particles. Performance of Protective Clothing: Second Symposium, ASTM STP 989. Mansdorf, S. Z., Sager, R. & Nielsen, A. P., Eds. Philadelphia: American Society for Testing and Materials, 832-846.

[27] Rehrmann, J. A. & Jonas, L. A. (1978). Dependence of Gas Adsorption Rates on Carbon Granule Size and Linear Flow Velocity. Carbon. 16, 47-51.

., Harder, C.A. & Bigles, B. E. (1974). rtridge Efficiency Studies: VI. Effects of . Dept. UCRL-76184. Lawrence Livermore

ıer, C. F. (1981). Air Pollution Its Origin econd Ed. NY: Harper Collins.

Tewari, Y.B., & Sansone, E.B. (1979). Adsorption Rate Constants of Activated Carbon for Various Vapors. Carbon. 17, 345-349.

APPENDIX

APPENDIX A

Appendix A. Chemical Properties and Toxicity of TCE.

CHARACTERISTIC	TRICHLOROETHYLENE
Chemical Formula	C2Cl3H3
Molecular Weight (g/mole)	133.39
Gas Density (kg/m^3)	4.450
Liquid Density(kg/m^3)	1465.0
Boiling Temperature at atmospheric pressure(°C)	86.7
Latent Heat of vaporization (kJ/kg)	240
Vapor pressure of pure compound (kPa @ 20 °C)	7.61
CAS Number	79-01-6
OSHA-PEL (8-hr)	100 ppm

STANDARD	CONCENTRATION OF TCE
Odor Threshold	28 ppm
OSHA-PEL (8-hr) Ceiling limit 5 min any 2 hr Maximum peak	100 ppm 200 ppm 300 ppm
NIOSH (10-hr)	25 ppm
ACGIH (8-hr) STEL	50 ppm 200 ppm
New York Air Quality Standards SGC AGC	 33,000 $\mu g/m^3$ 0.45 $\mu g/m^3$
BIF Rules RsD	7.7E+00 $m^3/\mu g$
LC50 (4-hr exposure rats)	8000 ppm
LD50 (orally in rats)	4.92 ml/kg

APPENDIX B

```
7 REM
10 REM Program to calculate delta for a given time and determine the value
20 REM of C/Co for each time increment. This is an itterative solution and
30 REM will use limits of C/Co = .99 to .01. This describes the limits of
40 REM of the adsorption wave and states that 1% of Co is the leading edge
50 REM of the wave.
51 REM
55 REM ------------------------------------------------------------------
56 REM
60 PRINT "IMPORTANT NOTE: USE CONSISTANT UNITS (eg. mks)!"
70 INPUT "Velocity of the carrier gas, m/s";VA
80 INPUT "Density of the adsorbent, kg/m^3 ";RHOAD
90 INPUT "Alpha, kg/m^3";ALPHA
100 INPUT "Beta";BETA
110 INPUT "Inlet concentration, kg/m^3";CO
120 INPUT "K value, s^-1";K
130 INPUT "Length of the adsorption bed, m"; L
190 REM
200 REM ----------Print of the initial inputs to the output----------------
210 REM
220 LPRINT "The Input bed conditions are:"
240 LPRINT "Velocity of the carrier gas, m/s";VA
260 LPRINT "Density of the adsorbent, kg/m^3 = ";RHOAD
280 LPRINT "Alpha, kg/m^3 = ";ALPHA
300 LPRINT "Beta = ";BETA
320 LPRINT "Inlet concentration, kg/m^3 = ";CO
340 LPRINT "K value, s^-1 = ";K
360 LPRINT "Length of the adsorption bed, m = "; L
490 REM
500 REM ------------------------------------------------------------------
501 REM
520 REM This is based on Equation 6-6b p.267 of Wark and Warner. This
540 REM equation calculates the velocity of the adsorption wave through the
560 REM bed of activated carbon. This adsorption wave velocity is then used
580 REM to determine the value for DELTA1A in equation 6-10 line _____.
590 REM
600 REM ------------------------------------------------------------------
610 REM
620 VAD = (VA/RHOAD)*(ALPHA^(1/BETA))*(CO^((BETA-1)/BETA))
640 PRINT VAD
660 LPRINT "Adsorption wave velocity = ";VAD
990 REM
1000 REM -----------------------------------------------------------------
1001 REM
1050 REM This is based on equation 6-10 page 269 of Wark and Warner. It is
1100 REM modified to replace the ma, A, rhoa with the velocity of the gas, VA.
1150 REM This equation calculates the value of DELTA1BMAX (x-x1) for the
1200 REM maximum boundary condition where the initial concentration is 1 and
1250 REM the outlet concentration is .01.
1300 REM
1350 REM -----------------------------------------------------------------
1370 REM
1400 B1 = BETA-1
1450 B = 1/B1
1460 PRINT " Beta - 1 =";B1
1461 LPRINT " Beta - 1 =";B1
1470 PRINT " 1/B1 = ";B
1471 LPRINT " 1/B1 = ";B
1500 DELTA1BMAX = (VA/K)*(LOG(.99/.01)+B*LOG((1-.01^B1)/(1-(.99)^B1)))
1550 LPRINT "DELTA1BMAX (I.E. TRUE DELTA) = ";DELTA1BMAX
1990 REM
2000 REM -----------------------------------------------------------------
2001 REM
```

```
2050 REM This section uses an loop to range the breakthrough time from
2100 REM zero to 3696 seconds. Then the calculation of the delta for that time
2150 REM is made. Once this is done the second delta is calculated. A maximum
2200 REM and minimum value is then determined and compared to the value
2300 REM associated with the original time. This section is based on equation
2350 REM 6-11 of Wark and Warner p. 270. It uses the depth of the bed, L;
2400 REM VAD is the adsorption wave velocity; and TB is the time at which
2450 REM a value of delta is being calculated for. This method steps through
2500 REM the time increments and allows for as much or little resolution
2550 REM dependant solely on the user.
2570 REM
2600 REM ------------------------------------------------------------------
2650 I = 24000
2700 J = 0
2750 FOR TB =  24 TO I STEP 24
2770 REM
2800 REM ---------------------- W&W equation 6-11 -------------------------
2820 REM
2850 DELTA1A = L - VAD*TB
2900 REM
2950 REM This is the check to determine if the value calculated is out of the
3000 REM limits of the maximum delta for the system which is being evaluated.
3050 REM
3100 IF DELTA1A > DELTA1BMAX GOTO 10200
3150 IF DELTA1A < 0 GOTO 10500
3190 REM
3200 REM ------------------------------------------------------------------
3201 REM
3250 REM This section defines the concentrations using equation 6-10 of
3300 REM Wark and Warner to determine the actual distances which the wave
3350 REM travels. The values of C1 (i.e. C) increase in a .01 step until
3400 REM Co/C1 is equal to 1.
3449 REM
3450 REM ------------------------------------------------------------------
3451 REM
3500 FOR C1 = .99 TO J STEP -.01
3550 Z = LOG(.99/C1)
3600 Y = LOG((1 - (C1)^(B1))/(1-(.99)^(B1)))
3650 DELTA1B = (VA/K)*(Z + B*Y)
3700 X = DELTA1A - DELTA1B
3750 IF X <= 0 THEN GOTO 3900
3800 IF X > 0 THEN GOTO 3850
3850 NEXT C1
3900 PRINT "C/Co = ";C1,"       TB = ";TB
3950 LPRINT "C/Co = ";C1,"       TB = ";TB
4000 REM
10000 REM -----------------------------------------------------------------
10001 REM
10100 GOTO 10450
10200 PRINT "C/Co is less than .01 and TB =  ";TB
10300 LPRINT "C/Co is less than .01 and TB = ";TB
10400 GOTO 10450
10450 NEXT TB
10500 PRINT "C/Co is greater than .99 and TB = ";TB
10600 LPRINT "C/Co is greater than .99 and TB = ";TB
10800 END
```

```
10 REM this program is a modification of ADWAVET2.BAS to calculate
20 REM the values of delta for .01 increment in C/Co. By doing this
30 REM I hope to have the same mass adsorbed for a given amount of
40 REM carbon.
60 PRINT "IMPORTANT NOTE: USE CONSISTANT UNITS (eg. mks)!"
70 INPUT "Velocity of the carrier gas, m/s";VA
80 INPUT "Density of the adsorbent, kg/m^3 ";RHOAD
90 INPUT "Alpha, kg/m^3";ALPHA
100 INPUT "Beta";BETA
110 INPUT "Inlet concentration, kg/m^3";CO
120 INPUT "K value, s^-1";K
130 INPUT "Length of the adsorption bed, m"; L
140 INPUT "Area of the filter, m^2"; AF
150 REM LPRINT "The Input bed conditions are:"
160 LPRINT "Velocity of the carrier gas, m/s";VA
170 LPRINT "Density of the adsorbent, kg/m^3 = ";RHOAD
180 LPRINT "Alpha, kg/m^3 = ";ALPHA
190 LPRINT "Beta = ";BETA
200 LPRINT "Inlet concentration, kg/m^3 = ";CO
210 LPRINT "K value, s^-1 = ";K
220 LPRINT "Length of the adsorption bed, m = "; L
230 LPRINT "Area of the filter, m^2"; AF
240 REM
250 MT = CO*VA*AF*24
260 LPRINT "mt = ";MT
270 REM
280 VAD = (VA/RHOAD)*(ALPHA^(1/BETA))*(CO^((BETA-1)/BETA))
290 REM
300 LPRINT "Adsorption wave velocity = ";VAD
320 B1 = BETA-1
330 B = 1/B1
350 DELTA1BMAX = (VA/K)*(LOG(.99/.01)+B*LOG((1-.01^B1)/(1-(.99)^B1)))
361 TAB=DELTA1BMAX
362 MTW=0
363 LPRINT "DELTA= "TAB
365 SUMMAA=0
370 REM lPRINT "DELTA1BMAX (I.E. TRUE DELTA) = ";DELTA1BMAX
380 IF L - DELTA1BMAX < 0 GOTO 630
390 TB = (L - DELTA1BMAX)/VAD
400 TBW = TB
410 LPRINT "Tb = ";TB
420 MT1 = CO*VA*AF*TB
430 LPRINT "mt1 = ";MT1
440 REM
450 J = .99
460 FOR C1 = .02 TO J STEP .01
465 ZAP = TAB
470 IF C1 > .99 GOTO 580
480 Z = LOG(.99/C1)
490 Y = LOG((1 - (C1)^(B1))/(1-(.99)^(B1)))
495 TAB = (VA/K)*(Z + B*Y)
500 DELTA1B = ZAP - TAB
510 DT = DELTA1B/VAD
520 TBW = TBW + DT
530 MT2 = (((1-C1)+.005)*CO)*VA*AF*DT
532 REM MMP IS MAX POSSIBLE MASS IN INCREMENT DT
534 MMP=CO*VA*AF*DT
536 REM MASS ALREADY ADSORBED AT TB FOR THE INCREMENT DT
537 MAA=MMP-MT2
538 REM SUM OF MASS ALREADY ADSORBED IN WAVE
539 SUMMAA=SUMMAA+MAA
540 PRINT "C/Co = ";C1," MT2 = ";MT2," Tbw = ";TBW
550 LPRINT "C/Co = ";C1," MT2 = ";MT2," Tbw = ";TBW
560 MTW = MTW + MT2
570 NEXT C1
580 LPRINT "MTW = ";MTW
590 REM
600 MTT = MT1 + SUMMAA + MTW
605 LPRINT "SUMMAA = "SUMMAA
607 LPRINT "MT1 = "MT1
610 LPRINT "mtt = ";MTT
620 GOTO 650
630 PRINT "C/Co cannot be calculated since deltamax is exceeded"
640 LPRINT "C/Co cannot be calculated since deltamax is exceeded"
650 END
```

APPENDIX C

SAMPLE DIRECTORY/NUMBER: DATA1 /64
SAMPLE ID. super activated C
SUBMITTER: ccr
OPERATOR: ccr
UNIT NUMBER: 1
ANALYSIS GAS: Nitrogen

START 10:05:50 11.27.91
COMPL 17:13:25 11.27.91
REPT 17:13:26 11.27.91
SAMPLE WT: .2951 g
FREE SPACE: 57.4271 cc
EQUIL INTRVL: 5 sec

ANALYSIS LOG

RELATIVE PRESSURE	PRESSURE (mmHg)	VOL ADSORBED (cc/g STP)	ELAPSED TIME (HR:MN)	SATURATION PRESS.(mmHg)
			0:31	760.360
0.0582	44.262	571.4428	1:41	
0.1109	84.244	659.0431	1:55	
0.1695	128.713	736.8499	2:10	
0.2012	152.766	770.4448	2:22	
			2:36	759.331
0.2847	216.165	832.1522	2:46	
0.3239	245.905	849.6839	2:58	
0.3825	290.380	867.0791	3:08	
0.4697	356.575	882.9501	3:18	
0.5490	416.771	893.3771	3:27	
0.6470	491.189	904.1275	3:35	
0.7415	562.918	913.6401	3:45	
0.7946	603.204	918.6696	3:49	
0.8360	636.146	922.3585	3:54	
0.8750	664.227	927.4632	3:59	
0.9059	687.654	931.4060	4:04	
0.9286	704.927	934.8054	4:08	
0.9450	717.567	937.8865	4:12	
0.9584	727.475	940.9999	4:16	
0.9689	735.491	944.2546	4:20	
0.9768	741.438	947.3475	4:24	
0.9827	745.885	950.5076	4:28	
0.9877	749.661	954.1846	4:32	
0.9917	752.712	958.2371	4:36	
			4:36	759.021
0.9949	755.142	963.0500	4:41	
0.9850	747.644	959.1768	4:45	
0.9772	741.748	954.9618	4:49	
0.9702	736.422	951.5637	4:54	
0.9584	727.475	947.1711	4:59	
0.9441	716.615	943.3226	5:04	
0.9287	704.927	940.2872	5:09	
0.9131	693.136	937.8560	5:12	
0.8967	680.673	935.6818	5:16	
0.8727	662.417	932.9995	5:20	
0.8395	637.232	929.6882	5:24	
0.7979	605.686	925.9418	5:29	
0.7415	562.866	920.9042	5:35	
0.6316	479.450	910.8106	5:46	
0.5367	407.411	900.8309	5:54	
0.4498	341.422	887.6849	6:04	

US Army Surface Area Analysis SAC:2

-SAP 2000 V1.04 PAGE 1

SAMPLE DIRECTORY/NUMBER: DATA1 /64
SAMPLE ID: super activated 2
SUBMITTER: ccm
OPERATOR: ccm
UNIT NUMBER: 1
ANALYSIS GAS: Nitrogen

START 10:09:50 11/27/91
COMPL 17:12:25 11/27/91
REPRT 17:12:26 11/27/91
SAMPLE WT: 0.3541 g
FREE SPACE: 57.4273 cc
EQUIL INTRVL: 5 sec

ANALYSIS LOG

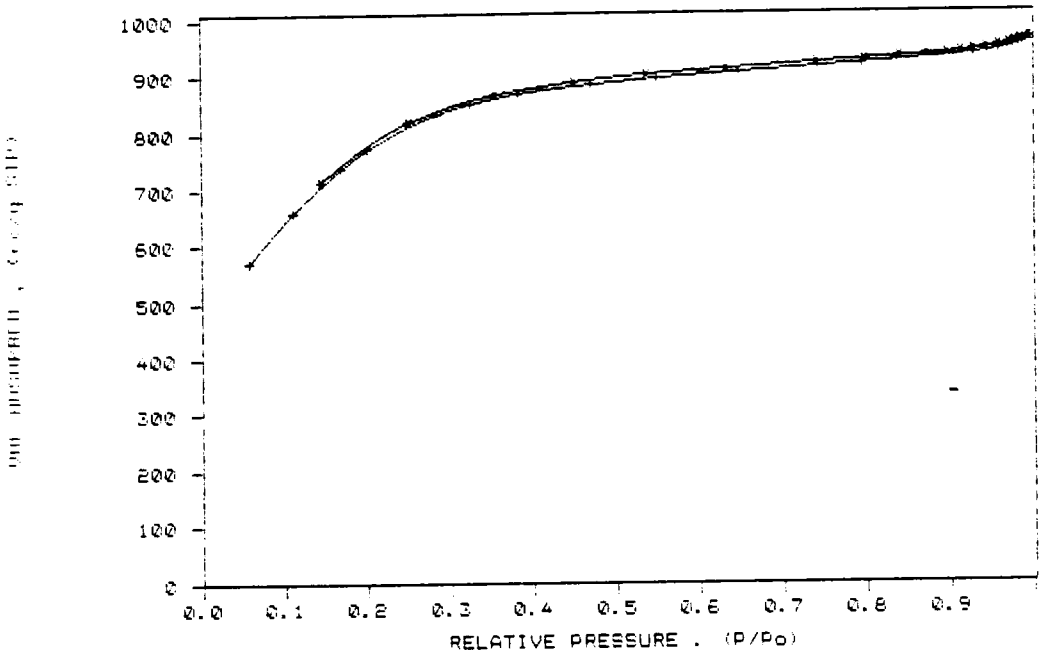
RELATIVE PRESSURE	PRESSURE (mmHg)	VOL ADSORBED (cc/g STP)	ELAPSED TIME (HR:MN)	SATURATION PRESS. (mmHg)
0.3551	269.539	866.1049	6:16	
0.2515	190.932	816.9157	6:36	
			6:37	759.176
0.1446	109.791	714.0021	7:03	

SAEP 2001 V1.04

SAMPLE DIRECTORY/NUMBER: DATA1 /e4
SAMPLE ID: super activated 2
SUBMITTER: ccn
OPERATOR: ccn
UNIT NUMBER: 1
ANALYSIS GAS: Nitrogen

START 10:09:50 11/27/91
COMPL 17:12:25 11/27/91
REPT 17:12:26 11/27/91
SAMPLE WT: 0.3941 g
FREE SPACE: 57.4071 cc
EQUIL INTRVL: 5 sec

ISOTHERM PLOT
+ ads, * des



SAMPLE DIRECTORY/NUMBER: DATA1 /64
SAMPLE ID: super activated 2
SUBMITTER: ccn
OPERATOR: ccn
UNIT NUMBER: 1
ANALYSIS GAS: Nitrogen

START 10:09:50 11/27/91
COMPL 17:12:25 11/27/91
REPRT 17:12:26 11/27/91
SAMPLE WT: 0.0941 g
FREE SPACE: 57.4272 cc
EQUIL INTRVL: 5 sec

BET SURFACE AREA REPORT

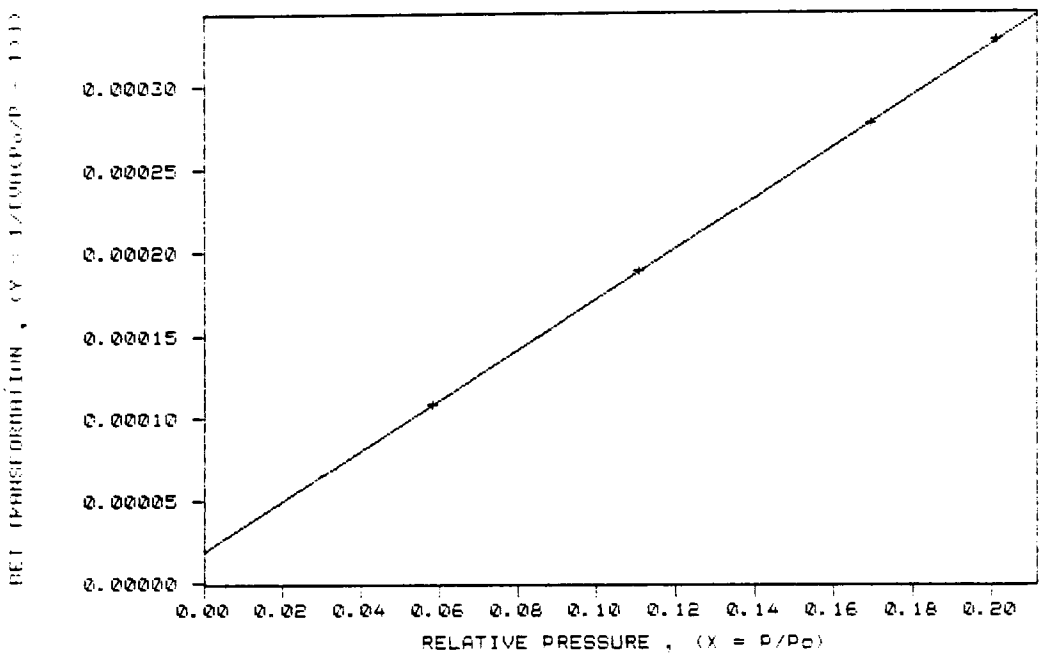
BET SURFACE AREA:	2819.2847	+/-	15.9003	sq. m/g
SLOPE:	0.001524	+/-	0.000009	
Y-INTERCEPT:	0.000020	+/-	0.000001	
C:	76.794037			
VM:	647.635193	cc/g STP		
CORRELATION COEFFICIENT:	9.99968E-01			

RELATIVE PRESSURE	VOL ADSORBED (cc/g STP)	1/ [VA(Po/P - 1)]
0.0583	571.4426	0.000108
0.1109	659.0431	0.000189
0.1695	736.8499	0.000277
0.2012	770.4445	0.000327

SAMPLE DIRECTORY/NUMBER: DATA1 /64
SAMPLE ID: super activated 2
SUBMITTER: cch
OPERATOR: cch
UNIT NUMBER: 1
ANALYSIS GAS: Nitrogen

START 10:09:50 11/27/91
COMPL 17:12:25 11/27/91
REPT 17:12:26 11/27/91
SAMPLE WT: 0.3941 g
FREE SPACE: 57.4272 cc
EQUIL INTRVL: 5 sec

BET PLOT



SAMPLE DIRECTORY/NUMBER: DATA1 /64
SAMPLE ID: super activated 2
SUBMITTER: ccr
OPERATOR: ccr
UNIT NUMBER: 1
ANALYSIS GAS: Nitrogen

START 10:09:50 11/27/95
COMPL 17:12:25 11/27/95
REPRT 17:12:26 11/27/95
SAMPLE WT: 0.3941 g
FREE SPACE: 57.4272 cc
EQUIL INTRVL: 5 sec

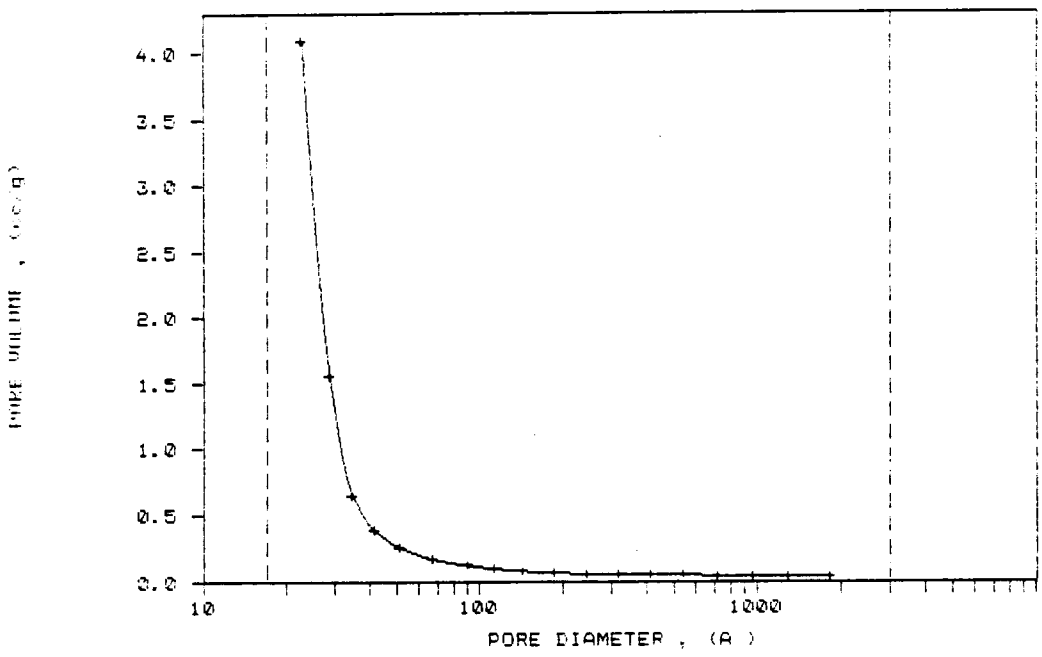
BJH ADSORPTION PORE DISTRIBUTION REPORT

PORE DIAMETER RANGE (A)	AVERAGE DIAMETER (A)	INCREMENTAL PORE VOLUME (cc/g)	CUMULATIVE PORE VOLUME (cc/g)	INCREMENTAL PORE AREA (sq. m/g)	CUMULATIVE PORE AREA (sq. m/g)
1580.5- 1586.5	1822.0	0.006643	0.006643	0.146	0.146
1136.6- 1136.6	1287.7	0.006079	0.012723	0.189	0.335
1136.6- 854.0	954.9	0.005273	0.017996	0.221	0.556
854.0- 642.4	717.9	0.005219	0.023215	0.291	0.846
642.4- 482.9	539.6	0.005580	0.028795	0.414	1.260
482.9- 370.7	411.6	0.005432	0.034227	0.528	1.788
370.7- 286.3	317.2	0.005480	0.039707	0.691	2.479
286.3- 219.0	243.2	0.006213	0.045921	1.022	3.501
219.0- 166.4	185.1	0.007482	0.053403	1.617	5.118
166.4- 129.4	141.9	0.008116	0.061519	2.272	7.390
129.4- 102.6	112.6	0.009320	0.070839	3.311	10.701
102.6- 81.8	89.6	0.011465	0.082304	5.119	15.820
81.8- 59.7	66.9	0.022593	0.104896	13.514	29.333
59.7- 46.1	50.9	0.028733	0.133629	22.596	51.929
46.1- 38.5	41.5	0.030155	0.163784	25.087	81.017
38.5- 32.1	34.6	0.051473	0.215257	59.574	140.591
32.1- 26.4	28.5	0.131949	0.347206	185.098	325.689
26.4- 20.7	22.7	0.428653	0.775859	756.949	1082.637

SAMPLE DIRECTORY/NUMBER: DATA1 /64
SAMPLE ID: super activatec 2
SUBMITTER: cch
OPERATOR: cch
UNIT NUMBER: 1
ANALYSIS GAS: Nitrogen

START 10:[illegible] 11/[illegible]
COMPL 17:10:[illegible] 11/[illegible]
REPRT [illegible] 11/[illegible]
SAMPLE WT: 0.[illegible] g
FREE SPACE: [illegible] cc
EQUIL INTRVL: 5 sec

dV/dlog(D) ADSORPTION PORE VOLUME PLOT



SAMPLE DIRECTORY/NUMBER: DATA1 /64
SAMPLE ID: super activated 2
SUBMITTER: ccn
OPERATOR: ccn
UNIT NUMBER: 1
ANALYSIS GAS: Nitrogen

START 10:09:5[illegible] 11/27/9[illegible]
COMPL 17:12:25 11/27/91
REPRT 17:12:2[illegible] 11/27/91
SAMPLE WT: 0.3941 g
FREE SPACE: 57.4072 cc
EQUIL INTRVL: 5 sec

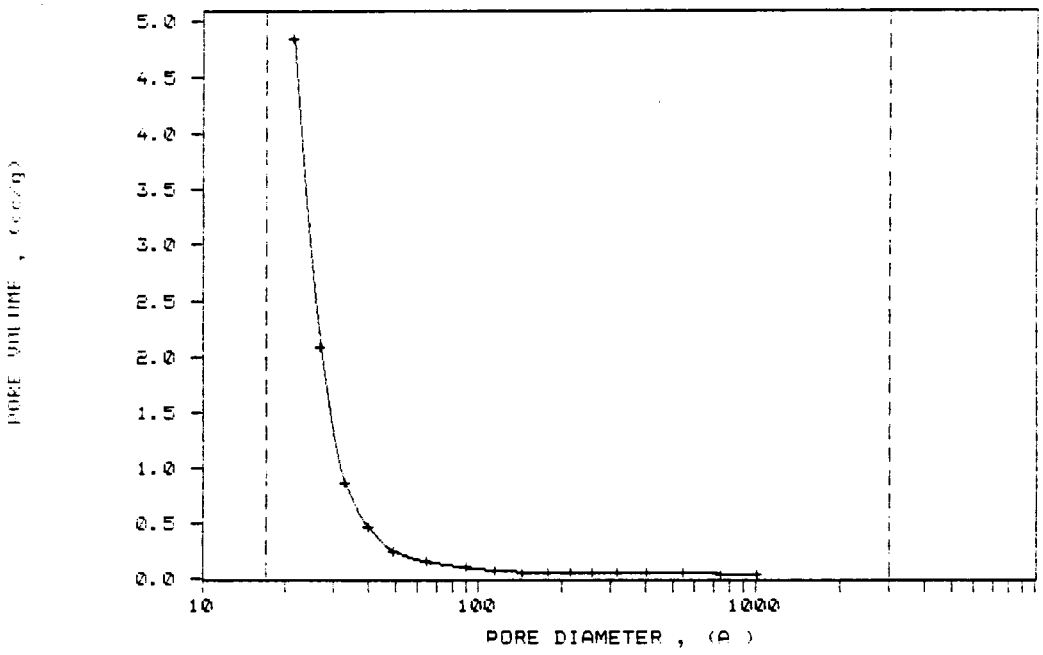
BJH DESORPTION PORE DISTRIBUTION REPORT

PORE DIAMETER RANGE (A)		AVERAGE DIAMETER (A)	INCREMENTAL PORE VOLUME (cc/g)	CUMULATIVE PORE VOLUME (cc/g)	INCREMENTAL PORE AREA (sq. m/g)	CUMULATIVE PORE AREA (sq. m/g)
1309.6-	869.7	1002.3	0.007109	0.007109	0.284	0.284
869.7-	668.7	742.6	0.005796	0.012905	0.312	0.596
668.7-	483.2	545.7	0.007612	0.020517	0.558	1.154
483.2-	362.6	405.2	0.006777	0.027294	0.669	1.823
362.6-	296.4	315.2	0.005425	0.032719	0.689	2.511
296.4-	236.7	256.5	0.004413	0.037132	0.686	3.199
236.7-	200.1	215.1	0.004016	0.041148	0.747	3.946
200.1-	163.4	177.8	0.005070	0.046218	1.141	5.087
163.4-	130.6	143.0	0.006499	0.052717	1.818	6.905
130.6-	104.3	114.2	0.007685	0.060402	2.692	9.597
104.3-	81.8	90.0	0.010940	0.071342	4.862	14.459
81.8-	57.2	64.6	0.024657	0.095999	15.275	29.733
57.2-	44.8	49.2	0.026803	0.122801	21.794	51.527
44.8-	36.9	39.9	0.039772	0.162574	39.873	91.401
36.9-	30.4	32.8	0.073290	0.235864	85.311	180.712
30.4-	24.7	26.8	0.187194	0.423058	279.907	460.619
24.7-	19.6	21.3	0.487795	0.910852	914.981	1375.600

SAMPLE DIRECTORY/NUMBER: DATA1 /64
SAMPLE ID: super activated I
SUBMITTER: ccm
OPERATOR: cch
UNIT NUMBER: 1
ANALYSIS GAS: Nitrogen

START 10:09:50 11/27/91
COMPL 17:12:25 11/27/91
REPRT 17:12:26 11/27/91
SAMPLE WT: 0.3941 g
FREE SPACE: 57.4272 cc
EQUIL INTRVL: 5 sec

dV/dlog(D) DESORPTION PORE VOLUME PLOT



SAMPLE DIRECTORY/NUMBER: DATA1 /a4
SAMPLE ID: super activated 2
SUBMITTER: ccr
OPERATOR: ccr
UNIT NUMBER: 1
ANALYSIS GAS: Nitrogen

START 10:09:50 11/27/9[illegible]
COMPL 17:12:25 11/27/9[illegible]
REPT 17:12:2[illegible] 11/27/9[illegible]
SAMPLE WT: 0.3541 g
FREE SPACE: 57.4174 cc
EQUIL INTRVL: 5 sec

SUMMARY REPORT

AREA

BET SURFACE AREA:	2819.2847	sq. m/g
SINGLE POINT SURFACE AREA AT P/Po 0.2012:	2679.2468	sq. m/g
BJH CUMULATIVE ADSORPTION SURFACE AREA OF PORES BETWEEN 17.0000 AND 3000.0000 A DIAMETER:	1082.6372	sq. m/g
BJH CUMULATIVE DESORPTION SURFACE AREA OF PORES BETWEEN 17.0000 AND 3000.0000 A DIAMETER:	1375.6001	sq. m/g

VOLUME

SINGLE POINT TOTAL PORE VOLUME OF PORES LESS THAN 1572.0005 A DIAMETER AT P/Po 0.9877:	1.475933	cc/g
BJH CUMULATIVE ADSORPTION PORE VOLUME OF PORES BETWEEN 17.0000 AND 3000.0000 A DIAMETER:	0.775859	cc/g
BJH CUMULATIVE DESORPTION PORE VOLUME OF PORES BETWEEN 17.0000 AND 3000.0000 A DIAMETER:	0.910852	cc/g

PORE SIZE

AVERAGE PORE DIAMETER (4V/A BY BET):	20.9405	A
BJH ADSORPTION AVERAGE PORE DIAMETER (4V/A):	28.6655	A
BJH DESORPTION AVERAGE PORE DIAMETER (4V/A):	26.4660	A

Alexander Carbon Surface Area Analysis

SF.3000+v1.04 PAGE 1

PLE DIRECTORY/NUMBER: DATA1 /75
PLE ID: US Army Project Alexander Carbon
BMITTER: Chris
ERATOR: Grad. Research Asst.
IT NUMBER: 1
ALYSIS GAS: Nitrogen

START 15:32:49 04/07/93
COMPL 19:22:05 04/07/93
REPRT 19:22:06 04/07/93
SAMPLE WT: 0.1530 g
FREE SPACE: 53.7248 cc
EQUIL INTRVL: 3 sec

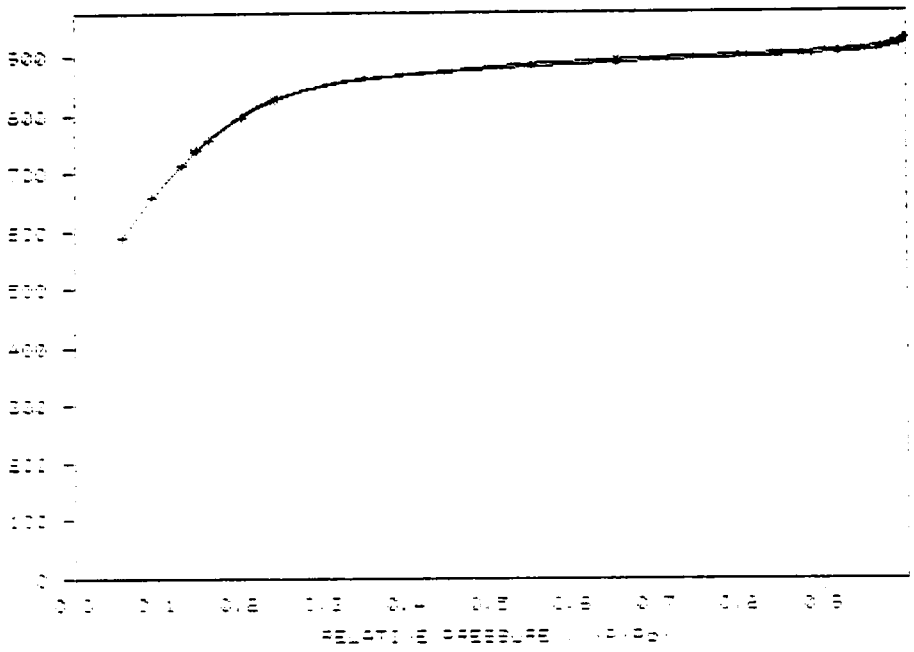
ANALYSIS LOG

RELATIVE PRESSURE	PRESSURE (mmHg)	VOL ADSORBED (cc/g STP)	ELAPSED TIME (HR:MN)	SATURATION PRESS. (mmHg)
			0:41	753.486
0.0572	43.130	638.4918	1:11	
0.0933	70.332	656.6757	1:18	
0.1300	97.948	714.7835	1:26	
0.1481	111.653	739.6071	1:32	
0.1624	122.409	757.1560	1:37	
0.2014	151.784	796.3663	1:46	
0.2439	185.347	826.9748	1:55	
0.3051	229.877	850.1461	2:02	
0.3516	268.029	859.9764	2:07	
0.4477	337.182	871.6964	2:11	
0.5013	415.789	880.5160	2:15	
0.6541	493.154	887.4441	2:19	
0.7465	562.514	892.8267	2:22	
0.8132	612.909	896.3734	2:24	
0.8520	642.775	898.8582	2:27	
0.8684	654.813	901.0908	2:29	
0.8855	667.516	903.2074	2:31	
0.9241	706.289	908.2432	2:32	
0.9443	727.413	908.8079	2:35	
0.9619	740.260	912.4653	2:37	
0.9715	741.048	917.9587	2:40	
0.9772	751.988	927.8251	2:46	
			2:47	734.305
0.7307	741.697	913.0887	2:51	
0.7698	771.199	914.0468	2:54	
0.8078	799.994	910.7700	2:57	
0.7722	702.736	906.7996	2:59	
0.9134	693.878	907.4722	3:01	
0.9025	660.4ee	90e.2010	3:03	
0.8781	665.822	904.8181	3:05	
0.8401	635.405	902.8125	3:08	
0.7999	603.122	900.2580	3:10	
0.7812	588.06	897.0029	3:13	
0.8277	623.562	899.9774	3:16	
0.8518	641.747	885.2864	3:20	
0.7854	591.747	874.5155	3:25	
0.7511	561.128	851.1807	3:30	
0.2408	181.311	129.2716	3:36	
0.1478	108.478	737.8577	3:48	

SAMPLE ID: UC Army Project Alexander Carbon
OPERATOR: Brad. Research Asst.
ADSORB: Nitrogen

START 10:02: 8 04/07/93
COMPL 15:03:15 14/07/93
ANALYSIS 15:03:06 14/07/93
SAMPLE WT: 0.1850 g
FREE SPACE: 35.7043 cc
EQUIL INTERVAL: 8 sec

ISOTHERM PLOT
- ads, * des



Alexander Carbon Surface Area Analysis

FILE DIRECTORY NUMBER: DATA\ 778	START [illegible]
FILE ID: US Army Project Alexander Carbon	DONE [illegible]
SITTER: Conlin	USER [illegible]
OPATOR: Grad. Research Asst.	SAMPLE WT: [illegible] g
T NUMBER: 1	FREE SPACE: 80.7348 cc
LYSIS GAS: Nitrogen	EQUIL INTRVL: 5 sec

BET SURFACE AREA REPORT

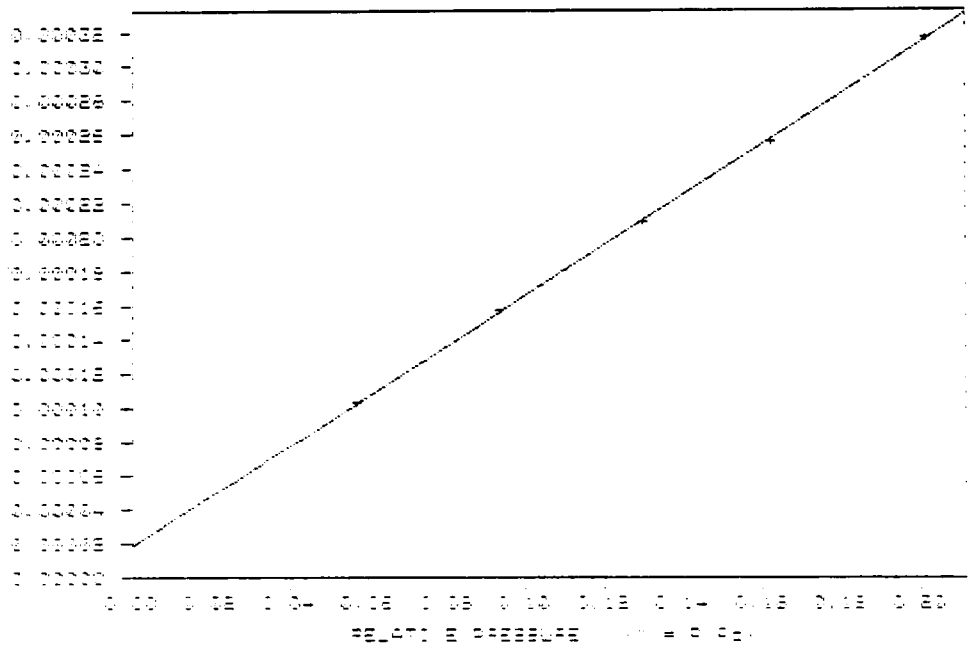
BET SURFACE AREA:	2918.6842	+/-	[illegible] sq. m/g
SLOPE:	[illegible]	+/-	[illegible]
Y-INTERCEPT:	[illegible]	+/-	[illegible]
C:	[illegible]		
Vm:	[illegible] cc/g STP		
CORRELATION COEFFICIENT:	[illegible]		

RELATIVE PRESSURE	VOL ADSORBED cc/g STP	1/ [illegible]
[illegible]	[illegible]	[illegible]
[illegible]	[illegible]	[illegible]
[illegible]	[illegible]	[illegible]
[illegible]	[illegible]	[illegible]
[illegible]	[illegible]	[illegible]

FILE DIRECTORY/NUMBER: DATA1 /TE
FILE ID: LB Arm Project Alexander Carbon
OPERATOR: Grad. Research Asst.
SAMPLE NO.: 1
ANALYSIS GAS: Nitrogen

START
COMPL
REPRT
SAMPLE WT: 0.0530 g
FREE SPACE:
EQUIL INTRVL: 1 sec

BET PLOT



FILE DIRECTORY/NUMBER: DATA1 /75
FILE TO: US Army Project Alexander Carbon
SUBMITTER: Chris
OPERATOR: Grad. Research Asst.
RUN NUMBER: 1
ANALYSIS GAS: Nitrogen

START 15:33:49 04/07/93
COMPL 19:22:05 04/07/93
REPRT 19:22:06 04/07/93
SAMPLE WT: 0.1830 g
FREE SPACE: 53.7048 cc
EQUIL INTRVL: 5 sec

BJH ADSORPTION PORE DISTRIBUTION REPORT

RD DIAMETER RANGE (A	AVERAGE DIAMETER (A)	INCREMENTAL PORE VOLUME (cc/g)	CUMULATIVE PORE VOLUME (cc/g)	INCREMENTAL PORE AREA (sq. m/g)	CUMULATIVE PORE AREA (sq. m/g)
1A.7- [illegible]	1506.8	0.009125	0.009125	0.279	0.279
66.1- 568.7	676.4	0.016705	0.025830	0.396	0.676
38.7- 000.6	393.5	0.005697	0.031527	0.579	1.255
29.6- 251.9	251.3	0.003405	0.034931	0.454	1.709
25.2- 1[illegible]	206.3	0.004.63	0.039099	0.800	2.509
22.7- [illegible]	187.5	0.004016	0.043115	1.095	3.604
[illegible]	1[illegible]	0.003364	0.046479	1.656	5.290
[illegible] 4	93.4	0.007710	0.054188	3.320	8.611
[illegible]	68.7	0.010536	0.064724	7.549	16.160
[illegible]	51.4	0.018479	0.083203	14.356	30.516
[illegible]	40.2	0.026139	0.109341	26.097	56.613
[illegible]	33.6	0.039253	0.148593	46.156	104.768
[illegible]	28.1	0.057796	0.206389	101.111	205.879
[illegible]	[illegible]	0.[illegible]	0.[illegible]	736.561	[illegible]

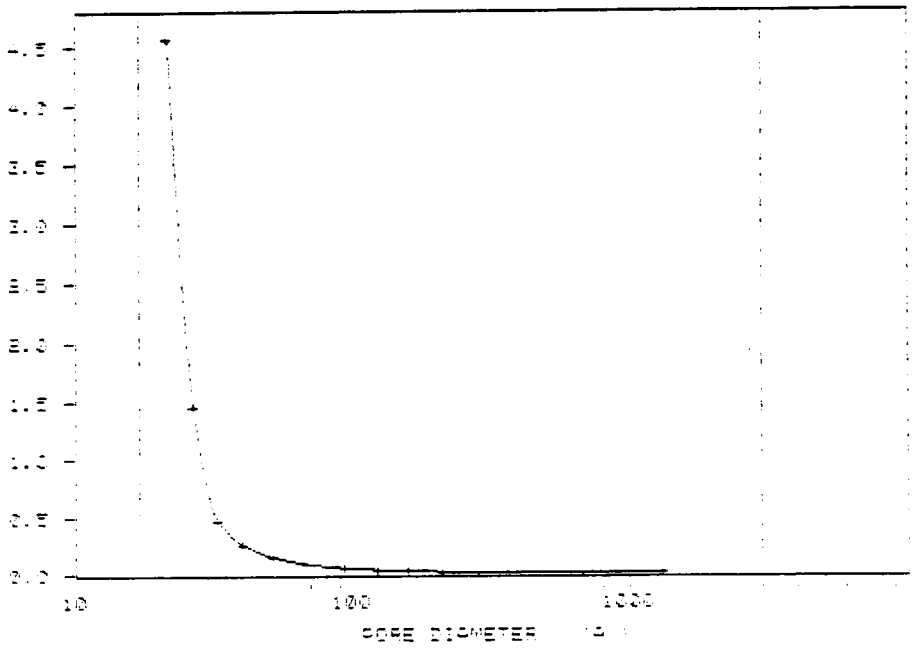
Alexander Carbon Surface Area Analysis

SP 2000 V1.04 PAGE 6

FILE DIRECTORY/NUMBER: DATA1 /75
FILE ID: US Army Project Alexander Carbon
SUBMITTER: Chris
OPERATOR: Grad. Research Asst.
RT NUMBER: 1
ALYSIS GAS: Nitrogen

START 10:30:49 04/07/93
COMPL 19:22:05 04/07/93
REPRT 19:22:06 04/07/93
SAMPLE WT: 0.1830 g
FREE SPACE: 33.7248 cc
EQUIL INTRVL: 5 sec

dV/dlog(D) ADSORPTION PORE VOLUME PLOT



FILE DIRECTORY/NUMBER: DATA1 /73
FILE ID: US Army, Project Alexander Carbon
WRITTER: Carlos
OPRATOR: Grad. Research Asst.
UNIT NUMBER: 1
ANALYSIS GAS: Nitrogen

START 10:33:44 04/07/93
COMPL 14:22:03 04/07/93
REPRT 14:22:16 04/07/93
SAMPLE WT: 1.1551 g
FREE SPACE: 50.7540 cc
EQUIL INTRVL: 5 sec

BJH DESORPTION PORE DISTRIBUTION REPORT

PORE DIAMETER RANGE (A)		AVERAGE DIAMETER (A)	INCREMENTAL PORE VOLUME (cc/g)	CUMULATIVE PORE VOLUME (cc/g)	INCREMENTAL PORE AREA (sq. m/g)	CUMULATIVE PORE AREA (sq. m/g)
1038.9-	659.2	781.4	0.000138	0.009233	0.424	0.424
779.2-	606.9	661.5	0.000668	0.014382	0.5.8	0.942
606.9-	370.1	555.5	0.000349	0.017847	0.419	1.362
471.1-	258.1	372.7	0.000303	0.020246	0.780	1.741
370.0-	211.6	288.8	0.000238	0.022571	1.407	2.148
211.6-	180.3	190.9	0.000151	0.025722	1.688	2.836
180.3-	171.1	144.7	0.000408	0.029637	1.062	3.898
171.1-	165.7	110.1	0.000459	0.034218	1.619	5.517
165.0-	91.1	94.1	0.000714	0.041427	2.152	7.669
91.1-	87.8	87.8	0.000110	0.042532	0.141	7.810
87.8-	48.4	61.4	0.000771	0.050301	17.871	25.681
48.4-	37.1	41.8	0.000275	0.053075	22.959	48.640
37.1-	31.1	33.6	0.000148	0.054566	17.787	66.427
31.1-	26.1	28.1	0.000134	0.055917	19.141	85.568
26.1-	22.2	24.0	0.000102	0.056943	17.041	102.609

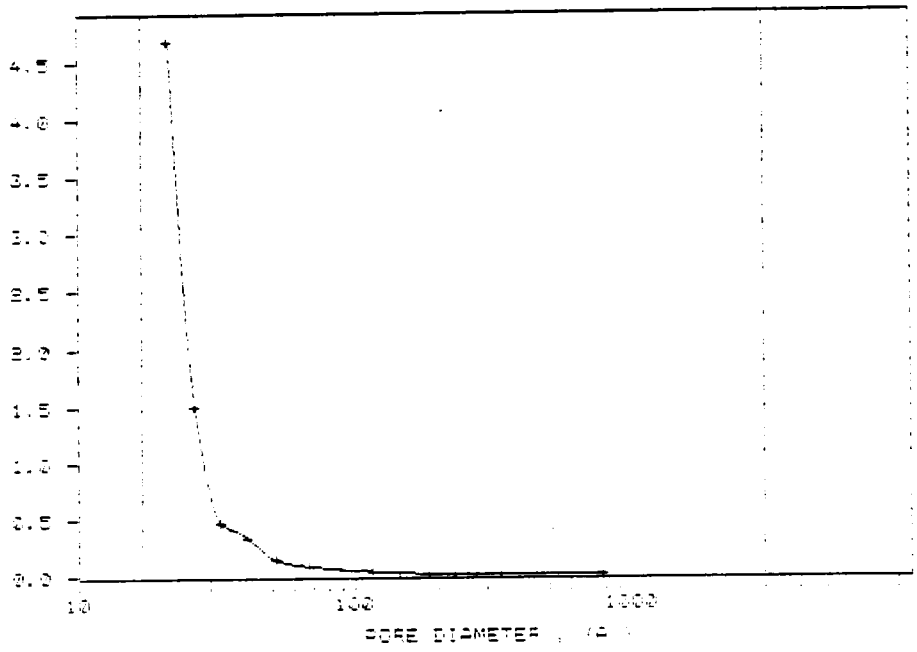
Alexander Carbon Surface Area Analysis

SF 2000 V1.04

MPLE DIRECTORY/NUMBER: DATA1 /75
PLE ID: US Army Project Alexander Carbon
MITTER: Chris
RATOR: Grad. Research Asst.
T NUMBER: 1
LYSIS GAS: Nitrogen

START 18:00:49 04/07/93
COMPL 19:22:05 04/07/93
REPT 19:22:06 04/07/93
SAMPLE WT: 0.1530 g
FREE SPACE: 53.7248 cc
EQUIL INTRVL: 5 sec

dV/dlog(D) DESORPTION PORE VOLUME PLOT



MPLE DIRECTORY/NUMBER: DATA1 /75
MPLE ID: US Army Project Alexander Carbon
BMITTER: Chris
ERATOR: Grad. Research Asst.
T NUMBER: 1
ALYSIS GAS: Nitrogen

START 15:32:49 04/07/93
COMPL 19:22:05 04/07/93
REPRT 19:22:06 04/07/93
SAMPLE WT: 0.1530 g
FREE SPACE: 53.7148 cc
EQUIL INTRVL: 5 sec

SUMMARY REPORT

AREA

T SURFACE AREA:	2918.6868	sq. m/g
NGLE POINT SURFACE AREA AT P/Po 0.2014:	2768.6509	sq. m/g
M CUMULATIVE ADSORPTION SURFACE AREA OF PORES BETWEEN 17.0000 AND 3000.0000 Å DIAMETER:	1093.2385	sq. m/g
CUMULATIVE DESORPTION SURFACE AREA OF PORES BETWEEN 17.0000 AND 3000.0000 Å DIAMETER:	1142.4407	sq. m/g

VOLUME

NGLE POINT TOTAL PORE VOLUME OF PORES LESS THAN 1581.8750 Å DIAMETER AT P/Po 0.9925:	1.419018	cc/g
CUMULATIVE ADSORPTION PORE VOLUME OF PORES BETWEEN 17.0000 AND 3000.0000 Å DIAMETER:	1.087771	cc/g
CUMULATIVE DESORPTION PORE VOLUME OF PORES BETWEEN 17.0000 AND 3000.0000 Å DIAMETER:	0.718548	cc/g

PORE SIZE

AVE PORE DIAMETER (4V/A BET):	19.4874	Å
ADSORPTION AVERAGE PORE DIAMETER (4V/A BET):	25.3187	Å
DESORPTION AVERAGE PORE DIAMETER (4V/A BET):	25.1710	Å

US Army Surface Area Analysis Fisher 50-200.I

ASAP 2000 V1.04

SAMPLE DIRECTORY/NUMBER: DATA1 /63
SAMPLE ID: Fisher 50-200
SUBMITTER: ccn
OPERATOR: ccn
UNIT NUMBER: 1
ANALYSIS GAS: Nitrogen

START 09:08:34 11/26/91
COMPL 12:13:30 11/26/91
REPRT 12:13:3[illegible] 11/26/91
SAMPLE WT: [illegible] g
FREE SPACE: 54.5041 cc
EQUIL INTRVL: 5 sec

ANALYSIS LOG

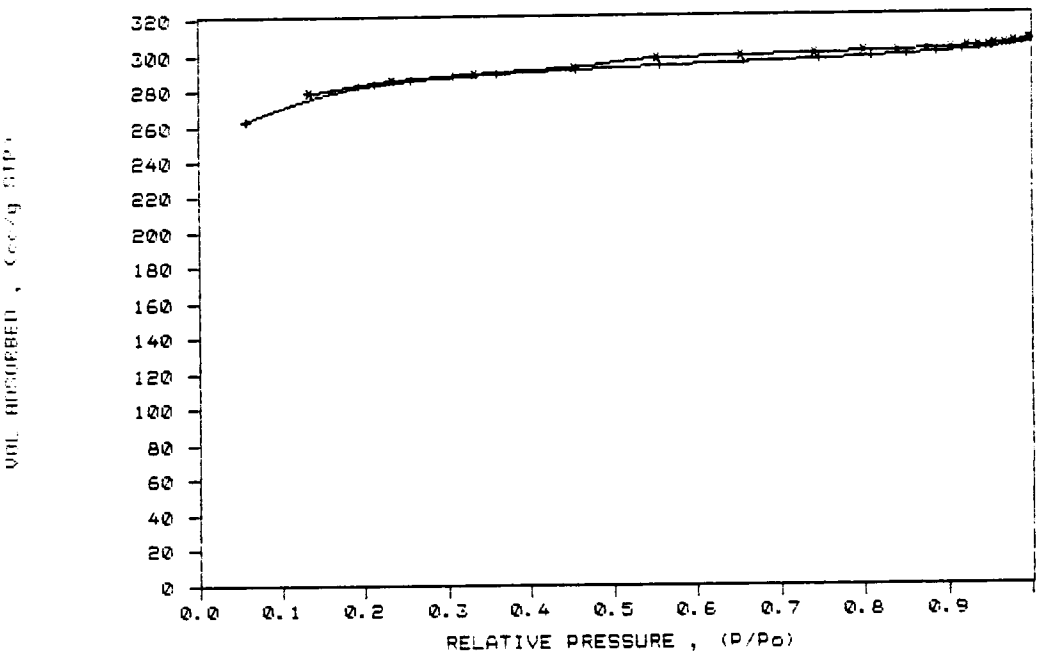
RELATIVE PRESSURE	PRESSURE (mmHg)	VOL ADSORBED (cc/g STP)	ELAPSED TIME (HR:MN)	SATURATION PRESS. (mmHg)
			0:30	760.107
0.0574	43.596	263.1909	1:08	
0.1943	147.698	281.9189	1:15	
0.2123	161.403	283.1061	1:18	
0.2564	194.862	285.3050	1:23	
0.3074	233.700	287.2619	1:27	
0.3592	273.055	288.8622	1:31	
0.4548	345.715	291.0642	1:35	
0.5559	422.563	292.9490	1:38	
0.6564	498.946	294.6622	1:42	
0.7467	567.572	296.2961	1:45	
0.8093	615.150	297.5928	1:48	
0.8514	647.213	298.6190	1:51	
0.8870	674.208	299.5799	1:53	
0.9174	697.377	300.4913	1:55	
0.9386	713.460	301.2708	1:57	
0.9544	725.458	301.9485	1:59	
0.9752	741.283	303.1295	2:02	
0.9862	751.160	304.3647	2:05	
0.9961	757.211	306.4760	2:11	
0.9782	743.610	304.8949	2:14	
0.9683	736.060	304.1930	2:16	
0.9552	726.130	303.5201	2:19	
0.9489	721.321	303.1778	2:21	
0.9367	712.012	302.7836	2:23	
0.9238	702.238	302.4071	2:25	
0.9044	687.499	301.9731	2:27	
0.8752	665.262	301.4301	2:30	
			2:31	760.159
0.8395	638.163	300.8900	2:33	
0.7997	607.910	300.3520	2:35	
0.7413	563.538	299.6345	2:38	
0.6526	496.205	298.5768	2:41	
0.5513	419.098	297.2796	2:44	
0.4521	343.698	292.4438	2:51	
0.3331	253.197	289.0117	2:55	
0.2334	177.434	285.3794	2:59	
0.1344	102.185	278.5366	3:05	

SAP 2000 V1.04

SAMPLE DIRECTORY/NUMBER: DATA1 /63
SAMPLE ID: Fisher 50-200
SUBMITTER: cch
OPERATOR: cch
UNIT NUMBER: 1
ANALYSIS GAS: Nitrogen

START 09:08:34 11/26/91
COMPL 12:13:30 11/26/91
REPRT 12:13:31 11/26/91
SAMPLE WT: 0.5189 g
FREE SPACE: 54.5241 cc
EQUIL INTRVL: 5 sec

ISOTHERM PLOT
+ ads, * des



SAMPLE DIRECTORY/NUMBER: DATA1 /63
SAMPLE ID: fisher 50-200
SUBMITTER: ccn
OPERATOR: ccn
UNIT NUMBER: 1
ANALYSIS GAS: Nitrogen

START 09:08:34 11/26/91
COMPL 12:13:30 11/26/91
REPT 12:13:31 11/26/91
SAMPLE WT: 0.5169 g
FREE SPACE: 54.5241 cc
EQUIL INTRVL: 5 sec

BET SURFACE AREA REPORT

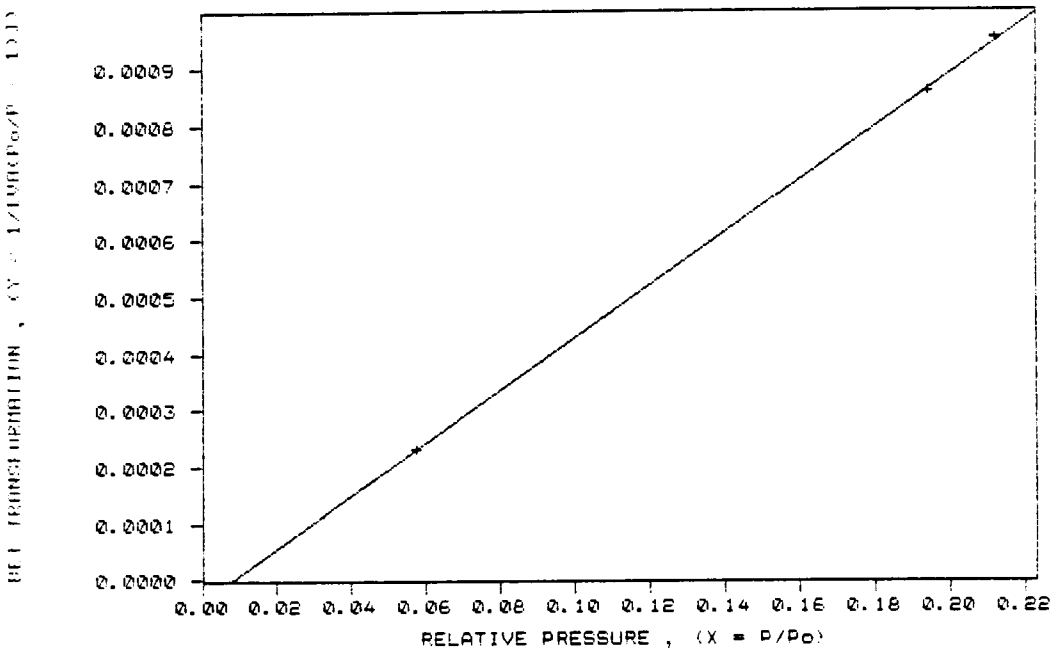
BET SURFACE AREA:	949.9671	+/-	16.8578	sq. m/g
SLOPE:	0.004617	+/-	0.000080	
Y-INTERCEPT:	-0.000034	+/-	0.000014	
C:	-133.007645			
VM:	218.227341	cc/g STP		
CORRELATION COEFFICIENT:	9.99849E-01			

RELATIVE PRESSURE	VOL ADSORBED (cc/g STP)	1/ [VA(Po/P - 1)]
0.0574	263.1909	0.000231
0.1943	281.9189	0.000855
0.2123	283.1061	0.000952

SAMPLE DIRECTORY/NUMBER: DATA1 /67
SAMPLE ID: Fisher 50-200
SUBMITTER: ccn
OPERATOR: ccn
UNIT NUMBER: 1
ANALYSIS GAS: Nitrogen

START 09:06:34 11/26/91
COMPL 12:13:30 11/26/91
REPT 12:13:31 11/26/91
SAMPLE WT: 0.5169 g
FREE SPACE: 54.5241 cc
EQUIL INTRVL: 5 sec

BET PLOT



SAMPLE DIRECTORY/NUMBER: DATA1 /63
SAMPLE ID: Fisher 50-200
SUBMITTER: ccm
OPERATOR: ccm
UNIT NUMBER: 1
ANALYSIS GAS: Nitrogen

START 09:06:34 11/26/91
COMPL 12:13:30 11/26/91
REPT 12:13:31 11/26/91
SAMPLE WT: 0.5169 g
FREE SPACE: 54.5241 cc
EQUIL INTRVL: 5 sec

LANGMUIR SURFACE AREA REPORT

LANGMUIR SURFACE AREA:	1266.7949	+/-	2.6495	sq. m/g
SLOPE:	0.002436	+/-	0.000007	
Y-INTERCEPT:	0.000021	+/-	0.000001	
C:	164.428635			
VM:	291.003235	cc/g STP		
CORRELATION COEFFICIENT:	9.999998E-01			

RELATIVE PRESSURE	VOL ADSORBED (cc/g STP)	1/ [VA*Po/P]
0.0574	263.1909	0.000215
0.1947	281.9189	0.000685
0.2123	283.1061	0.000750

SAMPLE DIRECTORY/NUMBER: DATA1 /67
SAMPLE ID: Fisher 50-200
SUBMITTER: ccn
OPERATOR: ccn
UNIT NUMBER: 1
ANALYSIS GAS: Nitrogen

START 09:08:[illegible] 11/[illegible]/9[illegible]
COMPL 12:13:30 11/2[illegible]/9[illegible]
REPRT 12:13:31 11/2[illegible]/9[illegible]
SAMPLE WT: 0.5156 g
FREE SPACE: 34.5241 cc
EQUIL INTRVL: 5 sec

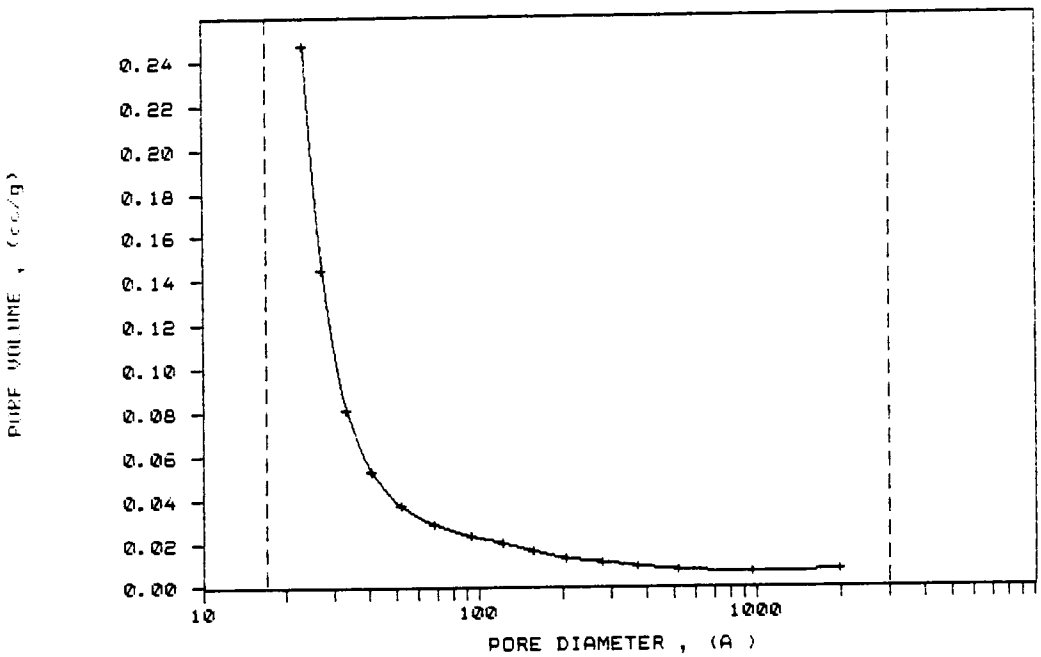
BJH ADSORPTION PORE DISTRIBUTION REPORT

PORE DIAMETER RANGE (A)	AVERAGE DIAMETER (A)	INCREMENTAL PORE VOLUME (cc/g)	CUMULATIVE PORE VOLUME (cc/g)	INCREMENTAL PORE AREA (sq. m/g)	CUMULATIVE PORE AREA (sq. m/g)
4996.7- 1655.5	1977.0	0.003448	0.003448	0.070	0.070
1655.5- 799.8	956.9	0.002043	0.005491	0.085	0.155
799.8- 441.6	522.3	0.002020	0.007511	0.155	0.310
441.6- 331.0	370.0	0.001187	0.008698	0.128	0.438
331.0- 248.5	277.6	0.001408	0.010106	0.203	0.641
248.5- 183.4	205.6	0.001706	0.011813	0.332	0.973
183.4- 140.7	156.0	0.001882	0.013695	0.482	1.455
140.7- 110.4	121.5	0.002102	0.015797	0.692	2.147
110.4- 83.5	92.6	0.002800	0.018597	1.207	3.355
83.5- 61.4	68.6	0.003798	0.022394	2.213	5.568
61.4- 46.9	51.9	0.004328	0.026722	3.337	8.904
46.9- 37.3	40.8	0.005271	0.031993	5.173	14.078
37.3- 30.6	33.1	0.006906	0.038900	8.339	22.417
30.6- 24.9	27.0	0.012953	0.051853	19.186	41.603
24.9- 21.9	23.1	0.013880	0.065732	23.989	65.591

SAMPLE DIRECTORY/NUMBER: DATA1 /63
SAMPLE ID: fisher 50-200
SUBMITTER: cch
OPERATOR: cch
UNIT NUMBER: 1
ANALYSIS GAS: Nitrogen

START 09:08:34 11/26/91
COMPL 12:13:30 11/26/91
REPRT 12:13:31 11/26/91
SAMPLE WT: 0.5189 g
FREE SPACE: 54.5241 cc
EQUIL INTRVL: 5 sec

dV/dlog(D) ADSORPTION PORE VOLUME PLOT



SAMPLE DIRECTORY/NUMBER: DATA1 /63
SAMPLE ID: fisher 50-200
SUBMITTER: cch
OPERATOR: cch
UNIT NUMBER: 1
ANALYSIS GAS: Nitrogen

START 09:08:34 11/26/91
COMPL 12:13:30 11/26/91
REPRT 12:13:31 11/26/91
SAMPLE WT: 0.5189 g
FREE SPACE: 54.5241 cc
EQUIL INTRVL: 5 sec

BJH DESORPTION PORE DISTRIBUTION REPORT

PORE DIAMETER RANGE (A)		AVERAGE DIAMETER (A)	INCREMENTAL PORE VOLUME (cc/g)	CUMULATIVE PORE VOLUME (cc/g)	INCREMENTAL PORE AREA (sq. m/g)	CUMULATIVE PORE AREA (sq. m/g)
509.4-	629.8	718.9	0.001210	0.001210	0.067	0.067
629.8-	450.0	509.6	0.001179	0.002389	0.092	0.160
450.0-	395.8	419.3	0.000608	0.002997	0.058	0.218
395.8-	321.3	350.5	0.000701	0.003698	0.080	0.298
321.3-	266.6	290.0	0.000683	0.004381	0.094	0.392
266.6-	215.7	236.1	0.000799	0.005179	0.135	0.527
215.7-	166.6	184.4	0.001030	0.006209	0.223	0.751
166.6-	130.6	143.9	0.001059	0.007269	0.295	1.045
130.6-	105.2	114.9	0.001101	0.008370	0.383	1.429
105.2-	81.8	90.2	0.001552	0.009922	0.688	2.117
81.8-	60.8	67.7	0.002492	0.012414	1.472	3.589
60.8-	46.4	51.3	0.003382	0.015796	2.636	6.225
46.4-	37.1	40.5	0.015601	0.031397	15.423	21.648
37.1-	29.1	31.8	0.010638	0.042035	13.363	35.011
29.1-	23.8	25.7	0.012603	0.054638	19.599	54.610
23.8-	19.1	20.7	0.029558	0.084196	57.020	111.630

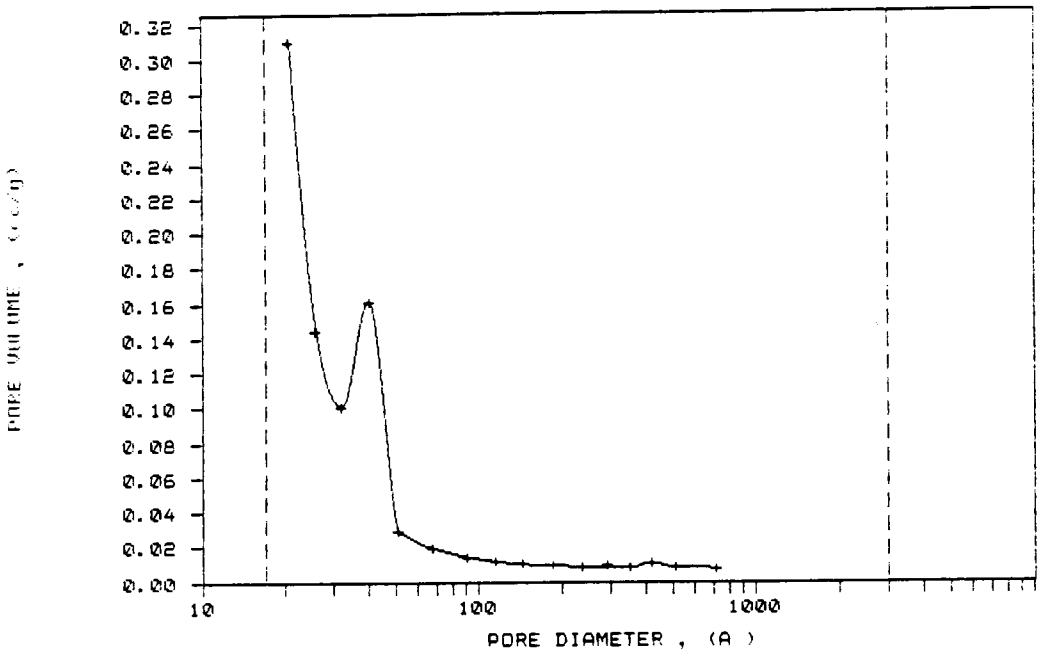
US Army Surface Area Analysis Fisher 50-200.2

SAP 2000 V1.04 PAGE 5

SAMPLE DIRECTORY/NUMBER: DATA1 /65
SAMPLE ID: fisher 50-200
SUBMITTER: cch
OPERATOR: cch
UNIT NUMBER: 1
ANALYSIS GAS: Nitrogen

START 09:08:34 11/26/91
COMPL 12:13:30 11/26/91
REPRT 12:13:31 11/26/91
SAMPLE WT: 0.5185 g
FREE SPACE: 54.5241 cc
EQUIL INTRVL: 5 sec

dV/dlog(D) DESORPTION PORE VOLUME PLOT



US Army Surface Area Analysis Fisher 50-200.2

ASAP 2000 V1.04

SAMPLE DIRECTORY/NUMBER: DATA1 /63
SAMPLE ID: fisher 50-200
SUBMITTER: cch
OPERATOR: cch
UNIT NUMBER: 1
ANALYSIS GAS: Nitrogen

START 09:08:34 11/26/91
COMPL 12:13:30 11/26/91
REPRT 12:13:31 11/26/91
SAMPLE WT: 0.5189 g
FREE SPACE: 54.5241 cc
EQUIL INTRVL: 5 sec

SUMMARY REPORT

AREA

BET SURFACE AREA:	945.9871	sq. m/g
LANGMUIR SURFACE AREA:	1266.7949	sq. m/g
SINGLE POINT SURFACE AREA AT P/Po 0.2123:	970.7305	sq. m/g
BJH CUMULATIVE ADSORPTION SURFACE AREA OF PORES BETWEEN 17.0000 AND 3000.0000 A DIAMETER:	65.5915	sq. m/g
BJH CUMULATIVE DESORPTION SURFACE AREA OF PORES BETWEEN 17.0000 AND 3000.0000 A DIAMETER:	111.6296	sq. m/g

VOLUME

SINGLE POINT TOTAL PORE VOLUME OF PORES LESS THAN 1640.3549 A DIAMETER AT P/Po 0.9882:	0.470791	cc/g
BJH CUMULATIVE ADSORPTION PORE VOLUME OF PORES BETWEEN 17.0000 AND 3000.0000 A DIAMETER:	0.065732	cc/g
BJH CUMULATIVE DESORPTION PORE VOLUME OF PORES BETWEEN 17.0000 AND 3000.0000 A DIAMETER:	0.084196	cc/g

PORE SIZE

AVERAGE PORE DIAMETER (4V/A BY LANGMUIR):	14.8656	A
BJH ADSORPTION AVERAGE PORE DIAMETER (4V/A):	40.0858	A
BJH DESORPTION AVERAGE PORE DIAMETER (4V/A):	30.1698	A

APPENDIX D

Appendix D. MIRAN 1A Information and Characteristics.

The MIRAN 1A is a single beam, variable filter spectrometer. It can be used in an automatic scanning mode or a fixed mode for determination of compound presence and concentration. The scanning absorption infrared spectral range is between 2.5 and 14.5 micrometers. The cell has an external pump which can be used to fill its 5.6 liter capacity. The detector is designed to provide continuous monitoring.

"The infrared source consists of a nichrome wire-wound resistor mounted within a cut-away type He6/U Crystal Can, which in turn is mounted upon supporting base. The resistor is heated to a constant temperature of about 900 degrees C by the regulated power supply described in section 5.5.2."

The theory which the detector operates on is found in the following references:

Brenchley, David L. et al. Industrial Source Sampling. Ann Arbor, Michigan: Science Publishers, Inc., 1973.

Colthup, N.B., Daly, L.H., and Wiberley, S.E. Introduction to Infrared and Raman Spectroscopy. New York: Academic Press, 1964.

APPENDIX E

Appendix E. Detailed Spreadsheet Mass Balance Analysis

Column 1

Time: formula for incrementing time in 24 second intervals.

Column 2

Inlet Concentration: assumed to be constant at 1700 ppm.

Column 3

Chart Reading: direct input from the strip chart recorder. Defined as the number of blocks at the corrisponding time.

Column 4

Outlet Concentration: value is recorded in ppm.

Formula:

= (Chart Reading)*(inlet concentration/calibration curve blocks)

the calibration curve blocks are the maximum value recorded by the strip chart recorder when the inlet flow by passes the filter holder assembly and runs through the detector.

Column 5

Amount Adsorbed, ppm

Formula:

=(inlet concentration)-(outlet concentration)

Column 6

Concentration Adsorbed, g/m^3

Formula:

= (amount adsorbed,ppm)*(molecular weight)*1000)/24.5 *(1 $g/10^6 \mu g$)

Column 7

Grams of TCE Adsorbed

Formula:

=(concentration adsorbed,g/m^3)*(Q,l/sec)*(T,sec)*(1 m^3/1000 l)

where Q = gas flow rate

T = time increment, 24 seconds

Column 8

Sum grams Adsorbed, g

This is a running total for the amount of TCE adsorbed at each of the time increments.

Column 9

Incremental g/g Adsorbed

Formula:

= (sum of grams adsorbed)/(weight of carbon on the filter)

The weight of carbon on the filter was determined by determining the area of the filter exposed to the TCE and then multiplying that area with the carbon loading reported for the filter.

VITA

Christopher (Chris) Charles Hood was born in Durham, North Carolina on August 2, 1964. He moved to Knoxville, Tennessee the following year. He attended elementary schools in the Knoxville area and graduated from Doyle High School in June, 1982. Following high school, Chris, attended the University of Tennessee, Knoxville and received a Bachelor of Science in Industrial Engineering in June, 1988. Upon completion of this degree he worked for three years as a sub-contractor at Oak Ridge National Laboratory. During the time at ORNL, he worked on the development of various human factors research related to control rooms and teleoperators. In August, 1991, Chris entered the University of Tennessee, Knoxville in the Environmental Engineering Masters program. He received his Master of Science degree from that program in December, 1993.

Chris is currently employed as an Environmental Engineer at Delta Research Corporation, an engineering consulting firm, located in Niceville, FL.